Mechanism of Formation and Age of the Ayyarmalai A-type Charnockite – Granite association from the South-Eastern Palghat- Cauvery Shear System, Southern India

Stephanie. E. Rowe

Tectonics Resources and Exploration (TRaX), Department of Geology and Geophysics, School of Earth and Environmental Sciences, University of Adelaide, South Australia.

E-Mail: Stephanie.rowe@student.adelaide.edu.au

OCTOBER 2010

Table of Contents

ABSTRACT **3**

1. INTRODUCTION **5**

1.1. Charnockite Definition & Problem **5**

1.2. Characteristics of Igneous and Metamorphic Charnockites **6**

2. GEOLOGICAL SETTING **8**

2.1. Geology of India **8**

2.1.1. Dharwar Craton & The Northern Granulite Terrain *8*

2.1.2. Southern Granulite Terrain *9*

2.2. Palghat-Cauvery Shear System **10**

3. FIELD RELATIONS & SAMPLE PETROLOGY **11**

3.1.Field Relationships ***12***

3.2.Ayyarmalai Quarry Massif Charnockite ***12***

3.2.1. Garnet & Hornblende Rich Charnockites *12*

3.2.2. Mafic Enclaves *14*

3.2.3. Charncokite Gneiss Zones *14*

3.3. Ayyarmalai Granite ***14***

3.3.1. Pink Alkali Granite *14*

3.3.2. Grey Granite *15*

3.3.3. Dehydration Zones *15*

3.3.4. Pegmatite *15*

4. ANALYTICAL PROCEDURES **16**

4.1. Petrography & Mineral Chemistry **16**

4.1.1 Pressure- Temperature Estimates *16*

4.2. Whole rock Major and Trace Elements **17**

4.2.1 Trace Elements *17*

4.3. U-Pb Zircon Dating **18**

4.4. Whole Rock Isotopic Analyses **19**

4.4.1. Radiogenic Isotopes *19*

4.4.2. Stable Isotopes *19*

5. RESULTS **20**

5.1. Mineral Chemistry **20**

5.1.1. Ayyarmalai Charnockite *20*

5.1.1.1. Garnet *20*

5.1.1.2. Pyroxenes *21*

5.1.1.3. Retrograde Minerals *21*

5.1.2.P-T Estimate (Charnockite) *22*

5.2. Whole Rock Geochemistry **22**

5.2.1. Ayyarmalai Charnockites *22*

5.2.2. Ayyarmalai Pink and Grey Alkali Granites *23*

5.3. U-Pb Zircon Geochronology **24**

5.3.1. Charnockite Zircons (SR-6 and SR-57) *25*

5.3.2. Ayyarmalai Granites (SR-68H and SR-63) *26*

5.4. Isotopes **27**

5.4.1. Radiogenic Isotopes *27*

5.4.1.1 Sm-Nd 27

5.4.1.2. Rb-Sr 27

5.4.1.3. Pb-Pb 28

5.4.2. Stable Isotopes *28*

5.4.2.1. $\delta^{18}O$ isotopes 28

6. DISCUSSION **29**

6.1. Petrographic and Geochemical Interpretation **29**

6.3. Timing and significance of charnockite and felsic magmatism in the PCSS **31**

6.4. Protolith and Crustal Evolution **33**

7. CONCLUSION **36**

8. ACKNOWLEDGEMENTS **37**

9. REFERENCES **37**

10. FIGURE CAPTIONS **45**

11. APPENDIX A – Supplementary Data Tables

12. APPENDIX B – Supplementary Figures

MECHANISM OF FORMATION AND AGE OF THE AYYARMALAI A-TYPE CHARNOCKITE – GRANITE ASSOCIATION FROM THE SOUTH-EASTERN PALGHAT-CAUVERY SHEAR SYSTEM, SOUTHERN INDIA

ABSTRACT

The Ayyarmalai A-type charnockite and A-type alkali granite lies on the south-eastern margin of the Palghat-Cauvery Shear System and provides an example of co-magmatism that was later overprinted with granulite facies metamorphism at ~2.45-2.5Ga. The Palghat-Cauvery Shear System represents an intriguing zone with Neoproterozoic aged granulites (~800-500 Ma) to the south and Archaean granulites (~3000-2500 Ma) to the north; the origins of which are still often disputed. This study presents whole rock major and trace element compositions, mineral chemistry, pressure-temperature estimates and whole rock Sm-Nd, Rb-Sr, Pb-Pb and $\delta^{18}O$ isotopic compositions of this A-type charnockite-granite association found at Ayyarmalai, Tamil Nadu, Southern India. The subsequent data from this study suggests that: (1) the Ayyarmalai charnockites from the Palghat-Cauvery Shear System have zircon ages that are synchronous with events in the Northern Granulite Terrain; (2) The Dharwar Craton is a strong candidate for the protolith of these rocks; (3) Evidence of a Neoproterozoic-Cambrian granulite metamorphic event (~520 Ma) appears to be absent in these rocks questioning the existence or location of a Neoproterozoic - Cambrian suture zone proposed for the Palghat-Cauvery Shear System recently.

U-Pb zircon ages show zoned igneous cores ~2.65-2.68 Ga ages in both rock types defining the crystallisation age, while the large metamorphic rim overgrowths date the Archaean granulite metamorphic event at ~2.45 - 2.5 Ga. Geochemical data of the Ayyarmalai charnockites reveal a very primitive, unfractionated REE pattern with no Eu-anomaly, ferroan, high K-calc-alkaline, with moderate enrichment of LREE with respect to HREE and fall within the field of high Ba-Sr type granitoids. Extraction of Pyroxene- Hornblende rich cumulates resulted in an intermediate charnockite driving the crystallisation towards the final A-type alkali granite. The A-type alkali granite show a more fractionated REE pattern with a significant Eu-anomaly, ferroan, high-K- calc-alkaline, with enrichment of LREE and depletion in the low Ba-Sr type granitoids. εNd and Nd model ages indicate

a highly evolved protolith ($\varepsilon_{Nd}(0)$ =-25.15 to -33.14) that encountered a crustal Archaean source (2.89-3.09 Ga) causing contamination as the magmas ascended. Harker diagrams, Nd data (isochron age, ~2519 Ma) and U-Pb zircon crystallisation ages suggest a co-magmatic relationship between the charnockite and alkali granite. Conventional geothermometry/barometry suggest minimum pressure-temperature conditions existed at 740 – 750°C and P=5.61 – 5.84 kbar.

The data presented from this study is consistent with a magmatic origin of these charnockites favouring the early crystallisation of orthopyroxene. The correlation with the data from the Dharwar Craton suggest that the study region may have encountered Dharwar Craton on magmatic ascent causing crustal contamination.

Keywords: A-type Charnockites, A-Type alkali Granite, Southern Granulite Terrain, Palghat- Cauvery Shear System, co-magmatism, Archaean – Palaeoproterozoic Boundary.

1. INTRODUCTION

Over a century ago, a hypersthene bearing granite was identified in a tombstone belonging to a Job Charnock in Calcutta by T.H. Holland. He located the source of the rock to quarries at Pallavaram, a suburb of Madras (now called Chennai). In a paper read to the Asiatic Society of Bengal, he detailed its petrological features and subsequently named it after the deceased by calling it a charnockite (Holland, 1900). The Southern Indian Granulite Terrain (SIGT) is well endowed with kilometres of charnockitic rock exposures which occur mainly as highland massifs lying along a network of major shear zones (Fig. 1a). The SIGT is separated into blocks and cratons divided by these shear zones that show traces of a dynamic tectonic history from Early Archaean to Cambrian (Chetty *et al*, 2006; Ghosh *et al.*, 2004). Charnockite formation makes up a significant part of the magmatic and metamorphic history of India and thus it is only fitting that these rocks have become subject to such extensive research over the last century.

1.1 Charnockite Definition and Problem

The IUGS define a charnockite as an *"Opx bearing granite composed mainly of quartz, perthite or antiperthite and Orthopyroxene (usually hypersthene), as an end member of the charnockite series"* (Le Maitre, 2002; Streckeisen, 1974, 1976). The charnockite series accounts for variants that have been recognised across different charnockites usually based on the differing modal abundance of the dominant feldspar i.e. opx- bearing granodiorites (charno-enderbite), opx-bearing tonalites (opdalite), opx- bearing monzonites (mangerites) and so forth (Le Maitre, 2002; Rajesh, 2004). Charnockites also vary from being acidic (and rich in quartz and feldspar) through to basic (and rich in olivine and pyroxene), which correspond mineralogically with many other igneous terms (Washington, 1916) i.e. diorites, norites and so on. Therefore charnockite is merely a general term (*senso lato)* that can be used until further geochemical analysis can discriminate the rocks into more specific categories.

The obvious ambiguity in this general term has led to a series of problems; one being the inconsistency and incorrect usage of nomenclature around when the term charnockite is applied. In

one case the term charnockite (an igneous term) has been applied to orthopyroxene (opx) bearing granites a part of an established igneous suite and on the other hand it has been applied to orthopyroxene bearing para and orthogneisses derived from granulite facies metamorphism. This has arisen through differing processes (igneous and metamorphic) that generate almost identical mineral assemblages (the key mineral in this case being hypersthene). Charnockites can be generated through several different mechanisms:

(1) Metasomatic dehydration granulite facies metamorphism involving the volatile fluxing of a low H_2O (high Pco_2) and/or alkali-halogen fluid. The influxing of a low H_2O fluid initiates the breakdown of hydrous minerals i.e. biotite and hornblende resulting in orthopyroxene (Smith *et al.*, 1979; Newton, 1989).

(2) Intrusion of water-undersaturated magma in dry crust during, or with subsequent, granulite facies metamorphism (Martignole, 1979).

(3) *In Situ* dry anatexis during granulite facies metamorphism (Martignole, 1979).

(4) Fractionation from enriched mantle-derived mafic magmas and/or crustal assimilation by mantle magmas. Differentiation of the parent magma can result in a cumulate or residue (after the granitic melt is removed) that is of charnockitic composition (Kilpatrick and Ellis, 1992; Field *et al.*, 1980; Frost and Frost, 2008; Pride & Muecke, 1980; Nesbitt, 1980). These charnockites also commonly display A-type granite characteristics.

There are several examples of igneous and metamorphic charnockites included in the literature, however given that charnockites are commonly found in granulite- facies metamorphic terrains, evidence of the original precursor are then reset or obliterated making it extremely difficult to distinguish which process crystallised the orthopyroxene resulting in a charnockite.

1.2. Characteristics of Igneous and Metamorphic Charnockites

In the SIGT, charnockites occur mainly as highland massifs and are usually interpreted as being the igneous type charnockites, as well as this; waxy green veinlets, selvages and patches occurring in the surrounding rocks that contain a charnockite composition were interpreted as incipient charnockites. Incipient charnockite is a term used to represent early stages of charnockite formation driven by the

influx of CO_2 rich fluids (Peucot *et al.*, 1989; Naha, 1988). There have been several research papers over the last decade that attributes the Southern Indian charnockites to be a product of the CO_2 metasomatic dehydration granulite facies metamorphism mechanism (Janardhan *et al.*, 1982; Bhattacharya & Sen, 2000; Santosh *et al.*, 1991; Frost & Frost, 1987; Bradshaw, 1989; Perchuk *et al.*, 2000; Hansen *et al.*, 1987, Raith & Srikantappa, 1993; Dobmeier & Raith, 2000; Tsunogae *et al.*, 2002; Santosh, 1985).

From many other localities around the globe there are clearly igneous charnockites that exist mainly as a part of a magmatic suite. This is where the magmas have differentiated into a series of rock types and in the case of charnockites there are several examples in the literature where charnockites occur a part of an Anorthosite-Mangerite-Charnockite-Granite Suite (AMCG Suite) around the globe e.g. The Adirondacks in New York (McLelland, 2002; Emslie, 1992); Korosten, Ukraine (Shumlyanskyy *et al.*, 2006) South-eastern Brazil (Janasi, 2002); Rogaland Complex in Southern Norway (Duchesne & Wilmart, 1997). Characterising these charnockites is difficult as the geochemistry, isotopic and mineral compositions are widely variable suggesting, a variety of tectonic settings. However, attempts to categorize igneous charnockites have suggested they are rich in TiO_2, K_2O and P_2O_5, have distinct iron-enrichment trends but due to the variable amongst individual charnockite plutons this is subject to debate (Kilpatrick & Ellis, 1992). Many attempts to split charnockite types into groups based on mineralogies have defined some interesting trends i.e. garnet-bearing vs. garnet-absent, low SiO_2 vs. high SiO_2 and garnet-rich vs. hornblende-rich. Rajesh (2008) shows that high SiO_2 charnockites display geochemical characteristics of alkali A-type granitoids, while low SiO_2 display similar trends with fractionated calc-alkaline granitoids similar to Caledonian type granitoids (Pitcher, 1982).

Santosh *et al.* (2005), has attributed charnockite formation in the SIGT to a CO_2 flushing origin, where CO_2 is derived from decarbonation of carbonate lithologies or from deep seated mantle sources leading to the generation of charnockite usually during granulite facies metamorphism (Santosh & Omori, 2005; Tsunogae *et al.*, 2008). Another model involves underplating of the crust by mantle-derived magmas (Tomson *et al.*, 2006; Newton, 1992; Rajesh, 2008). This study will compare these mechanisms with that of a subduction environment (where charnockite may be generated as syn-

accretion magmas), a compressional setting, an intraplate rift, or a plume-type setting, in hope to better constrain the tectonic environment in which these charnockite – granite associations were formed.

This paper will assemble valuable geochemical, petrological, isotopic (radiogenic and stable) and geochronological data on an A-type, high K calc-alkaline charnockite and alkali granite pair from Ayyarmalai; the south eastern end of the Palghat-Cauvery Shear System. The combined data aims to discriminate whether the charnockite from this area was crystallised from the mantle or was originally an igneous rock that was metamorphosed at granulite facies grade to a charnockite. This will hopefully provide some insight into links between charnockite – granite associates and where these rocks fit into the geological history of India and to a wider extent, eastern Gondwana.

2. GEOLOGICAL SETTING

2.1. Geology of India

2.1.2. Dharwar Craton and the Northern Granulite Terrain

During the Archaean, various cycles of geodynamic evolution took place in several cratons whereby an episode of island arc accretion was followed by the development and formation of tonalite - trondjhemite - granodiorite (TTG) greenstone terranes. This led to a period of reworking of the crust accompanied by tectonics, the emplacement of calc-alkaline granites and the development of high grade metamorphism. This is widely represented in the Dharwar Craton (central southern India) and contains some of the oldest rocks in the world (Chadwick, 1997; Jayananda *et al.*, 2000; Jayananda *et al*, 2006; Rogers, 1986) (Fig. 2a). In the northern part of the Dharwar Craton includes low to high grade volcanic-sedimentary rocks surrounded by more extensive areas of TTG Peninsular gneisses (Peucat *et al.*, 1989; Miller *et al.*, 1996; Mohan and Jayananda, 1999; Ghosh *et al.*, 2004). These TTG-greenstone terranes are intruded by a later synkinematic calc-alkaline to K-rich magmatic bodies along with a N-S sinistral shear zone dividing the Western and Eastern Dharwar Cratons (WDC and EDC respectively) (Chadwick *et al.*, 2000). In the WDC, Mesoarchaean TTG Peninsular gneisses are overlain by Late Archaean greenschist belts intruded by numerous granitic plutons (~2.6-2.68Ga) (Chadwick *et al.*, 2000; Jayamanda *et al.*, 2000). While in the EDC, the dominant lithologies consist

of Neoarchaean N-S trending granodiorite to granitic gneisses. The Archaean greenstone belts containing continental and oceanic-like volcano-sedimentary rocks that are interspersed within the granitic gneisses have experienced greenschist to amphibolite facies metamorphism (Miller *et al.*, 1996; Braun and Kriegsman, 2003; Ghosh *et al.*, 2004). Data suggests that protolith ages in the Dharwar craton range from 2.9-3.6 Ga (Beckinsale *et al.*, 1980; Harris, 1994; Bartlett *et al.*, 1998) and it is suspected that the southern part of the Dharwar craton experienced a late Archaean (~ 2.5 Ga) high temperature-low pressure metamorphic event (~8 kbar, 800°C) synchronous with the emplacement of granites (Buhl *et al.*, 1983; Hansen *et al*, 1984). This area of Archaean granulites is referred to in this study as the Northern Granulite Terrain (NGT), an area just north of the Palghat-Cauvery Shear System (Fig 2b). It is dominanted by large highland charnockitic massifs and lowland granitic ortho- and paragneisses varying from amphibolite to granulite grade of metamorphism (Ghosh *et al.*, 2004; Clark *et al.*, 2009; Mojeizes *et al*, 2003). Various data has suggested that these northern granulites are metamorphosed rocks from the Dharwar Craton (Ghosh *et al.*, 2004; Tomson *et al.*, 2006; Plavsa *et al.*,unpublished).

2.1.3. Southern Granulite Terrain

The Southern Indian Granulite Terrain (SIGT) is a significant terrain of high grade (amphibolite - granulite facies) rocks involving multiply deformed Archaean and Proterozoic magmatic and high grade metamorphic rocks (Santosh & Tsunogae 2003; Cenki & Kriegsman 2005; Chetty *et al.* 2006). Isotopic data, geological mapping and U-Pb geochronology of rocks from the SIGT in the past decade has indicated a diachronous evolution with regional thermotectonic and high-grade metamorphic events occurring at ~2.5 Ga and ~550 Ma. In the Southern Granulite Terrain, the older granulites are overprinted by a Neoproterozoic-Cambrian high T granulite event at around 0.55 Ga (Bartlet *et al.* 1995; Collins *et al.*, 2007; Clark *et al.*, 2009; Santosh *et al.*, 2003). The peak granulite facies metamorphism conditions calculated from various areas in the SGT constrain *P-T* conditions ranging from 700-1000°C and 5-12 kbar (Harris *et al.*, 1992; Raith *et al.*, 1997; Santosh *et al.*, 2003; Satish-Kumar *et al.*, 2002). Nd model ages range from 2.0 to 3.0 Ga (Bhaskar Rao *et al.*, 2003; Choudhary *et al.*, 1992; Harris *et al.*, 1994; Jayananda *et al.*, 1995; Brandon & Meen, 1995; Bartlett *et al.*, 1998;

Meissner *et al.*, 2002) except in the Achankovil Nd Unit where younger model ages are recorded (1.3–1.6 Ga; Harris *et al.*, 1994; Brandon and Meen, 1995; Bartlett *et al.*, 1998). This last metamorphism has been attributed to final accretion of Gondwana during the East African and Malagasy orogeny discussed later (Santosh *et al.*, 2003, 2009, Collins *et al.* 2007a, Collins *et al.* 2007b, Collins & Pisarevsky 2005).

2.2. Palghat-Cauvery Shear System

The Archaean and Neoproterozoic blocks of the SGT are separated by a prominent east-west tectonic zone (~70 x 400km), which in this study is referred to as the Palghat-Cauvery Shear System (PCSS) as it contains numerous narrow anastomosing network of dextral shear zones. This zone essentially separates the Neoproterozoic Southern Granulite Terrain from the Archaean/Palaeoproterozoic Northern Granulite Terrain and the Dharwar Craton. The zone also splits the SIGT into blocks called the Madras, North, Nilgiri and Madurai blocks. The Madurai block is separated by the Achankovil Zone further south from the Trivandrum block (Figure 2a). The PCSS, being at the interface of two different aged crustal blocks therefore represents an important zone for research. A number of tectonic models have been proposed for the PCSS, including:

(1) The PCSS forms the focus of either an ancient suture zone i.e. the continuation of the ancient Betsimisaraka suture of Gondwana that is evident in Madagascar and continues along this shear zone (Collins & Pisarevsky 2005; Collins *et al.* 2007; Cenki & Kriegsman 2005; Chetty *et al.* 2006, Santosh *et al.* 2009).

(2) It is a zone of transpressional tectonics in a convergent regime or merely a region of intense reworking of Archaean crust during the Proterozoic (Harris *et al*, 1994; Bhaskar Rao *et al*, 2003; Santosh *et al*, 2003).

(3) A dextral transcurrent shear belt (Drury *et al.*, 1984).

(4) A collapsed marginal basin (Drury and Holt, 1980) .

Geochronological signatures show three major ages at ca. 2.5 Ga, 1.8 Ga and 0.55 Ga which advocate a magmatic event, detrital zircon ages from metasediments and a granulite facies metamorphic event respecitvely. Rocks from the PCSS have given Nd model ages of 3.0-2.2 Ga suggesting that the shear

zone rocks are mainly reworked material from the high grade crustal domains to the north and south (e.g. Meiβner *et al.* 2002).

This study is located at Ayyarmalai, a site existing south east of the PCSS, a much understudied part of the system where the majority of the data has been obtained from the central and western sides. Limited knowledge on relationships between the SIGT and the adjacent Dharwar craton is also poorly understood therefore further data collection from this boundary would prove vital to delineating the tectonic history of Southern India.

3. FIELD RELATIONSHIPS & SAMPLE PETROGRAPHY

The samples collected for this study all lie within the PCSS near a small village called Ayyarmalai (10°52'48.48"N, 78°23'17.52"E); which is approximately 34km South East of Karur Township, 9km South of the Cauvery River, in Tamil Nadu, Southern India. Sample locations were recorded using Global positioning system (GPS) readings to record precise locations; Table 1 outlines sample locations, including GPS reading, rock type and the map units and Figure 2c shows a map of these localities. Samples were chosen to best represent the study area incorporating all of the mineralogical variability. Therefore the main rock types in the Ayyarmalai area have been categorised into: hornblende and garnet rich charnockite varieties, mafic charnockite zones, charnockitic gneiss zones, pink alkali granite, grey granite containing waxy green coloured dehydration zones and a later stage of cross-cutting hornblende-bearing pegmatites and quartzofeldspathic veins (Table 1).

3.1. Field Relationships

The field site for this study borders the town of Ayyarmalai (*Malai* meaning Hill), where a prominent 311m pink granite hill outcrops. The pink granite has a coarse, massive texture without any visible foliation but what appears to have flow induced folding. Pink feldspar is the dominant constituent with subordinate plagioclase and quartz and accessory biotite. The medium- to coarse-grained pink granite is veined locally by 0.5 to 1.0 m thick pegmatites and minor quartz. To the west

of the town there are excavated quarries where the rock types that have been exposed consist of extensive massif charnockites. The charnockite massif is faintly but recognizably foliated (the average trending Dip/Dip Direction, 38/250) and contains numerous quartz veins, large mafic blebs and pegmatites, all very dark in colour making it hard to distinguish between them in the field. Between the charnockite and the western front of the pink granite is a thick unit of grey granite contain green-grey waxy lenses and patches interpreted as dehydration zones.

3.2. Ayyarmalai Quarry Massif Charnockite

Charnockites have been subdivided into four types; the first two consist of hornblende rich charnockites existing to the western sides of the quarries and to then to the eastern sides of the quarries the assemblages are dominated more by garnet rather than hornblende. A third form of charnockite occurs as large mafic blebs consisting of dominantly hornblende, pyroxenes and Fe-Ti Oxides which appear to float in the homogenous massif charnockite and in this study these have been referred to as mafic charnockite zones. Visible on some walls of the quarries there are charnockites that have undergone high strain and formed a gneissosity with small sigma porphyroblasts that all have south side up movement indicators. These are referred to in the study as charnockitic gneiss zones.

3.2.1. Garnet & Hornblende Rich Charnockites

The charnockites are medium to dark greenish-grey rocks, within an even, medium-grained granoblastic texture, varying to porphyroblastic. K-feldspar (perthitic to mesoperthic and microcline), plagioclase and quartz are the main matrix minerals while hornblende, pyroxene and Fe-Ti oxides (ilmenite and magnetite) dominate the mafic minerals. Accessory minerals consist of apatite, iron oxides, magnetite, zircon and rarely allanite.

The mineral assemblage of these charnockites consists of:

(1) *Quartz + plagioclase + K-feldspar + orthopyroxene+ clinoproxene + hornblende + garnet ± Ilmenite ± biotite ± apatite ± magnetite ± zircon.*

The matrix assemblage in these samples consists of plagioclase, K-feldspar and quartz which have tight convolute interlocking (Figure 3q). Hornblende, ilmenite, magnetite and pyroxenes loosely define a foliation in some samples. Variable modal proportions of clinopyroxene and orthopyroxene in these rocks reach up to 20%. Where orthopyroxene occurs lying in close association is usually plagioclase, clinopyroxene, ilmenite and hornblende. In several instances, ilmenite is rimmed by clinopyroxene and hornblende and in some instances clinopyroxene occurs as cores within orthopyroxene. In these cases, clinopyroxene has a very high birefringence and displays lamellae textures. Hornblende displays a greenish-brown colour in plane light and displays well developed crystal cleavages. Hornblende is commonly intertwined with magnetite and biotite laths in these rocks. Plagioclase displays polysynthetic twinning while quartz shows some undulose extinction and there is minor myrmekite adjacent to biotite laths. Zircon abundance in charnockites appears quite high as numerous zircons over the assemblages apparent in thin section slides and even shows distinct zoning at this level. Small apatite crystals surrounded by radial cracks are also evident.

The assemblage of garnet rich charnockites from the Ayyarmalai quarries are the same as hornblende rich charnockite however the difference lays where garnet overtakes the dominance of hornblende. Garnet-rich charnockites have large garnet porphyroblasts dominating the assemblage and these occur closely with hornblende. Minor ilmenite, hornblende and quartz inclusions in garnet may represent an earlier stage (prograde) before the attainment of granulite facies conditions.

3.2.2. Mafic Charnockite zones

Amongst the homogenous charnockite are patches are very dark, mafic bleb zones. These zones appear to concentrically change in composition from the outer rim to inwards. The outermost rim is very rich in quartz and hornblende and then progressively inwards the middle of these patches is dominated by hornblende (dark green in thin section), magnetite/ ilmenite, pyroxene, quartz with minor plagioclase and garnet. These zones appear to float amongst the homogenous waxy green coloured hornblende and garnet rich charnockite varieties.

3.2.3. Charnockitic Gneiss Zones

The gneissosity in charnockitic rocks is defined by alternating bands and streaks of mafic and felsic minerals (Figure 3d). In these rocks the felsic bands are dominated by K-feldspar, Plagioclase and quartz, while the mafic bands which also defined to foliation through the alignment of these minerals consist of hornblende and biotite. In the mafic bands there are subordinate pyroxenes and reaction textures between biotite and myrmekite. Mineralogically, these charnockites differ in the modal abundance of quartz (5-20%) as opposed to the other charnockite samples that have a more granitic composition with a higher modal abundance of quartz (~20%).

3.3. Ayyarmalai Alkali Granites

3.3.1 Pink Alkali Granite

The dominant Ayyarmalai pink granites are medium grained, equigranular to granoblastic textures with a simple granitic composition. These are abundant in quartz (45%), K-feldspar (40%) with mafic minerals (10%) and accessory minerals (5%).

The mineral assemblage of these pink granitic rocks consists of:

(2) *K-feldspar + plagioclase + quartz+ biotite+ magnetite ± zircon ± titanate*

The Ayyarmalai pink granite has a granoblastic texture with convolute interlocking between grains. The matrix assemblage consists dominantly of K-feldspar (microcline and Perthite), plagioclase and quartz. Biotite in these assemblages contains ilmenite and quartz inclusions, are very rounded in shape. Other mineral features include plagioclase showing polysynthetic twinning and titanate which has radial cracks surrounding the mineral. In some samples hornblende and biotite define a lineation. Original igneous textures appear to have been obliterated by high grade metamorphism affecting the area. Zircons on top of the assemblages are clearly visible, however not as abundant as charnockite samples.

3.3.2. Grey Granite

Along the western front of Ayyarmalai consists of grey granite almost identical in modal compositions with the exception of the presence of bottle green clinopyroxene (Fig.3m-n). Clinopyroxene sometimes displays corroded cores and well developed crystal cleavages (Figure m-n). Microcline is the dominant K-feldspar mineral and again these have convolute interlocking textures in the matrix. The assemblages also contain titanite and ilmenite with radial cracking surrounding the grains. Other interesting features are the bright red colour of feldspars in hand sample specimens and the abundance of dehydration veins and selvages throughout the grey granite zone (Figure 3c).

3.3.3. Dehydration Zones

Waxy green-grey selvages run through the grey granite and bear striking resemblance to metamorphic charnockite (or "incipient charnockites"). The main assemblage of these dehydration zones consist of K-Feldspar + quartz + plagioclase ± Ilmenite ± magnetite. Microcline and microperthite dominate the felsic minerals. There is a high quantity of high birefringence fractures that intersect the minerals in these samples. The absence of orthopyroxene in these indicates that they are not charnockites, therefore these patches have been labelled as dehydration zones due to the absence of hydrous minerals.

3.3.4. Pegmatite

These a very coarse grained intrusions dominated by K-feldspar and quartz. Accessory minerals involve magnetite and hornblende. K-feldspar phenocrysts are large (<30cm in width) and the inner zones concentrate clusters of hornblende and magnetite (<3cm size grains). The pegmatites cross cut the pink granite and grey granite foliation (or flow induced folding), as well as the dehydration zones and quartz veins, representing the last stage of crystallisation.

4. ANALYTICAL PROCEDURES

4.1. Petrography

Identification of minerals and analysis of reaction textures of the various rock types were performed using field and lab petrography. First hand mineral identification was performed in the field by identification of hand specimens and field relationships. Standard thin sections of all the thirty two samples were made and used to identify minerals more closely examining mineral and reaction textures. This included 9 massif charnockites, 2 charnockitic gneisses, 5 mafic charnockite, 1 pegmatite from the quarry, 5 pink granites from Ayyarmalai, 3 grey granite, 2 dehydration veins occurring within the grey granite and 1 pegmatite samples from this area.

Quantitative analyses of the minerals were performed using polished thin sections of the main lithological types; garnet-rich charnockite, a hornblende-rich charnockite, the grey clinopyroxene-bearing granite and the pink alkali granite, were performed using Electron Microprobe CAMECA SX51 Electron Microprobe w SAMX Software housed at the University of Adelaide. The microprobe was calibrated to analyse minerals for the oxides Si, Mg, Fe, Ti, Al, Na, K, Ca, Mn, P, and also included F and Cl. This data was then recalculated using molecular weights of elements and minerals, the cation numbers as well as the oxygen numbers which then was used to calculate the cation quantities in the minerals. This determines the dominate end members involved in minerals occurring in these rocks.

4.1.1 Pressure-Temperature Estimates

Mineral chemistry data obtained from the Microprobe processes discussed above were used to input into a Plagioclase – Hornblende thermometry program to estimate pressure and temperature conditions. The procedure involves the input of the wt% chemistry of hornblende and plagioclase pairs assumed to be lying in equilibrium. Based on this information, this program provides a likely estimate based on a series of calculations to provide a constraint on temperature and pressure. Temperature estimates follow estimate procedures by Holland and Blundy, (1994); Blundy & Holland, (1990) while pressure estimates are given by Schmidt, (1992) and Anderson & Smith,

(1995). Given that hornblende and plagioclase are likely to be retrograde mineral features in these rock samples, the pressure-temperature conditions will only provide a minimum constraint on these estimates.

4.2. Whole Rock Major and Trace Elements

Analytical techniques and analysis for whole rock major and trace element concentrations were analysed at Amdel Bureau Vista. Thirty two samples were cleaned, jaw crushed and milled with a Tungsten Carbide mill into a very fine powder (<425 μm). Samples were sent to Amdel Bureau Vista, Thebarton, South Australia for analysis. Laboratories work to documented procedures in accordance to ISO 9001 Quality Management Systems standard. Three standard samples were analysed to ensure reproducibility of the study, which includes JG-3, BHN2A and MNT2A. Major elements analysed include; Al2O3 (0.01%), CaO (0.01%), Total Fe as Fe2O3 (0.01%), K2O (0.01%), MgO (0.01%), MnO (0.01%), Na2O (0.01%), P2O5 (0.01%), SiO2 (0.01%), TiO2 (0.005%) and Loss on Ignition (L.O.I).

4.2.1. Trace Elements

Six samples were also analysed to use more precise measurements used in isotopic calculations. Methods involved mixing approximately 10g of sample powder with 1ml of binder solution (Poly Vinyl Alcohol) and pressed to form a pellet. This was allowed to dry in air and was heated for a further 1 to 2 hours in a 60^{o}C oven to ensure that the pellet was completely dry before analysis. The samples were analysed using a Philips PW 1480 XRF Spectrometer, using several analysis programs covering suites of from 1 to 7 trace elements, with conditions optimised for the elements being analysed. The programs were calibrated against many (30 or more in some cases) local and international SRM's. The dual-anode Sc-Mo tube (operated at sufficient voltage to excite the Mo) and an Au tube were used for the analyses. Matrix corrections are made using either the Compton Scatter peak, or mass absorption coefficients calculated from the major element data. The extensive list of trace elements used in the analysis are reported in Table 2.

4.3. U-Pb Dating

Zircons obtained from samples SR-63, SR-6, SR-57 and SR-68H (see Table.1. for descriptions of samples), which involved garnet-rich and hornblende-rich charnockites, a clinopyroxene-bearing granite and a pink alkali granite from Ayyarmalai, were dated using U-Pb methods. Samples were washed, crushed with a dual jaw crusher and then separated with a meshed sieve to obtain a sand grain (79–300 μm) portion of the samples. Grains of zircons were obtained by panning out the heavy mineral portion of the grains and then scanned with a neodymium hand magnet to remove other minerals before being handpicked and mounted into epoxy resin blocks. These zircon mounts were then CL imaged using a Phillips XL-20 SEM with attached Gatan cathodoluminescence detector to determine and enhance any zonation or surface features of the zircon samples. U-Pb isotopic data were obtained using the Laser Ablation Inductively Coupled Plasma Mass Spectrometer (LA-ICPMS) in a He ablation atmosphere housed at the University of Adelaide. Standards Plesovich and BJWP (ca 720 Ma) were analysed simultaneously throughout the study to ensure reproducibility of the study. Laser pit diameter was 30 μm and analysed to a typical total depth of 40–50 μm.

U–Pb fractionation was corrected using the GEMOC GJ-1 zircon (TIMS normalisation data $^{207}Pb/^{206}Pb$ = 608.3 Ma, $^{206}Pb/^{238}U$ = 600.7 Ma and $^{207}Pb/^{235}U$ = 602.2 Ma (Jackson *et al.*, 2004). A number of zircon grains were excluded from analysis due to small size. Zircon cores larger than 40 μm in size were targeted, as well as some large metamorphic rims. In the data interpretation, a < 10% discordancy threshold was used for all grains analysed. Probability density plots have been constructed using Isoplot version 3.0 (Ludwig, 2003).

4.4. Whole Rock isotopic analyses

4.4.1 Radiogenic Isotopes

Analytical techniques and analyses for whole rock Sm–Nd isotopic data follow those of Payne *et al.* (2006) and were performed at the University of Adelaide. Seven samples; including 5 samples from Ayyarmalai, 1 blank sample and 1 standard sample (GSWP#2) were spiked with a ^{150}Nd–^{147}Sm

solution. HF was added to the sample in Teflon 'bombs' and evaporated. The samples were then oven-heated at 190°C for 5 days in HF in sealed Teflon bombs. The HF was then evaporated, with HNO_3 added shortly before samples were completely dry. 6 M HCl was added and samples were heated for 2 days at 160°C. REE were separated in Biorad Polyprep columns, and were further separated in HDEHP-impregnated Teflon-powder columns to isolate Sm and Nd. Nd was run on a Finnigan MAT 262 Thermal Ionisation Mass Spectrometer (TIMS) and Sm was run on a MAT 261 TIMS. The GSWP#2 standard gave a long term running average of 0.511834 ± 0.000018 (2σ, $n = 96$) and 0.512092 ± 0.000016 (2σ, $n = 164$) respectively. Epsilon values were calculated relative to a chondrite present day $^{143}Nd/^{144}Nd$ value of 0.512638 and $^{147}Sm/^{144}Nd$ value of 0.1966 (Goldstein *et al.*, 1984). Crustal residence ages relative to the depleted mantle (T_{DM}) assume present day $^{143}Nd/^{144}Nd$ value of 0.513114 and a $^{147}Sm/^{144}Nd$ DM value of 0.222 (REEs were separated in Biorad Polyprep columns again to further separate out Sr using the HDEHP-impregnated Teflon-powder columns to isolate Sr and Rb, which was dried and run on a Finnigan MAT 262 Thermal Ionisation Mass Spectrometer (TIMS). Pb was analysed using similar methods through separation with columns and run on the TIMS.

4.4.2. Stable Isotopes

Whole rock samples were analysed for oxygen isotopes by Professor Chris Harris at the University of Cape Town, Stable Isotope Laboratory. Powdered whole rock samples were weighed, approximately 10mg, and loaded into Ni reaction vessels and reacted with ClF_3 for > 3 hours. The O_2 gas produced was converted to CO_2 via a platinised carbon rod and yields of gas were measured to ensure that the reaction in each case was complete. The CO_2 gas was analysed using a Finnegan DeltaXP mass spectrometer in dual-inlet mode. Two aliquots of the internal standard MQ were analysed with each batch of 8 samples. The data for MQ were used to normalise the raw data to the SMOW scale. Further details of the analytical method can be found in Harris & Ashwal (2002). The $\delta^{18}O$ values are reported in table 3d**,** these values have been reported as delta values relative to SMOW (Standard mean ocean water). The equation (3), converts the measured isotope ratios to $\delta^{18}O$

values. A sample with a positive δ value is enriched in ^{18}O relative to SMOW and one with a negative value is depleted in ^{18}O relative to SMOW.

(3) $$\delta^{18}O = \left[\frac{(^{18}O/^{16}O)_{sam} - (^{18}O/^{16}O)_{SMOW}}{(^{18}O/^{16}O)_{SMOW}}\right] \times 10^3$$

5. RESULTS

5.1. Mineral Analysis

Representative mineral chemistry analyses are reported in Table 5a-f; the resulting oxide data has been converted to their relevant cation quantities for convenience. The analysis represents the dominant minerals from the main charnockite rock type assemblages; including a garnet rich charnockite (SR – 84) and a hornblende rich charnockite (SR – 57).

5.1.1. Ayyarmalai Charnockites

5.1.1.1. Garnet

Garnet porphyroblasts are quite variable in their chemistry (Table 5f). Garnets in the hornblende rich charnockite are dominantly enriched in almandine (Fe^{2+} rich garnet) and grossular (Ca rich Garnet), and to a lesser extent andradite (Fe^{3+} rich garnet) and spessartine (Mn rich garnet) i.e. $Alm_{52.61 - 60.78}$, $Grs_{11.2 - 34.4}$, $And_{4.3\text{-}22.4}$, $Sps_{1.5\text{-}14.3}$). Chemical zonations from core to rim appear to exist with enrichment of pyrope (Mg garnet) increasing towards the core i.e. Rim values X_{Mg} (1.2 – 3.33) to core values X_{Mg} (3.5 - 10.24). Other than that, there are no significant chemical zonations within the garnets and as well as this the various porphyroblasts have chemistry that is quite variable and inconsistent to be able to determine any definite zoning trends for this sample. Garnet porphyroblasts in the garnet rich charnockite are similar in composition to the hornblende rich charnockites with the exception of a higher concentration of pyrope.

5.1.1.2. Pyroxenes

Orthopyroxene and clinopyroxene are both present in the Ayyarmalai charnockites; with increased clinopyroxene occurring in the hornblende rich charnockites. The clinopyroxenes are associated with orthpyroxene sometimes preserved within orthopyroxene cores and others with ilmenite and ca-hornblendes. These clinopyroxenes are of the diopside-hedenburgite series and has lamellae textures when in the orthpyroxene cores. It is likely that the porphyroblastic clinopyroxenes were modified to diopside-hedenburgite by extensive fluid migration through the matrix. It can also be considered that the diopside-hedenburgite porphyroblasts with Ca-Al-amphibole cleavage overgrowths originally formed as a peak assemblage similar to that of the core clinopyroxenes but the composition was then altered during retrogression.

Orthopyroxene occurs as hypersthene (Fe,Mg rich) and is slightly enriched in Mn. Hypersthene in these charnockites occur in associate with hornblende, magnetite and ilmenite; more specifically hypersthenes rims ilmenite and sometimes magnetite. There is no evidence of chemical zonation from core to rim of hypersthenes porphyroblasts. Attempts to delineate whether orthopyroxene crystallised during igneous or metamorphic event in shown in Figure 6h; a plot with X_{Mg} vs X_{Al} of orthopyroxenes compiled from well known igneous and metamorphic charnockites which has indicated a differentiation trend (Santosh, 2010, submitted).

5.1.1.3. Retrograde Minerals (Amphibole, Plagioclase, Biotite, Symplectite)

Amphiboles are a retrograde mineral in the charnockite assemblage. These are enriched in calcium and aluminium with X_{Mg} varying from 0.08 – 0.24; which most likely resulted from the breakdown of clinopyroxene in the presence of garnet. The retrograde plagioclases associated with amphibole are enriched in albite ($Ab_{36.4-62.7}$; $An_{37.3-42.8}$) which complements the breakdown of Na-rich clinopyroxene with garnet. There is however no major chemical zonation existing from core to rim of hornblende and the chemical compositions are fairly consistent across both hornblende rich and garnet rich charnockite samples. Biotite occurs in close association on hornblende and generally symplectites

occur in partly as moats around hornblende- biotite clusters.

5.1.3. P-T estimate (Charnockite)

Hornblende-Plagioclase geothermometry provided a consistent pressure-temperature estimate likely to represent the retrograde conditions, at T= 745.1-754.3°C and P=5.61-5.38kbar using Andersons (1996) calculation format. This is a strictly minimum estimate given that hornblende and plagioclase are retrograde features in these assemblages.

5.2. Whole Rock Geochemistry

5.2.1. Ayyarmalai Charnockites

Representative geochemical data of all rock types in the Ayyarmalai area are reported in Table 1. Charnockite mineralogies include garnet-rich (SiO_2 53.9- 72.9%) and hornblende-rich (SiO_2 66.3 – 74.5%) which plot on the normative Ab-An-Or ternary diagram as quartz monzonites, while the mafic enclaves (SiO_2 – 45.1-57.6%) plot in the granodiorite field and the gneissic zones from the charnockite quarry (SiO_2-65.5-71.2%) in the granite field. With the variable silica contents, charnockites display (0.87-0.96) high Fe# (0.97-0.99), plotting as ferroan. In the Harker's binary diagram the major elements define linear trends (Fig. 5), and on the AFM triplot, trend from Calc-alkaline to tholeiitic in a straight line (Figure 6f) i.e. charnockites trend from Calc-alkaline to tholeiitic in a line, where the Ayyarmalai granite sits at the lowest part of the calc-alkaline field, then charnockites trend up in variably with the charnockitic gneisses into the tholeiitic field where it finishes with the restites.

With the exception of K_2O, concentrations for all major elements decrease with increasing silica for all the rock types. According to the ASI index (Figure 5j) the samples are divided into metaluminous and peraluminous varieties with the majority of the garnet rich charnockites plotting in the peraluminous field while the hornblende rich charnockites plot in the metaluminous field. These

charnockites plot in the Calc-alkalic to alkali-calcic field. They also plot in the A-type granitoid classification field.

Trace elements are also correlated with with SiO_2 (Figure 5k-r) for the variable charnockite varieties. Only Ba, La and Ce show notable scattering. The Ayyarmalai charnockite is rich in Ba and Sr, similar to high-Ba-Sr granitoids (Figure 6g; Rajesh & Santosh, 2004; Tarney & Jones, 1994). Ba contents and quite high (Ba 1500-2500ppm) while Sr is moderately low (Sr = 50-200ppm) whereas Ni and Cr contents are moderate (Ni = 7-19ppm and Cr = 10-40ppm). The Zr content is abnormally high (Zr = 300-2900ppm) with the very high Zr content existing in themafic enclaves. The REE contents are highly variable but generally characterized by high LREE contents (La_N= 367.85-59.95) and display a moderate to low fractionated REE patterns (La_N/Yb_N =25.06-4.3) and no to slightly positive Eu anomalies. Charnockites from Ayyarmalai show depletion in Ti, Sr and enrichment in Pb, Th and Zr when normalised to primitive mantle (Figure 7b). The charnockites fall in the high-k calc-alkaline to shonshonite series i.e. they are highly potassic. Shows chondrite normalised plot trending across the dehydration zone which indicates no significant change in elemental composition from the granite- to the dehydration zone and back into the granite.

5.2.2. Ayyaramalai Pink and Grey Granites

The pink and grey granitoids from the Ayyarmalai hill can be differentiated in mineralogy by the presence of clinopyroxene (diopside – hedenburgite) in the grey granite. Silica content varies from 73.9-77.8%, with high Fe# (0.97-0.99), plotting as ferroan higher than the charnockites (fig.5h) According to the AFM ternary diagram, the Ayyarmalai granitoids show a typical calc-alkaline differentiation trend (Fig.6f). The Ayyarmalai granites are fairly divided into metaluminous and peraluminous varieities, so this doesn't provide a distinct field. The MALI plot shows that the rocks from the Ayyarmalai area plot in the Calc-alkalic to alkali-calcic field (Figure 5i). They also plot in the A-type granitoid classification field (Figure 6e).

The Ayyarmalai granites are low in Ba and Sr, similar to low Ba-Sr granitoids (Figure 6g; Rajesh & Santosh, 2004; Tarney & Jones, 1994) granitoids. Ayyarmalai granites normalised to the bulk continental crust (Figure not shown) show small depletion anomalies in Ba and Nb, significant depletion anomalies in Cs, Sr and Ti and enrichment peaks at Rb and Th.

The REE patterns are moderately fractionated (La_N/Yb_N =20.05-6.01) which don't significantly differentiate them from the charnockites. When normalised to primitive mantle (Figure 7b), the alkali granites are highly depleted in Sr, P and Ti and enriched in Pb, Ba, Th and U. Trace element plots show some strong trends against silica, where Zr, Ti, mg# and Ni decrease with increasing silica content while Rb, A/CNK, K_2O/Na_2O increase with increasing silica (Figure 5k-v). The Ayyarmalai granite however shows LREE enrichment (La_N= 340 – 57.22), similar to the charnockites but does differ with a significant Eu depletion anomaly (Figure 7a).

5.3. U-Pb Zircon Geochronology

U-Pb analysis data has been presented in Table 4. Five different rock lithologies from Ayyarmalai were zircon dated using U-Pb methods including; hornblende rich charnockite (SR-57), garnet rich charnockite (SR-6), pink alkali granite (SR-68H), Grey granite (SR-63) and charnockitic Gneiss (SR-55).

5.3.1. Charnockite Zircons (SR-6 and SR-57)

All zircon grains from the charnockite from Ayyarmalai quarry range from 50 - 400µm in size, they are subrounded to prismatic shaped, some contain xenocrystic cores as well as zoned, unzoned (or very weakly zoned) grains and convolute chaotic core textures (Figure 4c-d). Cathodoluminescent (CL) images show that most of the zircon grains very chaotic textures display, typical granulite facies zircons (Pidgeon *et al.*, 2000). Some domains evolve as marginal bands and as lobes that locally penetrate the interior of grains, locally they also form amoebic zones entirely enclosed in the centre of the grains. Many of the cores are characterized by distinct oscillatory zoning resembling the former magmatic zircon (Fig 4c-d). Dark rims are found on some zircon grains, although these tend to

parallel the earlier more luminescent bands and are interpreted to represent the last phase of zircon growth rather than a younger phase of new zircon. The Th/U ratios of the zircons from charnockites are generally slightly higher in the cores (Th/U = ~0.2-0.6) while the rim overgrowths have lower ratios (Th/U = ~0.08 – 0.1). This indicates a low Th and high U (diagnostic of metamorphic overgrowths) in the rims whereas the high Th, low U contents are diagnostic of magmatic zircons (Hoskin & Schaltergger, 2003). The possibility of two events is consistent with the relatively high concentrations of U, low Th/U, and the structureless nature of the rims in these samples which is consistent with a metamorphic origin for the rims of zircon. As well as this, relatively low concentrations of U, high Th/U, and oscillatory zoning in the cores is consistent with a magmatic origin for the cores of the zircon grains.

The analysed cores from SR-57 (hornblende-rich charnockite) zircons provided an upper intercept age of 2652 ± 27 Ma and a lower intercept of 1151 ± 240Ma, MSWD = 3.5 (Figure 4d). The large overgrowths provided an upper intercept age of 2509 ± 40 Ma and a lower intercept age of 984 ± 430Ma, MSWD = 3.5. Therefore two Discordia lines are interpreted for the spread of data and this is well represented in the Concordia Diagrams (Fig 4d). Smearing of data between the two populations of zircons are a likely cause for the high MSWD error. The core ages range from 2.5 – 2.68 Ga with varying ages in the layers in the oscillatory zoning. The large span of ages of metamorphic zircons from 2.2 – 2.5 Ga indicates either a prolonged metamorphic event of significant Pb loss during metamorphism.

Analysed cores and rims from SR-6 (garnet rich charnockite) have provided only one Discordia line with an upper intercept age from the cores of the zircons being 2684 ± 36 Ma and a lower intercept age of 1584 ± 340 Ma, MSWD = 2.8 (Figure 4c). The overgrowth rim age could not be determined due to the high degree of metamictisation causing a high discordancy that was without the 10% threshold.

5.3.2. Ayyarmalai Granites (SR-68H and SR – 63)

All zircon grains from the charnockite from Ayyarmalai quarry range from 70 - 200μm in size and have subrounded to prismatic to pyramidal elongated shapes. CL images show some grains contain xenocrystic cores as well as zoned, unzoned (or very weakly zoned) grains and convolute chaotic core textures (fig 4a-b). Many of these zircons have complex oscillatory zoning at the cores while others display metamiticisation. Large highly luminescent rims exist around the cores. The Th/U ratios of the zircons from granites are generally slightly higher in the cores (Th/U = ~0.2-0.8) while the rim overgrowths have lower ratios (Th/U = ~0.2 – 0.3). This indicates a low Th and high U (diagnostic of metamorphic overgrowths) in the rims whereas the high Th, low U contents are diagnostic of magmatic zircons (Hoskin & Schaltergger, 2003), suggesting two separate events similar to the charnockite samples.

The analysed cores from SR-68H (Pink alkali granite) zircons provided an upper intercept age of 2638 ± 47 Ma and a lower intercept of 570 ± 1200Ma, MSWD = 3.5 (Figure 4b). The large overgrowths provided an upper intercept age of 2465 ± 56 Ma and a lower intercept age of 521 ± 1500Ma, MSWD = 4.0. Therefore two Discordia lines are interpreted for the spread of data and this is well represented in the Concordia Diagrams (Fig 4b).

The analysed cores from SR-63 (Grey granite) zircons provided an upper intercept age of 2677 ± 90 Ma and a lower intercept of 1351 ± 680Ma, MSWD = 8.4 (Figure 4b). The large overgrowths provided an upper intercept age of 2567 ± 37 Ma and a lower intercept age of 1112 ± 460Ma, MSWD =0.83. Therefore two Discordia lines are interpreted for the spread of data and this is well represented in the Concordia Diagrams (Fig 4b). Similarly to the charnockites there is a high degree of smearing of data between the two populations of zircons due to Pb loss in the older zircons during metamorphism; a likely cause for the high MSWD error. However, the most important feature is that both the granites and the charnockites contain similar core-rim structures, overgrowth patterns and ages.

5.4. Isotopic Data

5.4.1. Radiogenic Isotopes

Mineral-whole rock Sm-Nd, Rb-Sr and Pb-Pb dating of the charnockite from the Ayyarmalai location (Fig.1) is listed in table 3a-c respectively. Further additional samples are reported from other areas relating to Eastern Gondwana i.e. samples from Palghat-Cauvery Shear System, Southern Granulite Terrain, Northern Granulite Terrain, Dharwar Craton, Madagascar, Sri Lanka and East Antartica (See References in Tables 2a-b).

5.4.1.1. Sm-Nd

Three of the Ayyarmalai charnockite samples analysed (SR-1, SR-57 and SR-84) yielded εNd(0) values which range between -25.15 to -33.14. The two Ayyarmalai granite samples analysed (SR-68H and SR-861) also range from -25.15 – 32.4. The core ages represented in the zircons of these samples were around 2.65Ga while the metamorphic overgrowths are consistent with a granulite facies metamorphic that occurred in the NGT (~2.5 Ga) (Rajesh & Santosh, 2004; Rajesh, 2008). Therefore, the εNd(2.65 Ga) values of the charnockites range from -2.97 to -4.57 and εNd(2.5 Ga) range from -4.7 to -4.57 (Table 3a). The two alkali granite samples had ε_{Nd} (2.65 Ga) values range from -3.8 to -5.31, while the ε_{Nd}(2.5 Ga) range from -5.39 to -6.86. An errorchron age for the charnockites and granites combined of 2515 ± 620 Ma is calculated based on the Sm-Nd data (initial $^{143}Nd/^{144}Nd$ of 0.50910±0.00049, MSWD = 1.7) (Figure 9a). The $^{147}Sm/^{144}Nd$ ratios of all the samples lie within the range of 0.1081 – 0.134. Although the error is quite large, these points all lie in line with each other and correspond with the crystallisation ages of these rocks, indicating possible co-magmatism. The T_{DM} (Depleted Mantle) model ages range from 2890 – 3090Ma in these samples, ages significantly older than the crystallisation ages. Results are plotted in the ε_{Nd} evolution diagram (Figure 8a).

5.4.1.2. Rb-Sr

Obtained Rb-Sr data and calculations are reported in Table 2b on samples from Ayyarmalai. The calculation of the inital ratio ($^{87}Sr/^{86}Sr$) can be used to compare with the standard value of 0.706, a

number that represents that anything lower than this the rock was derived from partial melting of the mantle. Four samples from Ayyarmalai have initial ratios calculated at 2.5Ga of between 0.7019 and 0.7344. Sample SR-861 shows an impossible initial ratio of 0.5598 which is probably due to post Archaean alteration. An errorchron age for the charnockites of 2536 ± 1200 Ma is calculated based on the limited Sr-Rb data (Initial $^{87}Sr/^{86}Sr$ =0.7±1.5, MSWD = 11.7) (Figure 9b).

5.4.1.3. Pb-Pb

The $^{207}Pb/^{206}Pb$ isochron, reports an errorchron age of 3496±1100 Ma, MSWD = 4.3. This is significantly older than the predicted Nd model ages, therefore this age estimate has a significant error due to the limited number of samples analysed and the significant uranium loss that is likely to have occurred since the Archaean age.

5.4.2. Stable Isotopes

5.4.2.1.δ^{18} O isotopes

Whole-rock oxygen isotope analysis was performed on samples that were to represent a traverse from Hornblende rich charnockite – garnet rich charnockite – grey granite – dehydration zone – pink Ayyarmalai granite. The hornblende rich charnockites shows an abnormally low $\delta^{18}O$ value of -0.11 ‰, while the rest of the samples have increasingly higher $\delta^{18}O$ values, with none higher than 5.4%. The range of $\delta^{18}O$ values typical for igneous rocks like between +6 and 15%. Garnet rich charnockites have $\delta^{18}O$ values that lie closer in to the typical igneous rocks range, whereas the dehydration veins, granites and hornblende rich charnockite have very low $\delta^{18}O$ values. Low $\delta^{18}O$ values can indicate that these rocks crystallised from low $\delta^{18}O$ magma (Valley *et al.*, 1986; Taylor *et al.*, 1991; Hoefs, 1980), or most likely, the protolith had its $\delta^{18}O$ lowered by exchange with meteoric water prior to peak metamorphism. On determination of $\delta^{18}O$ of Quartz for three samples which are almost the same (slightly higher) than the whole rock values determine the samples were in O-isotope equilibrium at high-temperature. This suggests that the low $\delta^{18}O$ values were a part of the high-*T* mineral assemblage (Valley *et al.*, 1986; Taylor, 1987; Taylor *et al.*, 1991; Hoefs, 1980).

6. DISCUSSION

6.1. Petrographic & Geochemical Interpretation

Sampling for this study has essentially incorporated as many of the mineralogical varieties in the field area. Field and petrographic studies clearly delineate garnet-rich, intermediate hornblende-rich charnockites as well as low silica hornblende-rich mafic varieties within the Ayyarmalai charnockite massif. Based on the differences between the major and trace elements compositions, strong linear trends in harker diagrams and the REE patterns, the combined data suggests that the charnockites and alkali granites at Ayyarmalai formed from the same parent magma. This involves the mafic samples that trend down towards the intermediate charnockites and charnockite gneiss zones and finishes at the silica, K-rich granites. The low silica rocks have the highest REE but with no negative Eu anomaly and then progressively moving towards the alkali granite is the development of a significant Eu anomaly (Figure 7a). Given that these hornblende rich mafic samples have similar iron concentrations as the other samples (Figure 5b), low Cr, anomalously high Zr and occur as blocks/blebs within the charnockite quarry walls it's not likely that these mafic samples are derived from primitive mafic magma. One possibility of the origin of these mafic charnockites is that they are hornblende-pyroxene-Fe-Ti oxide-plagioclase adcumulates that when separated from the melt resulted in the intermediate charnockite composition this driving crystallisation towards the alkali granite. This is consistent with the nature of these mafic charnockites that is, brought out in blocks/blebs in the waxy green-grey homogenous charnockites. If this is the case, this would put the parent magma at a composition between the mafic cumulates and intermediate charnockites.

The dehydration zones in the grey granite at the western base of the pink alkali granite have almost identical geochemical (major and trace) concentrations as the grey granite. While several attempts were made to obtain the most representative samples in the area, no orthopyroxene was identified in these selvages. These dehydration veins contain a simple assemblage of quartz, plagioclase, feldspar (in the form of microcline) and ilmenite/magnetite. Unless non-sampled selvages exist in the field that contain orthopyroxene in their assemblages it suggests that these veins are not charnockites (or "incipient" charnockites representing an early stage of charnockite formation

initiated from movement of high pressure CO_2 rich fluids travelling through channels and fractures in the surrounding rock) and do not represent the generation of charnockites through metamorphic mechanisms. Interestingly, these selvages still encompass that waxy green-grey colour that is a feature of many charnockites. It is interesting to note that the waxy green colour was still produced regardless and deceptively looks almost identical to incipient charnockites such as at Kalbbadurga (Bhattacharya & Sen, 2000). This now requires thin section microscopy and mineral chemistry analysis to confirm in other cases whether orthopyroxene is present in these veins.

The other dominant feature of these charnockites and granites from Ayyarmalai is the alkali ferroan A-type signature that is widely report in the literature (Figure 6e) (Whalen *et al.*, 1987; Eby, 1990; Chappell & White, 1992; Frost *et al.*, 2001). A-type granitoids (i.e. anorogenic granitoids) are those that intrude into non-orogenic settings, are generally higher in SiO_2 (~77%), alkalis, Fe/Mg, halogens (F and Cl), REE, Ga/Al, Zr, Nb, Ga, Y and Ce and lower in trace elements compatible in mafics (Co, Cr, Ni) and feldspars (Ba, Sr) than I-types (Whalen *et al.*, 1987; Eby, 1990). However, post orogenic granitoid compositions range from strictly peraluminous S-types, to metaluminous I-types and hybrids, to those with A-type chemical characteristics; therefore the discriminate tectonic setting with A-type granitoids can be deceiving. The R_1-R_2 diagram plot shown in Figure 10, shows that the majority of the samples from Ayyarmalai share similarities with a post orogenic and syn-collision geodynamic setting. Though these samples from Ayyarmalai are regarded as A-type, within plate granites the geochemistry suggests that these may be ascribed to a post-orogenic geodynamic setting at the time of emplacement. Alternatively, a two stage melting model, involving basaltic underplating proposed by Rajesh (2008), can result in the formation of A-type calc-alkaline charnockite and alkali A-type granites from the Nilgiri and Madurai blocks. Trends in the geochemistry indicated in Figure 5, show some similarities with the Munnar granite from the Madurai Block which would make this model plausible.

This study favours the early crystallisation of orthopyroxene in granitic melts like charnockites and lacks metasomatic alteration. This is similar to cases when associated with anorthosites and mangerites within AMCG suites (Esmlie, 1991; Duchesne & Wilmart, 1997; Markl *et al.*, 1989).

Ayyarmalai is likely to exist as part of an AMCG suite and to determine this identification as well as collection of U-Pb zircon and monazite, Sm-Nd and geochemical data of anorthosites and mangerites surrounding Ayyarmalai would help find possible relationships.

6.2. Timing & Significance of Charnockite and Feslic Magmatism in the PCSS

Rocks from the PCSS have displayed multiple ages of 2.5 Ga, 1.8 Ga and 0.55 Ga. These have been attributed to date the crystallisation age, detrital zircons in metasediments and a metamorphic event respectively. The 0.55 Ga metamorphic event is widely reported in the literature as relating to the final stages of Gondwana accretion resulting in a granulite facies metamorphic event. The Ayyarmalai Pink Granite (2.67-2.63 Ga) has similar ages to the charnockite (i.e. 2.68-2.65 Ga) with the same overgrowth rims interpreted as the age of a granulite metamorphic event (2.45-2.5 Ga). This again indicates that these two rock types formed at the same time, again consistent with these rocks being co-magmatic. Curiously, the U-Pb zircon ages of the overgrowth rims suggest a granulite facies metamorphic event at 2.45-2.5 Ga. No evidence of the 0.55 Ga metamorphic event is evident in these Ayyarmalai A-type charnockites and alkali granites. Given this, Raith *et al.* (2010), recently presented U-Pb detrital zircon data from corundum bearing leucosomes from Kupprattipatti, west of Ayyarmalai. These detrital zircons had inherited concordant domains between 2502 and 1992Ma, a discordia with upper and lower intercept ages of 2481 ± 37 and 532 ± 63 Ma and a concordant age of 529 ± 9Ma. This presents a dilemma as to why the charnockites and granites from Ayyarmalai do not contain these Cambrian age overgrowths while leucosomes analysed at a small town only a few kilometres from Ayyarmalai do. Further zircon dating and structural mapping in the area would be required to better constrain the age of events and any structural barriers that occur between these areas.

The 2.45-2.5Ga metamorphic overgrowth rims do not correlate with ages in the SGT, however it does correlate with a widespread granulite thermal event synchronous with tectonism in the adjacent Salem Block (or NGT) occurring at 2.5-2.55Ga. The zircons from the charnockite and the pink granite

from Ayyarmalai also show very similar age structures to those from granites in the Madras, Salem & Nilgiri blocks, which are north of the PCSS. Most of these plutons have zircon core ages of 2.9 - 2.6Ga and are surrounded by metamorphic rims of 2.4-2.5Ga (Santosh *et al,* 2003; Vinogradov *et al,* 1964). Like the NGT, Ayyarmalai also lacks any of the Neoproterozoic-Cambrian metamorphic overgrowths (Clark *et al* 2009). This suggests that the NGT represents reworked Dharwar Craton as suggested in Collins *et al* (2010) or primary, late stage growth of the craton. Some U-Pb zircon data has suggested there may have been a metamorphic event dated at ~2.5Ga in the Dharwar Craton representing a magmatic event dominated by voluminous granite magmatism. The Ayyarmalai Pink granite displays similar geochemical and petrological characteristics of late Neoproterozoic granites, however, these geochronological results conclusively show them to be Archaean. Consideration of a late Archaean magmatic and tectonic event in the Dharwar craton has been explained by a rising megaplume that produced such granitoids as the Closepet and Bangalore Granitoids (Peucat *et al*, 1993; Choukroune *et al.*, 1995). Given that samples from Ayyarmalai display similar geochemical characteristics with the Dharwar craton rather than the SGT this origin needs to be considered. This involves a rising plume into a mature crust which causes softening in the crust, inverse diapirism and thus induces metamorphism. However, there are certain features of a plume that are inconsistent with observations from Ayyarmalai data. For instance, plume magmatism has been known to display more juvenile Nd magmatic signatures (sometimes with small crustal signatures) and the results from Ayyarmalai suggest a much evolved source with a large crustal input. This is illustrated in the Closepet and Bangalore Granitoids and on comparison between the isotopic compositions between them and Ayyarmalai; the granitoids do not appear to be correlated. As well as these differences in composition between the two rock types at Ayyarmalai lying in such close association is unlikely to occur, whereby a plume might produce a much more homogeneous rock type over a larger area. Therefore, a plume model in the case of Ayyarmalai appears to be unlikely.

The other possibility in relation to the ages obtained from granites within the PCSS relates to the evolution of Gondwana. As Gondwana formed, the Mozambique Ocean closed and its suture was identified in Madagascar, known as the Betsimisaraka suture (Collins & Windley, 2002; Collins *et al.*,

2007). Collins *et al* (2007) suggested that the PCSS is an ideal candidate for the continuation of this suture due to the correlation of tectonic units; however this is still often disputed (Shackleton, 1996; Collins & Windley, 2002; Meert, 2003). The Cambrian metamorphic ages (~500 Ma) found in several places along the PCSS also exist along the Betsimisiraka suture belt (Collins *et al.*, 2003); suggested to correspond with the closure of the ocean and subsequent collision of India with Azania (called the Malagasy Orogeny ~540-520Ma) (Collins & Pisarevsky, 2005). Collins *et al* (2002) suggested that the Antananarivo block of Madagascar, south of the Betsimisiraka suture has <2.6 Ga rocks exposed which may correlate with rocks from the Madurai Block, the Karur-Kambam-Painavu-Trichur shear zone (KKPT) and PCSS. The Antananrivo Block is separated from the Antongil Block (suspected to be the Dharwar craton) by a paragneiss belt that is highly deformed and contains ultramafics and some Neoproterozoic sediments (Collins *et al*, 2002; Collins & Windley, 2006). If samples from Ayyarmalai did strongly correlate with those from the Antananarivo block, it would suggest that the microcontinent Azania extends to encompass these areas. It would also suggest that there is possibly a belt of pre-Neoproterozoic crust that extends from the northern Madurai Block (separated from metamorphosed Dharwar craton by the PCSS) that extends through the Antananarivo Block. Given that charnockites and granites from Ayyarmalai do not contain evidence of the Neoproterozoic-Cambrian metamorphic age Andean-style plate boundary, it may also suggest that the suture zone actually cuts south of the PCSS and that this shear zone represents the northern limit of the Neoproterozoic and early Cambrian magmatism, metamorphism and orogenesis.

6.3. Protolith and Crustal Evolution in the PCSS

In discussion of the reconstruction of eastern Gondwana, it is important to compare the isotopic composition of the Ayyarmalai charnockites and granites with potentially adjacent terrains in the supercontinent. As Pb data are scare and Rb-Sr is highly sensitive to fractionation, Sm-Nd isotope data presented in this study are compared with data from the Dharwar Craton, NGT, PCSS, SGT, East Antarctica, Sri Lanka and Madagascar (Table 3a; Figure 8a).

The charnockites and granites from Ayyarmalai have model ages between 2.8 – 3.09Ga, ages that are slightly older than their crystallisation ages. The proposition that the charnockites and granites are co-magmatic are confirmed by the similar model ages which clearly verify the crystallisation ages (Figure 9a). The negative εNd(t) values (between -4.7 to -6.86) and older Archaean T_{DM} model ages suggest that these rocks could be generated (i) either by melting of a contaminated depleted mantle source; (ii) by melting of an enriched mantle source (not solely derived from depleted mantle and are likely to be contaminated), or (iii) through contamination of mafic magmas from the depleted mantle and contamination by crust with older T_{DM} values (>2.8-3.09 Ga). Figure 8a indicates that the charnockites and granites from Ayyarmalai correlate with charnockites from the NGT given the similar Nd characteristics and zircon U-Pb crystallisation ages (Bhaskar Rao *et al.*, 2003; Meiβner *et al*, 2002); however these samples have a more juvenile magma input. As well as this, Figure 8; 9d, suggests that the rocks from Ayyarmalai fall in the field of TTG basement of the Dharwar craton which suggests a possible source of crustal contamination. The samples also closely relate to the ~2.55 Ga granites that intruded the Dharwar craton i.e. Late Archaean K-granites from the AB suite, Bangalore granites and some TTG gneisses (Jayananda *et al.*, 2000; Rickers *et al.*, 2001). Based on limited published data of basement gneiss in the Antananarivo block, the data suggests that this is not a likely source for crustal contamination of the Ayyarmalai samples (Kroener, 2000). This further supports the possibility that the Ayyarmalai consists of metamorphosed Dharwar Craton. Given Sm-Nd data is limited in the Antananarivo block; further data collection would prove beneficial to support this theory.

The granite samples from Ayyarmalai analysed for $\delta^{18}O$ could indicate features about the type of magma these rocks crystallised from. Granites that exhibit near-equilibrium oxygen isotope fractionations for constituent minerals are characterized by magmatic O-isotopic compositions (~+6-8‰), however this is not the case with the Ayyarmalai granitoids as they are lower than the magmatic compositions. The Ayyarmalai granitoids all have low $\delta^{18}O$ whole rock values of –0.11 to +4.4 indicating contamination with reworked sediments that are mixed with meteoric water (not a viable mechanism on mass balance grounds). However, given the high amount of crustal contamination in

these rocks of Archaean age (T_{DM} model ages of 2.7-3.04 Ga), this may suggest that the low $\delta^{18}O$ source comes from the Archaean crustal block that the magma intruded and mixed with. The suggestion from this study that the intermediate charnockite crystallised orthopyroxene early is favoured by contamination of mafic mantle derived melts with siliceous crustal rocks; these values are supported by the $\delta^{18}O$ values. In this case, possible scenarios include involvement from the Dharwar Craton as suspected in this study as the crustal contamination source given its similar protolith age. Alternatively, this signature may be related to the Antananarivo Block of Madagascar where it is proposed that the Betsimisiraka Suture zone just above the Antananarivo Block is a continuation of the Palghat-Cauvery Shear System in which where these samples were taken (Figure 11; Collins & Windley, 2002; Collins *et al.* 2007). However, the Nd model ages of Ayyarmalai do not appear to correlate with the Antananarivo Block but instead do correlate with the adjacent Northern Granulite Terrain and average Dharwar Craton basement.

Low $\delta^{18}O$ values have been widely associated with subsolidus hydrothermal alteration for several igneous rocks worldwide (Criss & Taylor 1986; Harris & Ashwal, 2002). Granites that exhibit near-equilibrium oxygen isotope fractionations for constituent minerals are characterized by magmatic O-isotopic compositions (~+7‰), however this is not the case with the Ayyarmalai granitoids as they are lower than the magmatic compositions (Valley *et al.*, 1986; Taylor, 1987; Taylor *et al.*, 1991; Hoefs, 1980). The Ayyarmalai granitoids all have quite low $\delta^{18}O$ whole rock values of –0.11 to +4.4. It is therefore necessary to establish whether the low $\delta^{18}O$ values of the A-type Ayyarmalai charnockites and granites reflect the composition of the original magmas, or result from subsequent fluid–rock interaction. To establish this, it is rendered necessary to analyse the $\delta^{18}O$ of separated minerals (not analysed in this study) from the samples to determine equilibrium; this would indicate if in fact the magma had the low $\delta^{18}O$ signature. In this case, low $\delta^{18}O$ values imply that either this is a characteristic of the source, was acquired during the evolution of the magma or was created through mixing with or assimilation of material that contained very low $\delta^{18}O$ values (Harris & Ashwal, 2002). A likely scenario for these rocks would be a large high-temperature exchange with water at some stage in the protolith history, or sometime prior to peak metamorphism.

Given the limited extent of oxygen isotope data obtained from adjacent terranes, it would be useful for future research to compare this data with whole rock and mineral oxygen isotope data collected from the Dharwar craton, the Southern Indian Granulite Terrain and the Antananarivo and Antongil blocks of Madagascar.

7. CONCLUSION

Several interesting conclusions can be made about the evolution of the Ayyarmalai A-type charnockite-granite association:

(1) The crystallisation age of the charnockites (2.68-2.64Ga) and granites (2.63-2.67Ga) from the south eastern PCSS are Archaean and depict a granulite facies metamorphic event occurring at 2.45-2.5Ga.

(2) Strong co-linear trends in Harker diagrams, similar Nd model ages and U-Pb zircon ages and Nd errorchrons strongly suggest that the Ayyarmalai A-type Charnockite-Granite have experienced the same Nd evolution history and are co-magmatic.

(3) The lack of orthopyroxene in the dehydration zones would suggest that the Ayyarmalai charnockites were not generated from CO_2 fluxing, and thus favours early crystallisation of orthopyroxene.

(4) Nd isotopic values suggest the protolith is late Archaean in age (2.9-3.09 Ga) which have similarities with isotopic data from Dharwar Craton. However, similarities also exist with the Antananrivo Block of central Madagascar that was suggested as an extension of the Madurai Block by Collins *et al.* (2007).

(5) Oxygen isotopic data suggests that the protolith had its $\delta^{18}O$ lowered by exchange with meteoric water prior to peak metamorphism.

(6) Geochemistry suggests a late syn to post tectonic setting (possibly post collisional). A two stage model of basaltic underplating combined fractional crystallisation with partial crystallisation may account for the varying compositions at Ayyarmalai.

8. ACKNOWLEDGMENTS

I would like to thank the Australian Government for supporting this work through an Australia-India Strategic Research Fund Grant. A huge thank you to my supervisors John Foden and Alan Collins for your endless knowledge and wisdom on the subject of rocks. Many thanks to Santosh and Chetty for the most welcomed assistance and hospitality in India and Alan for ensuring a smooth transition into a new country (and putting up with my inability to tolerate chilli). Thank you to William Teale and Vaddi Venkatasivappa for being my main field buddies and also Diana, Jade, Libby and Mohanty (India wouldn't have been the same without you guys). A massive thank you to Professor Chris Harris from the University of Cape Town for your valuable assistance with analysing my samples at short notice for oxygen isotopes and even when they couldn't be done in time still did them in the name of science. Your knowledge and wisdom on the topic was greatly valued and appreciated. Thank you to Justin Payne and Ben Wade for all the help and guidance in the labs. Finally, thanks to all the honours students, what a great year!

9. REFERENCES

ANANTHA IYER, G.V. & NARAYANAN KUTTY, T.R., 1978. Geochemical comparison of Archaean granulites in India with Proterozoic granulites in Canada. Developments in Precambrian Geology, 1, 269-288

ANDERSON, J.L., SMITH, D.R., 1995, The effect of temperature and oxygen fugacity on Al-in hornblende barometry. AM mineral 80, 549-59.

BALASURBRAHMAYAN, M.N., 2006, Geology and Tectonics of India: An Overview, *International Associated for Gondwana Research,* Memoir no. 9, p. 39-45.

BARROS, C.E.M., DALL'AGNOL, R., BARBAY, P., BOULLIER, A., 1997. Geochemistry of the Estrela Granite Complex, Carajás region, Brazil: an example of an Archaean A-type granitoid, *Journal of South American Earth Sciences,* 10 (3-4), 323-330.

BARTLETT J.M., DOUGHERTY-PAGE, J.S., HARRIS, N.B.W., HAWKESWORTH, C.J. and SANTOSH, M., 1998. The application of single zircon evaporation and model Nd ages to the

interpretation of polymetamorphic terrains: an example from the Proterozoic mobile belt of south India. Contributions to Mineralogy and Petrology, 131: 181-195.

BECKINSALE , R.D., *1980*. Granite magmatism in the tin belt of southeast Asia. In: M.P. Atherton and J. Tarney (Editors), Origin of Granite Batholiths, Geochemical Evidence Shiva Publishing Ltd, London (1980), *pp*. 34--44.

BHATTACHARYA, S., SEN, S.K., 2000, New insights into the Origin of Kabbaldurga Charnockites, Karnataka, South India. *Gondwana Research,* 3 (4), 489-506.

BHASKAR RAO, Y.J., JANARDHAN, A.S., VIYAYA KUMAR, T., NARAYANA, B.L., DAYALl, A.M., TAYLOR, P.N. and CHETTY, T.R.K., 2003. Sm-Nd Model Ages and Rb-Sr Isotopic Systematics of Charnockites and Gneisses across the Cauvery Shear Zone, Southern India: Implications for the Archaean - Neoproterozoic Terrane Boundary in the Southern Granulite Terrain. Memoir Geological Society of India, 50: 297-317.

BHASKAR RAO, T., TOMSON, J.K., VIJAYA KUMAR, V. J., MALIKHARJUNA RAO, J., 2006. Charnockite genesis across the Archaean–Proterozoic terrane boundary in the South Indian Granulite Terrain: Constraints from major–trace element geochemistry and Sr–Nd isotopic systematics, Gondwana Research 10, 115–127

BLUNDAY, J.X., HOLLAND, T.J., 1990, Calcic ampbiole equilibrian and a new amhinole-plagioclase geothermometer. Contrib Mineral Petrol, 104, 208-24.

BRADSHAW, J.Y., 1989. Early Cretaceous vein related garnet granulite in Fiorland, southwest New Zealand: a case for infiltration of mantle derived CO_2 rich fluids. *J Geol,* 97, 697-717.

BRANDON, A. D., and MEEN K. 1995. Nd isotopic evidence for the position of southernmost Indian terranes within East Gondwana. *Precambrian Res.* 70:269-280.

BRAUN, I., KREIGSMAN, L.M., 2003. Proterozoic crustal evolution of the southernmost India and Sri Lanka. In: M. Yoshida, B.F. Windley and S Dasqupta (Editors), Proterozoic East Gondwana: Supercontinent Assembly and Breakup. *Geological Society*, London, Special Publications, London, 169-202.

BUHL, D, GRAUERT, R, RAITH, M, 1983. U–Pb zircon dating of Archean rocks from the South Indian Craton: results from the amphibolite to granulite facies transition zone at Kabbal Quarry, southern Karnataka. Fortschr Mineral 61:43–45

CENKI, B. & KREIGSMAN, L.M., 2005. Tectonics of the Neoproterozoic southern granulite terrain south India. *Precambrian Research*, 138, 337-356.

CHADWICK, B., VASUDEV, V.N., HEDGE, G.V., 2000. The Dharwar Craton, southern India, interpretated as the result of Late Archaean oblique convergence. *Precambrian Research*, 99, 91-111.

CHAPPELL, B.W., WHITE, A.J.R., 1974. Two contrasting granite types. Pacific Geology 8, 173–174.

CHETTY, T.R., RAO, B. & Y.J, 2006. Strain pattern and deformational history in the eastern part of the Cauvery shear zone, southern India. *J. Asian Earth Science*, 28, 46-54.

CHOUNDHARY, A.K., HARRIS, N.B.W, VAN CALSTEREN, P., HAWKESWORTH, C.J., 1992. Pan African charnockite formation in Kerala, South India, Geol Mag, 129, 257-264.

CLARK, C., COLLINS. A.S., TIMMS, N.E., KINNY, P.D., CHETTY, T.R.K, SANTOSH, M., 2009a. SHRIMP U-Pb age constraints on magmatism and high grade metamorphism in the salem block, southern India. *Gondwana Research*, 16, 27-36.

CLARK, C., COLLINS, A.C., SANTOSH, M., TAYLOR, R., WADE, B.P., 2009b. The *P-T*-t architecture of a Gonwana suture: REE, U-Pb and Ti-in-zircon thermometric contrsaints from the Palghat Cauvery Shear System, South India, *Precam. Res,* 174, 129-144.

COLLINS, A.S. & PISAREVSKY, S.A., 2005. Amalgamating eastern Gondwana: The evolution of the Circum-Indian Orogens. *Earth-Science Reviews*, 71(3-4), 229-270.

COLLINS, A.S., CLARK, C., SAJEEV, K., SANTOSH., KELSEY, D.E., HAND, M., 2007a. Passage through India : the Mozambique Ocean suture , high-pressure granulites and the Palghat-Cauvery shear zone system. *Terra*, 141-147.

COLLINS, A.S., SANTOSH, M., BRAUN, I., CLARK, C., 2007b. Age and sedimentart provenance of the southern granulites, Southern India,: U-Th-Pb SHRIMP secondary ion mass spectrometry, *Precambrian Research,* 155, 125-138.

COLLINS, A.C., WINDLEY, B.F., 2002. The tectonic evolution of central and northern Madagascar and its place in the final assembly of Gondwana. *Journal of Geology,* 110 (2), 325-339.

COLLINS, A.C., CLARK, C., CHETTY, A.R.K, SANTOSH, M., 2010. Geodynamic Regimes, Global Tectonics and Evolution of Precambrian Cratonic Basins in India, Indian Journal of Geology, Vol.80, Nos. 1-4, (2008) p.23-40

CONDIE, K.C., BOWLING, G.P., ALLEN, P., 1985. Missing Eu anomaly and Archaean high-grade granites, *Geology,* 13, 633-636.

CONDIE, K.C., BOWLING, G.P., ALLEN, P., 1986. Origin of granites in an Archaean high-grade terrane, southern India, *Contrib Mineral Petrol,* 92:93-103.

CRISS, R.E, TAYLOR H.P Jr ,1986. Meteoric–hydrothermal systems. In: Valley JW, Taylor HP Jr, O'Neil JR (eds) Stable isotopes in high-temperature geological processes. *Mineral Soc Am*, Rev Mineral 16:373–424

DOBMEIER, C., RAITH, M., 2000. On the origin of 'arrested' charnockitization in the Chilka Lake area, Eastern Ghats Belt, India: a reappraisal, *Geol Mag.,* 137, 27-37.

DRURY, S.A. and HOLT, R.W., 1980. The tectonic framework of the south Indian craton: A reconnaissance involving Landsat imagery. Tectonophysics, 65: T1-T15.

DUCHESNE, J-C., WILMART, E., 1997. Igneous charnockites and related rocks from the Bjerkreim-Sokndal layered intrusion (southweat Norway):a jotunite (hypersthenes monzodiorite)-derived A-type granitoid suite. *J Petrol,* 38, 337-369.

EBY, G.N., 1990. The A-type granitoids: a review of their occurrence and chemical characteristics and speculations on their petrogenesis. Lithos 26, 115–134.

EMSLIE, R. F. & HUNT, P. A., 1990. Ages and petrogenetic significance of igneous mangerite-charnockite suites associated with massif anorthosites, Grenville Province, Canada, *J Geology*, 98,pp. 213-231.

FIELD, S.A., DRURY, S.A., COOPER, D.C., Rare-earth and LIL fractionation in high-grade charnockitic gneisses, south Norway. *Lithos* 13:281-289.

FOWLER, T.J., 2001. Pan-African granite emplacement mechanism in the Eastern Desert, Egypt. *Journal of African Earth Sciences,* 32 (1), 61-85.

FRIEND, C.R.L., 1981, Charnockite and Granite formation and influx of Co2 at Kabaldurga, Nature, Vol. 294.

FROST, B.R., FROST, C.D., 1987. CO_2 melts, and granulite metamorphism. *Nature,* 327, 503-506.

FROST, B.R. & FROST, C.D., 2008. On charnockites. *Gondwana Research*, 13, 30 - 44.

FROST, B.R., BARNES, C.G., COLLINS, W.J., ARCULUS, R.J., ELLIS, D.J., FROST, C.D., 2001, A Geochemical Classification for Granitic Rocks, *Journal of Petrology,* 42, 11, p. 2033

GHOSH, J.G., DE WIT, M.J., ZARTMAN, R.E., 2004. Age and tectonic evolution of Neoproterozoic ductile shear zones in the Southern Granulite Terrain of India, with implications for Gondwana studies, *Tectonics,* 23.

GOLDSTEIN, S., O'NOINS, R.K., HAMILTON, P.J., 1984. A Sm-Nd isotopic study of atmospheric dusts and particulates from major river systems. Earth and Planetary Science Letters, 70: 221-236.

HARRIS, N.B.W., SANTOSH, M. and TAYLOR, P.N., 1994. Crustal Evolution in South India: Constraints from Nd Isotopes. The Journal of Geology, 102: 139-150.

HARRIS, C., ERLANK, A.J., 1992. The production of large-volume, lowdelta 18O rhyolites rifting of Africa and Antarctica; the Lebombo Monocline, Southern Africa. *Geochim Cosmochim Acta* 56:3561–3570

HARRIS, C., ASHWAL, L.D., 2002.The origin of low d18O granites and related rocks from the Seychelles, Contrib Mineral Petrol, 143: 366–376.

HANSEN, E.C., NEWTON, R.C., JANARDHAN, A.S., 1984. Fluid inclusions inrocks from the amphibolites facies gneiss to charnockite progression in southern Karnataka, India:direct evidence concerning the fluids of granulite metamorphism. *Journal of Met. Geology,* 2, 249-264.

HANSEN, E.C., JANARDHAN, A.S., NEWTON, R.C., PRAME, W.K.B.N., RAVINDRA KUMAR, G.R., 1987. Arrested charnockite formation in southern india and Sri Lanka. *Contrib Mineral Petrol,* 96, 225-244.

HASLAM, H.W., 1989. Charnockites at Mchinji, Malawi: the nature and origin of igneous charnockites. *Journal of African Earth Sciences,* 8 (1), 11-18.

HOEFS, J., 1980.Stable Isotope Geochemistry. Springer verlag Berline.

HOLLAND, T.M., 1900. The charnockite series, a group of Archaean hypsthenic rocks in Peninsula India. Mem. Geol. Surv. India 28, 119-249.

HOLLAND, T. & BLUNDY, J. 1994. Non-ideal interactions in calcic amphiboles and their bearing on amphibole-plagioclase thermometry. CONTRIB MINERAL PETROL 116, 433-47

HOSKIN, P.W.O, SCHALTEGGER, U., 2003. The composition of zircon and igneous and metamorphic petrogenesis. *Rev Mineral Geochem*, 53, 27-62.

JACKSON, S.E., PEARSON, N.J., GRIFFIN, W.L., BELOUSOVA, E.A., 2004. The application of laser ablation-inductively coupled plasma-mass spectrometry to in situ U/Pb zircon geochronology. Chemical Geology, 211(1-2): 47-69.

JANARDHAN, A.S., NEWTON, R.C, HANSEN , E.C., 1982. The Transformation of Amphibolite Facies Gneiss to Charnockite in Southern Karnataka and Northern Tamil Nadu, Contrib Mineral Petrol, 79:13~149 India

JANASI, V.D.A., 2002, Elemental and Sr-Nd isotope geochemistry of two Neoproterozoic mangerite suites in SE Brazil: implications for the origin of the mangerite – charnockite - granite series, *Precambrian Research,* 119, 301-327.

JAYANANDA, M., JANARDHAN, A.S., SICASUBRAMANIAN, P. and PEUCATt, J.J., 1995. Geochronological and isotopic constraints on granulite formation in the Kodaikanal area, southern India. Memoir Geological Society of India, 34: 373-390.

JAYANANDA, M., MOYEN, J.F., MARTIN, H., PEUCAT, J.J., AUVRAY, B., MAHABALESWAR, B., 2000. Late Archaean (2550-2520Ma) juvenile magmatism in the Eastern Dharwar craton, southern India: constraints from geochronology, Nd-Sr isotopes and whole rock geochemistry. *Precambrian Research*, 99, 225-254.

JAYANANDA, M., CHARDON, D., PEUCAT, J.-J., CAPDEVILA, R., 2006. 2.61 Ga potassicgranites and crustal reworking in the western Dharwar craton, south India: tectonic, geochronologic and geochemical constraints. Precambrian Research 150, 1–26.

KAIYI, W., YUEHUA, Y., RUIYING, Y., YIFEI,C., 1985. REE Geochemistry of early Precambrian charnockites and tonalitic-granodioritic gneisses of the Qianan reigon, Eastern Hebei, North China, *Precambrian Research,* 27, 63-84.

KRONER, A., ,HEGNER, E., COLLINS, A.S, WINDLEY, B.F., BREWER, T., RAZAKAMANANA, T., PIDGEON, R.T., Age and magmatic history of the Antananarivo block, central Madagascar, as derived from zircon geochronology and Nd isotopic systematic , American J. Sci, 300, 251–288

KILPATRICK, J.A., ELLISA, D.J., 1992. C-type magmas: igneous charnockites and their extrusive equivalents. Transactions of the Royal Society of Edinburgh. Earth Sciences 83, 155–164.

LADENBERGER, B., and COLLINS, W.J., 1996. Derivation of A-type Granites from a dehydrated charnockitic lower crust: vidence fromthe Chaelundi Complex, Eastern Australia, *Journal of Petrology,* 37 (1), 145-170.

LE MAITRE, RW (ed)., 2002. Igneous rocks: A classification and glossary of terms, *Cambridge University Press*.

LUDWIG, K.R., 2003. Users manual for Isoplot/Ex, version 3.00, A Geochronological Toolkit for Microsoft Excel. Berkeley Geochronology Centre, Berkeley, CA.

MARKL, G., FROST, B.R., BUCHER, K., 1989. The origin of anorthosites and related rocks from the Lofoten Islands, Northern Norway: I. Field relations and estimation of intrinsic variables. Journal of Petrology 39, 1425–1452.

MARTIGNOLE, J., 1979. Charnockite genesis and the proterozoic crust, *Museum*, 9, 303-310.

MARTIGNOLE, J., STEVENSON, R. & MARTELAT, J., 2005. A Grenvillian anorthosite-mangerite-charnockite-granite suite in the basement of the Andes : The Ilo AMCG suite (southern Peru). *Symposium A Quarterly Journal In Modern Foreign Literatures*, 481-484.

MCLELLAND, J.M., Shrimp II Geochronology of the Adriondack AMCG Suite II: Granitoids, Gabbros and Cross curtting Dikes. *Geology Society of America,* Abstracts with Programs, 34 (6), 241.

MEERT, J.., 2003. A synopsis of events rela- ted to the assembly of eastern Gondw- ana. Tectonophysics, 362, 1–40.

MEIβNER, B., DETERS, P., SRIKANTAPPA, C., KOHLER, H., 2002. Geochronological evolution of the Moyar, Bhavani and Palghat shear zones of southern India: implications for east Gondwana correlations. Precambrian Research, 114: 149-175.

MILLER, J.S., SANTOSH, M., PRESSLEY, R.A., CLEMENTS, A.S., ROGERS, J.J.W., 1996. A Pan-African thermal event in southern India, *Journal of Southeast Asian Earth Sciences,*14(3/4), 127-136.

MOHAN, A., JAYANANDA, M., 1999. Metamorphism and Isotopic Evolution of Granulites of Southern India: Reference to Neoproterozoic Crustal Evolution. *Gondwana Research,* 2 (2): 251 – 262.

MUNASINGHE, T. and DISAANAYAK, C.B., 1980. Are Charnockites metamorphosed Archaean volcanic rocks? A case study from Sri Lanka, *Precambrian Research,* 12, 459-470.

NAHA, K., SRINIVASAN, R., JAYARAM, S., 1993. Structural relations of charnockites of the Archean Dharwar Craton, Southern India, *Journal of Metamorphic Geology,* 11, 889-895.

NESBITT, H.W., 1980. Genesis of the New Quebec and Adirondack granu- Iites: evidence for their production by partial melting. *Contrib Mineral Petrol,* 72:303-310.

NEWTON, R.C., 1989. Metamorphic fluids in the deep crust, *Annual Review Earth and Planetary Sciences* 17, 385–412.

NEWTON, R.C., 1992. An overview of charnockite. *Precambrian Res*, 55, 399-405

ROGERS, J.J.W., 1986. The Dharwar Craton and the assembly of peninsular India. *J Geol,* 94, 129-144.

PAYNE, J., BAROVICH, K., HAND, M., 2006., Provenance of metasedimentary rocks in the northern Gawler Craton, Australia: Implications for Palaeoproterozoic reconstructions, Precambrian Research 148 (2006) 275–291

PETERSON, J. S. 1980: The zoned Kleivan granite - an end member of the anorthosite suite in southwest Norway. *Lithos 13,* 79-95. Oslo.

PERCHUK, L.L., SAFONOV, O.G., GERYA, T.V., FU, B., HARLOV, D.E., 2000. Mobility of components in metasomatic transformation and partial melting of gneisses: an examples from Sri Lanka. *Contrib Mineral Petrol,* 140, 212-232.

PEUCAT, J.J., VIDAL, P., BERNARD-GRIFFITHS, J., CONDIE, K.C., 1989. Sr, Nd and Pb Isotopic systematic in the Archaean Low – to High grade Transition zone of Southern India: Syn-Accretion vs Post Accretion Granulites. *Journal of Geology,* 97 (5): 537 – 549.

PRESS, C., 2010. Ultrahigh-Temperature NOTES in Madurai Granulites , Metamorphism Southern India : Evidence from Carbon Isotope Thermometry. *Carbon*, 108(4), 479-486.

PICHAMUTHU, C S, 1969, Nomenclature of charnockites. *Indian Mineralogist, 10,* 23-35.

PITCHER, W.S., 1982. Granite type and tectonic environment. In: Hsu, K.J. (Ed.), Mountain Building Process. *Academic Press*, London, pp. 19–40.

PLA CID, J., NARDI, L.V.S., CONCEICAO, H., BONIN, B., 2001. Anorogenic alkaline granites from northeastern Brazil: major, trace and rare earth elements in magmatic and metamorphic biotite and Ma-mafic minerals. *Journal of Asian Earth Sciences,* 19, 375-397.

PRIDE, C. and MUECKE, G.K., 1982. Geochemistry and origin of granitic rocks, Scourian Complex, NW Scot- land. Contrib. Mineral. Petrol., 80: 379-385.

RAITH, H.M, SRIKANTAPPA, C., 1993. Arrested charnockite formation at Kottavattom, Southern India. *Journal of Metamorphic Geology,* 11, 815-832.

RAITH, M.; KARMAKAR, S..BROWN, M. 1997. Ultra-high- temperature metamorphism and multistage decom- pressional evolution of sapphirine granulites from the Palni Hill ranges, southern India. J. Metamorph. Geol. 15:379-399.

RAITH, M.M., SENGUPTA, P., KOOIJMAN, E., UPADHYAY, D., SRIKANTAPPA, C., 2010. Corundum-leucosome-bearing aluminous gneiss from Ayyarmalai, Southern Granulite Terrain, India: A textbook example of vapour phase-absent muscovite-melting in silica-undersaturated aluminous rocks. *American Mineralogist,* 95, 897-907.

RAJESH, H.M., 2004. The igneous charnockite-high K-alkali calcic I-type granite-incipient charnockite association in Trivandrum Block, Southern India, *Contrib Mineral Petrol,* 147, 346-362.

RAJESH, H.M. & SANTOSH, M., 2004. Charnockitic magmatism in southern India. *J. Earth Syst. Sci.*, 113, 565-585.

RAJESH, H.M., 2008. Petrogenesis of two granites from the Nilgiri and Madurai blocks , southwestern India : Implications for charnockite – calc-alkaline granite and charnockite – alkali (A-type) granite link in high-grade terrains. *Precambrian Research*, 162, 180-197.

RAJESH, H.M., 2007. The petrogenetic characterization of intermediate and silicic charnockites in high-grade terrains : a case study from southern India. , 591-606.

RICKERS, K., MEZGER, K., RAITH, M.M., 2001. Evolution of the Continental Crust in the Proterozoic Eastern Ghats Belt, India and new constraints for Rodinia reconstruction: implications from Sm–Nd, Rb–Sr and Pb–Pb isotopes. *Precam Res*. 112, 183 – 210.

RIGBY, M, MOURI, H., BRANDL, G., 2008. A review of the pressure–temperature–time evolution of the Limpopo Belt: Constraints for a tectonic model, Journal of African Earth Sciences 50, 120–132

RIMSA, A, JOHANSSON, L., Whitehouse, M. 2007, *Contributions to Mineralogy and Petrology*, Vol 154, 3, pp. 357-369(13)

RUPASINGHE, M.S. and DISSANAYAKE, C.B., 1985. Charnockites and the genesis of gem minerals, *Chemical Geology,* 53, 1-16.

SANTOSH,M., 1985. Fluid evolution characteristics and piezothermic array of south Indian charnockites. *Geology,* 13, 361–363.

SANTOSH, M., JACKSON, D.H., HARRIS, N.B.W., MATTEY, D.P., 1991. Carbonic fluid inclusions in South India granulites:evidence for entrapment during charnockite formation, *Contrib Mineral Petrol,* 108, 318-330.

SANTOSH, M., OMORI, S., 2008. CO2 flushing: a plate tectonic perspective. Gondwana Research 13, 86–102 .

SANTOSH, M., TSUNOGAE, T., 2003. A RT I C L E S Extremely High Density Pure CO 2 Fluid Inclusions in a Garnet Granulite from Southern India. , 111(Touret 1985), 1-16.

SANTOSH, M., TANAKA., K., YOSHINURA, Y., 2005. Carbonic fluid inclusions in ultrahigh temperature graintoids from southern India. *Comp Rend Geosci*, 337, 326-335.

SATISH KUMAR M, HARLEY SL, 1998. An orthopyroxene-garnet thermometer and its applications to the Madras charnockites. *Contrib Mineral Petrol*. 88, 83-99.

SCHMIDT, M.W., 1992. Amphibole composition in tonalite as a function of pressure: an experimental calibration of the Al-in hornblende barometer. Contrib Miner Petrol, 110, 304-10.

SHUMLYANSKYY, L., ELLAM, R.M., MITROKHIN, O., The origin of basic rocks of the Korosten AMCG complex, Ukrainian shield: Implication of Nd and Sr isotope data. *Lithos,* 90, (3-4), 214-222.

SMITH, J.V., NEWTON, R.C., JANARDHAN, A.S., 1979. Signficance of granulite metamorphism for stabilisation of planetary crust: Charnockite formation at Kabbaldurga, S. India: Roles of CO_2 and H_2O; speculations on Venus and Mars, Abstr., Lunar Planetary Science, X: 1134-1136.

STRECKEISEN, A. L., 1974. Classification and Nomenclature of Plutonic Rocks. Recommendations of the IUGS Subcommission on the Systematics of Igneous Rocks. Geologische Rundschau. Internationale Zeitschrift für Geologie. Stuttgart. Vol.63, p. 773-785.

STRECKEISEN, A. L., 1978. IUGS Subcommission on the Systematics of Igneous Rocks. Classification and Nomenclature of Volcanic Rocks, Lamprophyres, Carbonatites and Melilite Rocks. Recommendations and Suggestions. Neues Jahrbuch für Mineralogie, Abhandlungen, Vol. 141, 1-14.

TARNEY, J., JONES, C.E., 1994. Trace element geochemistry of orogenic igneous rocks and crustal growth models. J Geol Soc Lond 151:855–868

TAYLOR, H.P., O'NEIL, J.R., KAPLAN, I.R., 1991. Stable Isotope Geochemistry: A tribute to Samuel Epstein, Special Publ. No 3. The Geochemical Society. San Antonio, TX.

TOMSON, J.K., BHASKAR RAO, Y.J., VIJAYA KUMAR, T., MALIKHARJUNA RAO, J., Y.J., 2006, Charnockite genesis across the Archaean–Proterozoic terrane boundary in the South

Indian Granulite Terrain: Constraints from major–trace element geochemistry and Sr–Nd isotopic systematic, *Gondwana Research* 10, 115–127.

TSUNOGAE, T., SANTOSH, M., OSANAI, Y., OWADA, M., TOYOSHIMA, T., HOKADA, T., 2002. Very high density carbonic fluid inclusions in sapphirine-bearing granulites from Tonagh Island in the Archaean Napier Complex, East Antarctica: implications for CO_2 infiltration during ultrahigh (T>1100°C) metamorphism. *Contrib Mineral Petrol,* 143, 279-299.

TSUNOGAE, T., SANTOSH, M. and DUBESSY, J., 2008. Fluid characteristics of ultrahigh-temperature metamorphism in southern India: a quantitative Raman spectroscopic study. *Precambrian Research,* 162, 198-211.

VALEEY, J.V. TAYLOR, H.P., O'NEIL, J.R., 1986. Stable Isotopes in High Temperatyre Geological Processes. Reviews in Mineralogy 16, Mineralogical Society of America Washing DC.

VINOGRADOV A, TUGARINOV A, ZHYGOV C, STAPINKOVA N, BIBIKOVA F and KHORRE, K 1964 Geochronology of Indian Precambrian; XXII Int. Geol. Cong. Report X 531–567

WASHINGTON, H.S., 1916. The charnockite series of igneous rocks, *Am J Sci,* 41, 321-338.

WENDLANDT, R F 1981 Influence of CO2 on melting of model granulite facies assemblages: a model for the genesis of charnockites; *Am. Mineral.* **66** 1164–1174

WHALEN, J.B., CURRIE, K., CHAPPELL, B.W., 1987. A-type granites: geochemical characteristics, discrimination and petrogenesis. Contributions to Mineralogy and Petrology 95, 407–419.

10. FIGURE CAPTIONS

Figure 1a). A geological diagram of Gondwana after Meert, 2010. The diagram show the the locations of continents arranged in the supercontinents, orogens. The fields in yellow depict Eastern Gondwana and the fiels in blue depict the arrangement of Western Gondwana.

Figure 2. (a) Simplified geological sketch of the Southern Granulite Terrain, south India (modified from Tomson *et al.*, 2006) showing major geological domains: Archaean and Neoproterozoic granulite blocks, the latter comprising Madurai Block (MB) and Trivandrum Block (TB), Cauvery Shear Zone system (CSZ), the Western and Eastern parts of Dharwar Craton (WDC and EDC). Abbreviations for charnockite massifs: Coorg (C), Biligiri Rangan (BR), Malai Mahadeva (MM), Shaveroy (SH), Pallavaram–Madras (MA), Nilgiri (NG), Kollimalai (KM), Palani–Kodaikkanal (KK) and Cardamon (CA). Major shear zones include: Moyar (Mo), Bhavani (Bh), Mettur (Mt), Salem–Attur (S–At), Gangavalli (Ga), Palghat–Cauvery (Pa–Ca), Karur– Oddanchatram (KOSZ), Karur–

Kambam–Painavu–Trichur (KKPT) and Acha9cnkovil (ASZ). **(b)** A simiplified geological map of the field region (modified after Raith *et al.*, 2010). **(c)** A geological map of the field site at Ayyarmalai showing lithological boundaries, structural features and sample locations.

Figure 3: Hand specimen photos from Ayyarmalai: (a) A massif charnockite showing the black-grey-green appearance of a charnockite. (b) Garnet rich charnockite. (c) Dehdyration zones occurring in a surrounding rock of grey granite characterized by red-feldspar, quartz, plagioclase, biotite and clinopyroxene. (d) A charnockitic gneiss zone showing individual prophyroblasts indicating south side up movement. (e) Pink granite with hornblende defining a lineation. (f)The boundary between the grey granite and pink alkali granite at Ayyarmalai. (g) Mafic charnockite with a quartz grain containing purple Amethyst. (h) Massif charnockite at Ayyarmalai quarry with zones of mafic patches/blebs. (i - q) Thin section photos (1cm = 10μm) showing relationships of minerals: i = hornblende rich charnockite, j =hornblende rich charnockite, k=hornblende rich charnockite, l = garnet rich charnockite, m= diopside with a corroded core in the grey granite in PL, l = diopside with a corroded core in the grey granite in XPL, m = Hornblende rich charnockite, n= Convolute textures in the pink granite, o= Granite dominated by microcline as the dominate feldspar, p= Convolute textures in hornblende rich charnockite. See text for further discussion.

Figure 4: a-d, Samples SR-63 (Grey Granite), 68H (Pink Alkali Granite), 57 (Hornblende rich Charnockite) and 6 (Garnet rich Charnockite) showing U-Pb Concordia diagrams and CL images of individual zircons in samples with their relevant analysed ages.

Figure 5: a-j: Harker Diagrams i.e. major elements vs SiO_2. Shaded areas represent Massif charnockite compositions taken from the Palghat-Cauvery Shear System in the Northern Central Madurai Block area (Tomson *et al.*, 2006). Apatite and Titanite geotherms follow that f Watson and Harrison (1984) LOI = Loss on ignition. (h) Fe*/(Fe*+MgO) plot, shaded fields represent calc-alkaline granitoids and alkali A-type granitoids (Bryant *et al*, 1999; Eby, 1990). (i) A MALI Plot. (j) An ASI plot showing the fields where metaluminous and peraluminous granites fall. (k-r) Trace elements vs SiO_2.

Figure 6: Discrimination Diagrams: (a) A K/Rb vs. K2O plot, (b)Rb vs Sr plot, the field represents typical mantle values. (c)A Th/U vs La/Th diagram with shaded zone representing typical values of igneous rocks and directions where U or Th loss occurs. (d) An-Ab-Or diagram showing the Ayyarmalai charnockite composition in terms of nortmative An-Ab-Or. (e) A-type discrimation diagram showing the domains where I, S and A-type granites typically fall (Whalen *et al*, 1987). (f) An AFM diagram showing calc-alkaline and tholeiite series trends (Irvine and Barager, 1971). (g) A Rb-Sr-Ba triplot showing two distinct types of granitoids i.e. a low Ba-Sr Granitoid and a high Ba-Sr Granitoids. Fields of Low Ba-Sr Granitoids are from Fowler *et al* (2001), while High Ba-Sr granitoids are from Tomson *et al* (2006). (g) X_{Al} vs X_{Mg} plot comparing orthopyroxenes from metamorphic dehydrations zones with orthopyroxenes that are clearly igneous. Data compiled by Santosh (2010) submitted.

Figure 7. Chondrite-normalised REE patterns (Sun and McDonough, 1989) incorporating all the rock types (b) Primitive mantle normalised REE patterns (Sun and McDonough, 1989).

Figure 8. Isotope Plots (a) An εNd vs time (Ga) plot of Ayyarmalai samples compared with samples from Sri Lanka, Plaghat-Cauvery Shear sysem, Madagascar, East Antarctica, Dharwar Craton, Northern Granulite Terrina, Madurai Block. Shaded domains represent basement of the Dharwar craton and Madagascar.

Figure 9. (a) 143Nd/144Nd vs 147Sm/144Nd plot. (b) 87Sr/86Sr vs 87Rb/86Sr plot. (c) εNd vs 87Sr/86Rb plot, shaded area represents a wide range of basement values of the TTG Gneisses of the Dharwar Craton.

Figure 10. A tectonic discrimination plot, R1-R2 diagram model from Bachelor & Bowden, (1985) showing Ayyarmalai samples dominantly plotting in a post-orogenic field.

Figure 11. The proposed continuation of Azania into southern India (after Collins *et al.* 2007) where the continuation of the PCSS could be the Betsimisiraka suture in Madagscar. Abbreviations: PCSS = Palghat-Cauvery shear zone; KKPT = Karur-Kamban-Painavu-Trichur shear zone; MB= Madurai Block; TB= Trivandrum Block.

Table 1. Lithological descriptions, structural features and GPS localities of rock samples from Ayyarmalai, Tamil Nadu, Southern India.

Sample	Lithology	Structure	Locality	Longitude	Lattitude	Image
SR-1	Massif fine grained, equigranular charnockite consisting of dark smoky coloured quartz, grey feldspars, brown weathered opx and possibly some cpx.	F 70/238	Quarry 1	10°52'32.8"N	78°22'25.5"E	
SR-2	Light Pink, equigranular and medium grained granitic composition rock. It has abundant quartz 45%, K-feldspar 40% and 10% black minerals which appears to be hornblende? Some of the black mineral specs are magnetic indicating the presence of Magnetite.	-	Western base of Ayyarmalai	10°52'30.4"N	78°22'45.9"E	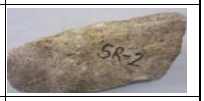
SR-3	Divided sample -one side blocky quartz vein and other is pink felsic granite with same lithology as SR-2	-	Western base of Ayyarmalai	10°52'30.4"N	78°22'45.9"E	
SR-4	Large pegmatite vein which cross cuts folding in the felsic granite, black dark veins run through the centre of the pegmatites which consist of magnetite.	-	Western base of Ayyarmalai	10°52'30.4"N	78°22'45.9"E	
SR-6	A light green-grey coloured garnet bearing charnockite, not as dark as the majority of samples in quarry.	-	Quarry 1	10°52'31.1"N	78°22'24.1"E	
SR-9	Grey-pink quartz, k-feldspar, biotite, mafic minerals hard to distinguish. Sample taken from gneissic zone within the quarry.	-	Quarry 2	10°52'31.8"N	78°22'24.0"E	
SR 50(1)(2)	Charnockite enveloped by coarse hornblende and quartz rich, glossy zones. Possibly a restite? (1) is the hornblende rich zone (2) is charnockite.	-	Quarry 3	10°52'26.1"N	78°22'26.2"E	
SR-51	Fine grained massif charnockite	-	Quarry 3	10°52'26.1"N	78°22'26.2"E	
SR - 52	Pegmatite Vein - K-feldspar, quartz and large phenocrysts of hornblende	-	Quarry 3	10°52'26.1"N	78°22'26.2"E	
SR - 53	Gneissic zone with porphyroblast indicators showing south side up.	vertical	Quarry 3	10°52'26.1"N	78°22'26.2"E	
SR - 55	Gneissic zone with porphyroblast indicators showing south side up.	vertical	Quarry 3	10°52'26.1"N	78°22'26.2"E	
SR - 56	Fine grained massif charnockite ± garnets?	-	Quarry 5	10°52'24.4"N	78°22'24.7"E	
SR-57	Waxy green coloured, fine grained massif charnockite, little to no visible garnet, dominate mineral is hornblende.	F 38/249	Quarry 5	10°52'29.7"N	78°22'24.2"E	
SR - 58	Fine grained massif charnockite ± garnets?	F 38/250	Quarry	10°52'29.7"N	78°22'24.2"E	
SR-59	Glossy rim surrounding the charnockite, dominated by quartz	-	Quarry	10°52'29.7"N	78°22'24.2"E	
SR - 60	Mafic hornblende rich rim lining the quartz rim	-	Quarry	10°52'29.7"N	78°22'24.2"E	
SR - 61	Dark halo dominated with quartz, hornblende.	-	Quarry	10°52'29.7"N	78°22'24.2"E	
SR - 62	North side of quarry is light grey -green colour charnockite, dominated by hornblende, however no visible opx, appears more felsic variety. Looks like fesics from hill.	-	North side of Quarry 2	10°52'32.8"N	78°22'25.5"E	
SR - 63	Grey granite consisting of pink - red coloured feldspar, plagioclase, biotite?, some magnetite.	-	Western base of Ayyarmalai	10°52'32.3"N	78°22'46.3"E	
SR - 64	Pink granite - k-feldpar, quartz, plagioclase ± dark minerals.	F 80/314	Ayyarmalai	10°52'32.3"N	78°22'46.3"E	
SR -67	Pegmatite vein within the pink granite	-	Ayyarmalai	10°52'27.4"N	78°22'47.6"E	
SR - 68H	Pink granite - k-feldpar, quartz, plagioclase ± dark minerals.	F 62/236	Ayyarmalai	10°52'27.4"N	78°22'47.6"E	
SR - 70	Lineated pink granite - lineation defined by large hornblende phenocrysts alligned within the pink K-feldspar and quartz matrix.	L 40→267	Southern side of Ayyarmalai base	10°52'25.1"N	78°22'49.7"E	
SR - 71	Pink granite - k-feldpar, quartz, plagioclase ± dark minerals.	-	Sample obtained from further up the hill on southern side			
SR - 80	Grey granite consisting of pink - red coloured feldspar, plagioclase, biotite?, some magnetite. Abundant green waxy dehydration veins running through the outcrops.	-	Northern side of Ayyarmalai base	10°52'32.3"N	78°22'47.1"E	
SR - 82	Lineated pink granite - lineation defined by large hornblende phenocrysts alligned within the pink K-feldspar and quartz matrix.	L 58 →260	Southern side of Ayyarmalai base	10°52'36.3"N	78°22'47.5"E	
SR - 84	Garnet rich charnockite, garnets are quite large in size (<2mm) in respect to other charnockites in the quarry.	-	Quarry 1	10°52'31.1"N	78°22'24.1"E	
SR - 85	Another dehydration similar to sample SR - 86	-	North western side of Ayyarmalai	10°52'32.3"N	78°22'47.1"E	
SR - 86	Abundant veins and splodges of the green waxy rock lithology. Samples taken across the green " incipient charnockite" zone. Quartz is identifiable in the green zone, as well as hornblende. No OPX is visibly identifiable. K-feldspar in the surrounding grey coloured granite appears garnet coloured red and is less abundant than the pink K-feldpar granite behind it. This granite is dominated by quartz 55%, 35% K-feldspar and 10% black minerals. Green vein requires thin section analysis for identification of fine grained minerals.	-	Western Side of Ayyermalai	10°52'32.3"N	78°22'46.3"E	
SR - 87	Another dehydration similar to sample SR - 86	-	South western side of Ayyarmalai	10°52'36.3"N	78°22'47.5"E	

Table 2. Geochemistry, C.I.P.W normalised values and relevant calculations of rock samples from Ayyarmalai

	Sample	SR-1	SR-56	SR-57	SR-58	SR-59	SR-62	SR-70	SR-84	SR-6	SR-9	SR-50(1)	SR-50(2)	SR-51	SR-60	SR-61	SR-53	SR-55
	Rock Type	GCH	GCH	HCH	HCH	GCH	HCH	HCH	GCH	GCH	QPG	CMZ	CMZ	CMZ	CMZ	CMZ	GN	GN
Major Elements wt.%	SiO2	72.1	74.5	66.3	72.5	71.4	74	72.5	53.9	72.9	71.1	47.8	57.6	47.7	49.3	45.1	71.2	65.5
	TiO2	0.425	0.335	0.735	0.355	0.135	0.295	0.105	1.335	0.44	0.35	2.295	1.21	2.18	1.98	2.36	0.375	0.69
	Al2O3	12	12	13.4	12	13.2	11.8	13.2	14.5	11.5	13.4	15.9	15	16	13.7	14.5	12.5	13.5
	Fe2O3	3.39	2.91	7.73	3.52	2.66	2.85	1.24	16.5	4.34	3.09	18	11.5	17.4	21.2	23.3	4.12	6.44
	MnO	0.06	0.05	0.12	0.09	0.05	0.04	bd	0.23	0.11	0.04	0.28	0.17	0.28	0.32	0.35	0.07	0.11
	MgO	0.24	0.14	0.34	0.16	0.13	0.08	0.24	1.51	0.16	0.27	2.15	1.2	2.31	1.59	1.81	0.45	0.48
	CaO	1.4	1.2	2.58	1.21	1.01	0.94	1.28	5.46	1.53	1.52	7.76	5.1	8.24	6.08	7.74	1.88	2.84
	Na2O	2.34	2.26	2.78	2.1	2.52	2.31	3.02	2.04	1.85	2.38	4.14	3.62	4.07	2.76	3.14	2.79	3.22
	K2O	5.35	5.16	4.48	5.47	6.35	5.57	5.66	4.01	4.33	6.6	1.53	3.13	1.39	2.35	2.09	4.22	4
	P2O5	0.05	0.02	0.18	0.05	0.04	0.03	0.02	0.43	0.05	0.08	0.7	0.36	0.69	0.61	0.72	0.04	0.19
	LOI	0.23	0.2	0.22	0.12	0.81	0.2	0.57	0.12	0.27	0.53	-0.04	0.14	-0.05	0.56	0.3	0.68	0.38
	TOTAL	97.585	98.775	98.865	97.575	98.305	98.115	97.835	100.035	97.48	99.36	100.515	99.03	100.21	100.45	101.41	98.325	97.35
Calculations	K2O/Na2O	2.2863	2.2832	1.6115	2.6048	2.5198	2.4113	1.8742	1.9657	2.3405	2.7731	0.3696	0.8646	0.3415	0.8514	0.6656	1.5125	1.2422
	Na2O+K2O	7.6900	7.4200	7.2600	7.5700	8.8700	7.8800	8.6800	6.0500	6.1800	8.9800	5.6700	6.7500	5.4600	5.1100	5.2300	7.0100	7.2200
	A/CNK	1.3201	1.3921	1.3618	1.3667	1.3360	1.3379	1.3253	1.2598	1.4916	1.2762	1.1839	1.2658	1.1679	1.2243	1.1180	1.4061	1.3419
	Agpaitic index	0.6408	0.6183	0.5418	0.6308	0.6720	0.6678	0.6576	0.4172	0.5374	0.6701	0.3566	0.4500	0.3413	0.3730	0.3607	0.5608	0.5348
	Fe*	0.9339	0.9541	0.9579	0.9565	0.9534	0.9727	0.8378	0.9162	0.9644	0.9196	0.8933	0.9055	0.8828	0.9302	0.9279	0.9015	0.9306
	Fe#	0.9280	0.9502	0.9544	0.9529	0.9495	0.9708	0.8237	0.9086	0.9617	0.9124	0.8837	0.8970	0.8723	0.9240	0.9215	0.8926	0.9245
	Mg#	0.1230	0.0870	0.0802	0.0826	0.0883	0.0527	0.2772	0.1535	0.0681	0.1476	0.1914	0.1713	0.2083	0.1294	0.1334	0.1779	0.1287
	MALI	6.2900	6.2200	4.6800	6.3600	7.8600	6.9400	7.4000	0.5900	4.6500	7.4600	-2.0900	1.6500	-2.7800	-0.9700	-2.5100	5.1300	4.3800
	ASI	0.7953	0.8336	0.8641	0.8160	0.7866	0.7898	0.7932	0.8760	0.9149	0.7633	0.8839	0.8740	0.8821	0.8902	0.8362	0.8745	0.8632
C.I.P.W Norm	q	33.996	37.231	25.281	34.772	33.489	39.723	29.707	7.91	40.818	26.811	10.891	10.914	0.000	0.000	0.000	33.323	23.798
	An	5.612	5.75	10.198	5.6562	4.4006	1.9751	4.9214	18.711	7.3257	5.1284	36.126	14.851	23.297	21.345	21.345	8.4333	9.795
	Alb	20.755	19.712	25.135	18.565	20.697	21.11	25.399	19.675	16.57	20.678	15.486	34.018	38.941	30.697	30.697	24.879	29.433
	or	35.631	34.314	30.699	37.36	38.792	35.376	36.9	30.61	30.474	43.353	11.513	21.931	10.003	15.894	15.894	28.385	28.382
	mag	0.781	0.6551	1.8109	0.809	0.5672	0.3766	0.2792	4.12	1.0053	0.6976	4.7816	2.799	4.42	6.0643	6.0643	0.9546	1.5231
	zr	0.063	0.0441	0.1005	0.0536	0.0249	0.0176	0.0353	0.19	0.0633	0.0351	0.3067	0.1519	0.2972	0.3857	0.3857	0.054	0.1016
	hy	1.859	1.7365	4.433	2.2186	1.6239	0.8125	0.7278	11.96	2.5971	1.521	14.718	6.3906	0.000	0.000	0.000	2.9305	3.3998
	il	0.472	0.3671	0.8283	0.394	0.2034	0.27	0.119	0.6	0.4879	0.3765	2.882	1.4077	2.647	2.936	2.936	0.4195	0.7808
	di	0.687	0.000	1.1138	0.000	0.000	0.000	0.8375	5.22	0.000	1.2087	1.6775	5.7287	11.458	11.431	11.431	0.4714	2.3372
	Py	0.047	0.0344	0.0357	0.0349	0.0324	0.023	0.0345	0.08	0.1179	0.343	0.0932	0.0495	0.129	0.2116	0.2116	0.0704	0.0601
	Cor	0.000	0.1158	0.000	0.0382	0.0966	0.2971	0.000	0.000	0.4405	0.000	0.000	0.000	0.000	0.000	0.000	0.000	0.000
	Chr	0.000	0.000	0.000	0.000	0.000	0.000	0.000	0.000	0.000	0.000	0.000	0.000	0.009	0.000	0.000	0.000	0.000
	Ol	0.000	0.000	0.000	0.000	0.000	0.000	0.000	0.000	0.000	0.000	0.000	0.000	6.741	8.937	8.937	0.000	0.000
	Neph	0.000	0.000	0.000	0.000	0.000	0.000	0.000	0.000	0.000	0.000	0.000	0.000	0.541	0.4753	0.4753	0.000	0.000
	ap	0.099	0.0391	0.3649	0.0991	0.0736	0.0196	0.0392	0.93	0.1004	0.1558	1.5883	0.7584	1.5171	0.3857	1.6221	0.08	0.3894
LILE	Ba	2000	2500	2000	3200	1900	1800	1800	3100	3100	2800	470	950	295	1100	900	1700	2500
	Rb	130	75	120	130	165	125	85	60	85	115	24	60	25.5	43.5	22	75	65
	Sr	70	160	90	110	60	75	200	160	110	140	140	125	160	75	75	130	115
	Cs	0.1	bd	0.2	0.1	0.1	0.2	0.1	bd	bd	0.2	0.1	0.2	0.1	0.1	bd	0.2	0.1
	Pb	35	24	34.5	37.5	48.5	33	37	18.5	24	33	14.5	22	11.5	23	22.5	25	24
Incompatible. E.	Ni	4	bd	3	2	bd	bd	4	14	3	3	16	8	16	14	18	10	4
	Co	55	90	65	80	65	60	70	47	75	75	36	65	32	65	34.5	60	45
	Cr	bd	bd	bd	bd	bd	bd	bd	bd	bd	bd	30	bd	35	20	30	25	bd
	Cu	11	5.5	11.5	7	5	3.5	3.5	22.5	40	5.5	42	20	47	42	70	21.5	17
	Zn	80	35.5	150	55	65	43	24	235	50	48	310	195	260	435	500	75	120
	V	bd	bd	bd	bd	bd	bd	bd	45	bd	bd	85	45	95	60	75	bd	bd
Rare Earth Elements	La	39	22	80	75	135	44.5	105	70	90	49	60	38	55	105	100	80	44
	Ce	70	40.5	150	130	250	65	215	150	165	95	130	95	110	230	220	135	85
	Pr	8	4.6	17	14.5	25.5	6.5	20.5	20.5	18.5	12	18	14	15	30.5	28.5	15	10.5
	Nd	28.5	17	60	50	85	21.5	70	90	65	45.5	75	65	65	130	120	50	41
	Sm	6	4.1	13	10	14.5	4	13.5	21	11.5	11.5	18	19	14.5	33.5	31	9.5	9.5
	Eu	2.6	2.2	3.9	3.1	2.5	1.95	1.65	7.5	3.5	3.4	5.5	4.1	5.5	6	8	2.8	4.2
	Gd	6.5	4.4	13.5	9	11.5	3.6	10.5	20	11.5	12	21.5	24.5	17	39	37.5	8	10
	Tb	1	0.7	2.1	1.35	1.55	0.52	1.45	3.8	1.75	1.85	3.2	4.1	2.5	6	5.5	1.1	1.5
	Dy	6.5	4.4	12.5	8.5	8.5	3	7	22	11	10.5	19	26	14	35.5	33	6	9
	Ho	1.3	0.88	2.5	1.7	1.6	0.52	1.15	4.2	2.3	1.9	3.7	5	2.7	6.5	6	1.15	1.8
	Er	3.6	2.4	7	4.7	4.5	1.35	2.6	12	6.5	4.8	10	14	7.5	18.5	16.5	3.1	5
	Mo	2.5	1.8	4.7	3.2	2.4	3.1	1.2	2.3	1.8	1.2	5	3.6	4.3	10	9.5	1.4	2.6
	Tm	0.5	0.35	1	0.65	0.65	0.15	0.3	1.55	0.9	0.6	1.4	1.9	0.95	2.6	2.3	0.45	0.7
	Yb	3.6	2.3	7	4.5	4.4	1.2	1.6	11	6	3.7	9	12.5	6.5	18	15.5	3	4.7
	Lu	0.56	0.36	1.05	0.66	0.66	0.18	0.2	1.65	1.05	0.5	1.35	1.7	0.94	2.6	2.3	0.46	0.72
HFSE	Zr	550	340	850	480	210	385	300	1500	550	290	2200	1200	2200	2400	2800	440	800
	Th	12.5	5.5	34	27.5	75	12	80	9	35	17	6	7	6.5	24.5	19.5	30.5	6.5
	Nb	28.5	6.5	29.5	13.5	6.5	6.5	2	50	11.5	15	41.5	46	30.5	100	115	16	19.5
	U	1.3	0.3	6.5	1.9	2.8	1.2	2.3	0.5	1.5	0.8	4.3	2	2.9	7	4.4	1.2	0.7
	Y	30	20.5	65	42.5	38.5	12.5	28	95	55	45	90	125	70	170	150	28	42
	Sc	5	bd	10	bd	bd	bd	5	30	5	15	25	20	30	35	40	5	10
	Tl	0.5	0.3	0.4	0.4	0.5	0.4	0.3	0.2	0.3	0.4	0.2	0.3	0.1	0.2	0.2	0.3	0.3
Incompatible. E.	Ga	18.5	16.5	22.5	17.5	21.5	18	18.5	26.5	16	17	30	28	26	37	39	18	21
	Ag	0.2	bd	0.3	0.1	bd	bd	bd	0.6	0.2	0.1	0.5	0.5	0.4	0.8	1.1	0.1	0.2
	As	0.5	bd	0.5	bd	bd	bd	bd	bd	0.5	1	0.5	1	0.5	0.5	bd	bd	bd
	Bi	bd	bd	bd	bd	bd	bd	bd	bd	bd	0.1	bd	bd	bd	bd	bd	bd	bd
	Cd	0.1	bd	0.2	0.2	0.1	bd	bd	0.3	0.2	bd	0.5	0.4	0.3	0.7	0.8	0.1	0.2
	In	bd	bd	bd	bd	bd	bd	bd	bd	bd	bd	bd	bd	bd	bd	0.5	bd	bd
	Sb	bd	bd	bd	bd	bd	bd	bd	bd	bd	bd	bd	bd	bd	bd	bd	bd	bd
	Se	bd	bd	bd	bd	bd	bd	bd	bd	bd	bd	bd	bd	bd	bd	bd	bd	bd
	Te	bd	bd	bd	bd	bd	bd	bd	bd	bd	bd	bd	bd	bd	bd	bd	bd	bd
	W	800	950	750	1000	900	650	850	295	950	900	195	550	130	600	195	650	500
	S	0.04	0.03	0.03	0.03	0.03	0.02	0.03	0.06	0.1	0.03	0.07	0.04	0.1	0.05	0.16	0.06	0.05
Ratios	Rb/Ba	0.065	0.030	0.060	0.041	0.087	0.069	0.047	0.019	0.027	0.041	0.051	0.063	0.086	0.040	0.024	0.044	0.026
	Rb/Sr	1.857	0.469	1.333	1.182	2.750	1.667	0.425	0.375	0.773	0.821	0.171	0.480	0.159	0.580	0.293	0.577	0.565
	Nb/Zr	0.052	0.019	0.035	0.028	0.031	0.017	0.007	0.033	0.021	0.052	0.019	0.038	0.014	0.042	0.041	0.036	0.024
	Ce/Zr	0.127	0.119	0.176	0.271	1.190	0.169	0.717	0.100	0.300	0.328	0.059	0.079	0.050	0.096	0.079	0.307	0.106
	La_N/Yb_N	7.32	6.46	7.72	11.26	20.73	25.06	44.35	4.30	10.14	8.95	4.50	2.05	5.72	3.94	4.36	18.02	6.33
	Eu/Eu*	0.42	0.52	0.29	0.33	0.19	0.51	0.14	0.37	0.30	0.29	0.28	0.19	0.35	0.17	0.23	0.32	0.43
	Eu/Sm	0.43	0.54	0.30	0.31	0.17	0.49	0.12	0.36	0.30	0.30	0.31	0.22	0.38	0.18	0.26	0.29	0.44
	Eu/Gd	0.40	0.50	0.29	0.34	0.22	0.54	0.16	0.38	0.30	0.28	0.26	0.17	0.32	0.15	0.21	0.35	0.42
	Nd/Th	2.28	3.09	1.76	1.82	1.13	1.79	0.88	10.00	1.86	2.68	12.50	9.29	10.00	5.31	6.15	1.64	6.31
	Nb/Ce	0.41	0.16	0.20	0.10	0.03	0.10	0.01	0.33	0.07	0.16	0.32	0.48	0.28	0.43	0.52	0.12	0.23
	Ce/Yb	19.44	17.61	21.43	28.89	56.82	54.17	134.38	13.64	27.50	25.68	14.44	7.60	16.92	12.78	14.19	45.00	18.09
	La/Lu	69.64	61.11	76.19	113.64	204.55	247.22	525.00	42.42	85.71	98.00	44.44	22.35	58.51	40.38	43.48	173.91	61.11
	Ba/La	51.28	113.64	25.00	42.67	14.07	40.45	17.14	44.29	34.44	57.14	7.83	25.00	5.36	10.48	9.00	21.25	56.82
	Sr/Y	2.33	7.80	1.38	2.59	1.56	6.00	7.14	1.68	2.00	3.11	1.56	1.00	2.29	0.44	0.50	4.64	2.74

Table 2. (Cont.) - Geochemistry, C.I.P.W normalised values and relevant calculations of rock samples from Ayyarmalai

	Sample	SR-2	SR-3	SR-68H	SR-71	SR-82	SR-63	SR-80	SR-64	SR-52	SR-85(1)	SR-85(2)	SR-85(3)	SR-85(4)
	Rock Type	PAG	PAG	PAG	PAG	PAG	DGG	DGG	DGG	PEG	DGG	DGG	DZ	DZ
Major Elements wt.%	SiO2	73.9	77.3	77.5	76.2	77.5	76.7	77.8	77	68.8	75.8	75.5	76.7	76.1
	TiO2	0.135	0.21	0.205	0.215	0.18	0.245	0.185	0.23	0.105	0.205	0.195	0.2	0.18
	Al2O3	12.5	10.5	10.7	11.3	11.5	11.4	11.3	10.7	15.1	10.7	11.4	11.2	11.7
	Fe2O3	1.42	1.82	1.66	1.68	1.5	2.16	1.68	2	1.86	1.9	1.81	2	1.71
	MnO	0.02	bd	bd	0.01	0.01	0.03	0.02	0.03	0.04	0.02	0.02	0.02	0.02
	MgO	0.02	0.04	0.03	0.03	0.04	0.04	0.03	0.05	0.22	0.04	0.04	0.04	0.05
	CaO	0.63	0.28	0.3	0.42	0.51	0.63	0.53	0.62	1.57	0.55	0.55	0.54	0.7
	Na2O	2.76	2.38	2.55	2.43	2.53	2.82	2.73	2.54	2.81	2.63	2.67	2.65	2.76
	K2O	6.02	5.06	5.3	5.6	5.83	5.67	5.57	5.05	7.47	5.42	5.5	5.51	5.61
	P2O5	bd	0.01	0.01	0.01	0.01	0.02	bd	bd	0.17	0.01	bd	0.02	bd
	LOI	0.32	0.53	0.48	0.45	0.21	0.27	0.27	0.6	0.58	0.11	0.52	0.17	0.5
	TOTAL	97.725	98.13	98.735	98.345	99.82	99.985	100.115	98.82	98.725	97.385	98.205	99.05	99.33
Calculations	K2O/Na2O	2.1812	2.1261	2.0784	2.3045	2.3043	2.0106	2.0403	1.9882	2.6584	2.0608	2.0599	2.0792	2.0326
	Na2O+K2O	8.7800	7.4400	7.8500	8.0300	8.3600	8.4900	8.3000	7.5900	10.2800	8.0500	8.1700	8.1600	8.3700
	A/CNK	1.3284	1.3601	1.3129	1.3373	1.2965	1.2500	1.2797	1.3033	1.2743	1.2442	1.3073	1.2874	1.2900
	Agpaitic index	0.7024	0.7086	0.7336	0.7106	0.7270	0.7447	0.7345	0.7093	0.6808	0.7523	0.7167	0.7286	0.7154
	Fe*	0.9861	0.9785	0.9822	0.9825	0.9740	0.9818	0.9825	0.9756	0.8942	0.9794	0.9784	0.9804	0.9716
	Fe#	0.9857	0.9772	0.9814	0.9816	0.9723	0.9809	0.9816	0.9740	0.8847	0.9782	0.9771	0.9793	0.9696
	Mg#	0.0271	0.0417	0.0346	0.0342	0.0502	0.0354	0.0342	0.0472	0.1899	0.0400	0.0419	0.0381	0.0548
	MALI	8.1500	7.1600	7.5500	7.6100	7.8500	7.8600	7.7700	6.9700	8.7100	7.5000	7.6200	7.6200	7.6700
	ASI	0.7733	0.7827	0.7560	0.7724	0.7511	0.7295	0.7440	0.7628	0.7588	0.7243	0.7608	0.7487	0.7551
C.I.P.W Norm	q	33.372	43.733	41.553	39.723	38.72	36.591	38.733	41.446	18.742	38.979	30.871	38.551	36.65
	An	2.9997	1.3025	1.3865	1.9751	2.365	1.3929	1.9009	2.6737	5.0647	1.1839	2.5832	2.1431	2.6976
	Alb	24.116	20.875	22.147	21.11	21.639	24.197	23.335	22.142	24.308	23.112	22.813	22.912	23.833
	or	38.058	32.03	33.283	35.376	35.866	35.302	34.33	31.773	48.923	34.431	33.964	34.431	35.005
	mag	0.3244	0.4165	0.3749	0.3766	0.3323	0.4815	0.369	0.4516	0.4257	0.4325	0.3983	0.4479	0.3802
	zr	0.0177	0.0177	0.0263	0.0176	0.0173	0.0433	0.0173	0.0264	0.0087	0.0355	0.0259	0.0349	0.0262
	hy	0.7416	0.9545	0.8274	0.8125	0.7308	0.6272	0.7382	0.9864	1.0418	0.2285	9.0893	0.979	0.7579
	il	0.151	0.228	0.2258	0.27	0.2329	0.2656	0.1164	0.2482	0.1178	0.5605	0.2116	0.2141	0.1924
	di	0.000	0.000	0.000	0.000	0.000	1.2075	0.3847	0.2304	1.0047	0.994	0.0215	0.2266	0.4155
	Py	0.0345	0.0346	0.0343	0.023	0.0225	0.0339	0.0562	0.0229	0.0341	0.0231	0.0225	0.0228	0.0227
	Cor	0.1645	0.3884	0.1217	0.2971	0.0559	0.000	0.000	0.000	0.000	0.000	0.000	0.000	0.000
	Chr	0.000	0.000	0.000	0.000	0.000	0.000	0.000	0.000	0.000	0.000	0.000	0.000	0.000
	Ol	0.000	0.000	0.000	0.000	0.000	0.000	0.000	0.000	0.000	0.000	0.000	0.000	0.000
	Neph	0.000	0.000	0.000	0.000	0.000	0.000	0.000	0.000	0.000	0.000	0.000	0.000	0.000
	ap	0.0196	0.0197	0.0195	0.0196	0.0173	0.0012	0.0192	0.000	0.3297	0.0197	0.000	0.000	0.0194
LILE	Ba	500	385	425	550	265	650	315	375	3200	430	430	420	435
	Rb	205	180	180	200	175	210	195	175	130	190	185	185	190
	Sr	19.5	20	13.5	20	18.5	18	12	27	185	13.5	13.5	14	14.5
	Cs	0.1	0.1	0.1	0.2	0.1	0.3	0.2	0.2	0.3	0.1	0.1	0.1	0.1
	Pb	42	41.5	36	42	40	47	46.5	40	39	37.5	38.5	37	38.5
Incompatible. E.	Ni	bd	bd	bd	bd	bd	bd	bd	bd	bd	bd	bd	bd	bd
	Co	75	70	95	100	100	70	85	120	40	95	95	135	135
	Cr	bd	bd	bd	bd	bd	bd	bd	bd	bd	bd	bd	bd	bd
	Cu	4	7.5	2	3	2.5	11	1.5	3	3	3	4.5	4.5	5
	Zn	36	38.5	43.5	35.5	33	75	65	50	27.5	60	55	55	49
	V	bd	bd	bd	bd	bd	bd	bd	bd	bd	bd	bd	bd	bd
Rare Earth Elements	La	45.5	85	65	21	65	100	85	105	26.5	105	85	85	80
	Ce	95	165	125	47.5	130	190	160	190	55	190	170	165	145
	Pr	9.5	19	13	4.6	12.5	19.5	16.5	20.5	6.5	21.5	17.5	17.5	16
	Nd	31.5	65	42.5	14	41.5	65	60	65	26	70	60	60	55
	Sm	6.5	13	8.5	3	8.5	13	12.5	13.5	7	14	12	12	10.5
	Eu	0.7	0.74	0.66	0.52	0.44	1.15	0.62	0.78	3.3	0.84	0.76	0.78	0.76
	Gd	6.5	11.5	7.5	2.5	7.5	13.5	11.5	13	8	14.5	12.5	12	10
	Tb	1.05	1.55	1.2	0.44	1.4	2.2	2.3	2.1	1.3	2.3	2.1	2	1.6
	Dy	6.5	7.5	7	2.7	8.5	13.5	14	13	8	14.5	13	12.5	10
	Ho	1.2	1.3	1.25	0.52	1.7	2.7	2.8	2.5	1.55	2.7	2.5	2.4	1.85
	Er	3.3	3.3	3.4	1.45	4.8	7.5	8.5	7	4.2	7.5	7	6.5	5
	Mo	1	1	1.3	1.2	1.7	1.7	1.3	1.6	12	1.3	1.3	1.6	1.6
	Tm	0.45	0.45	0.45	0.2	0.7	1.1	1.1	1	0.55	1.05	0.95	0.9	0.7
	Yb	3	2.8	2.9	1.45	5	7	8	6.5	3.5	6.5	6	6	4.4
	Lu	0.4	0.38	0.38	0.2	0.96	1	0.94	0.84	0.48	0.84	0.8	0.76	0.6
HFSE	Zr	155	180	205	155	155	335	185	255	55	265	220	195	200
	Th	28	46.5	44.5	33.5	47	50	55	60	10	55	47	46	43
	Nb	11	6	11	13.5	18	35	30.5	30	10.5	15.5	23	17	19
	U	2.4	2.9	2.2	2.7	8	8	6	3.9	1	4.1	3.6	3.2	4.3
	Y	28	31.5	29	13	38	70	70	65	36.5	70	65	60	45
	Sc	bd	bd	bd	bd	bd	bd	bd	bd	10	bd	bd	bd	bd
	Tl	0.7	0.8	0.6	0.7	0.6	0.7	0.6	0.6	0.4	0.6	0.6	0.6	0.6
Incompatible. E.	Ga	21	18	18.5	17.5	17	20	20	19	16.5	19	19	19	20
	Ag	0.1	0.2	bd	bd	0.1	0.3	0.3	0.2	bd	0.1	0.1	0.1	0.1
	As	bd	1.5	bd	bd	bd	0.5	bd	bd	bd	0.5	1	bd	bd
	Bi	bd	0.6	bd	bd	bd	bd	bd	bd	bd	bd	bd	bd	bd
	Cd	bd	bd	bd	bd	bd	bd	bd	bd	bd	bd	bd	bd	bd
	In	bd	bd	bd	bd	bd	bd	bd	bd	bd	bd	bd	bd	bd
	Sb	bd	bd	bd	bd	bd	bd	bd	bd	bd	bd	bd	bd	bd
	Se	bd	bd	bd	bd	bd	bd	bd	bd	bd	bd	bd	bd	bd
	Te	bd	bd	bd	bd	bd	bd	bd	bd	bd	bd	bd	bd	bd
	W	850	750	950	1300	1500	800	750	1500	500	600	1000	1100	1600
	S	0.03	0.03	0.03	0.02	0.02	0.03	0.02	0.02	0.03	0.02	0.02	0.02	0.02
Ratios	Rb/Ba	0.410	0.468	0.424	0.364	0.660	0.323	0.619	0.467	0.041	0.442	0.430	0.440	0.437
	Rb/Sr	10.513	9.000	13.333	10.000	9.459	11.667	16.250	6.481	0.703	14.074	13.704	13.214	13.103
	Nb/Zr	0.071	0.033	0.054	0.087	0.116	0.104	0.165	0.118	0.191	0.058	0.105	0.087	0.095
	Ce/Zr	0.613	0.917	0.610	0.306	0.839	0.567	0.865	0.745	1.000	0.717	0.773	0.846	0.725
	La_N/Yb_N	10.25	20.51	15.15	9.79	8.78	9.65	7.18	10.92	5.12	10.92	9.57	9.57	12.29
	Eu/Eu*	0.11	0.06	0.08	0.19	0.06	0.09	0.05	0.06	0.44	0.06	0.06	0.07	0.07
	Eu/Sm	0.11	0.06	0.08	0.17	0.05	0.09	0.05	0.06	0.47	0.06	0.06	0.07	0.07
	Eu/Gd	0.11	0.06	0.09	0.21	0.06	0.09	0.05	0.06	0.41	0.06	0.06	0.07	0.08
	Nd/Th	1.13	1.40	0.96	0.42	0.88	1.30	1.09	1.08	2.60	1.27	1.28	1.30	1.28
	Nb/Ce	0.12	0.04	0.09	0.28	0.14	0.18	0.19	0.16	0.19	0.08	0.14	0.10	0.13
	Ce/Yb	31.67	58.93	43.10	32.76	26.00	27.14	20.00	29.23	15.71	29.23	28.33	27.50	32.95
	La/Lu	113.75	223.68	171.05	105.00	67.71	100.00	90.43	125.00	55.21	125.00	106.25	111.84	133.33
	Ba/La	10.99	4.53	6.54	26.19	4.08	6.50	3.71	3.57	120.75	4.10	5.06	4.94	5.44
	Sr/Y	0.70	0.63	0.47	1.54	0.49	0.26	0.17	0.42	5.07	0.19	0.21	0.23	0.32

Table 2. (Cont.) - Geochemistry, C.I.P.W normalised values and relevant calculations of rock samples from Ayyarmalai

	Sample	SR-85(5)	SR-85(6)	SR-85(7)	SR-85(8)	SR-86(1)	SR-86(2)	SR-86(3)	SR-86(4)	SR-86(5)	SR-86(6)
	Rock Type	DGG	DGG	DGG	DGG	DGG	DGG	DZ	DGG	DGG	DGG
Major Elements wt.%	SiO2	75.2	76.3	76	78.1	76.3	75.8	75.8	76.2	75.8	76.9
	TiO2	0.18	0.19	0.195	0.195	0.21	0.215	0.225	0.21	0.21	0.23
	Al2O3	11.4	11.3	11	11.2	11.2	11.4	11.5	11.4	11.6	11
	Fe2O3	1.59	1.79	1.79	1.78	1.88	1.71	1.95	1.81	1.76	2.06
	MnO	0.02	0.02	0.02	0.02	0.02	0.03	0.02	0.02	0.02	0.02
	MgO	0.06	0.03	0.04	0.03	0.04	0.05	0.05	0.04	0.04	0.04
	CaO	0.81	0.57	0.54	0.55	0.55	0.63	0.66	0.59	0.64	0.63
	Na2O	2.76	2.72	2.6	2.6	2.5	2.59	2.69	2.64	2.67	2.79
	K2O	5.69	5.41	5.31	5.66	5.58	5.64	5.38	5.61	5.58	5.45
	P2O5	bd	bd	bd	bd	bd	bd	0.01	bd	bd	0.01
	LOI	0.7	0.28	0.2	0.18	0.29	0.26	0.39	0.27	0.62	0.2
	TOTAL	98.41	98.61	97.695	100.315	98.57	98.325	98.675	98.79	98.94	99.33
Calculations	K2O/Na2O	2.0616	1.9890	2.0423	2.1769	2.2320	2.1776	2.0000	2.1250	2.0899	1.9534
	Na2O+K2O	8.4500	8.1300	7.9100	8.2600	8.0800	8.2300	8.0700	8.2500	8.2500	8.2400
	A/CNK	1.2311	1.2989	1.3018	1.2713	1.2978	1.2867	1.3173	1.2896	1.3048	1.2401
	Agpaitic index	0.7412	0.7195	0.7191	0.7375	0.7214	0.7219	0.7017	0.7237	0.7112	0.7491
	Fe*	0.9636	0.9835	0.9781	0.9834	0.9792	0.9716	0.9750	0.9784	0.9778	0.9810
	Fe#	0.9608	0.9828	0.9768	0.9827	0.9780	0.9696	0.9733	0.9771	0.9764	0.9799
	Mg#	0.0696	0.0321	0.0424	0.0323	0.0404	0.0548	0.0483	0.0419	0.0431	0.0370
	MALI	7.6400	7.5600	7.3700	7.7100	7.5300	7.6000	7.4100	7.6600	7.6100	7.6100
	ASI	0.7234	0.7571	0.7580	0.7388	0.7542	0.7503	0.7709	0.7511	0.7618	0.7248
C.I.P.W Norm	q	35.978	38.285	39.453	39.249	38.868	37.564	37.808	37.733	37.337	38.138
	An	1.6949	2.3998	2.4365	1.9082	2.5972	2.5076	3.1149	2.4103	2.3336	1.128
	Alb	24.105	23.619	22.779	22.189	21.694	22.532	23.413	22.881	23.216	24.039
	or	35.904	33.959	33.637	34.839	35.125	35.602	33.92	35.174	35.238	34.156
	mag	0.3619	0.4048	0.4009	0.3905	0.4203	0.3832	0.4426	0.4054	0.3979	0.4579
	zr	0.0265	0.0263	0.0177	0.0172	0.0259	0.0345	0.0259	0.0259	0.0259	0.0326
	hy	0.1692	0.8227	0.9005	0.6985	0.9598	0.7437	0.9847	0.8225	0.6879	0.4818
	il	0.1946	0.2043	0.2169	0.2007	0.2326	0.2325	0.2433	0.222	0.2219	0.2436
	di	1.543	0.2448	0.1355	0.4857	0.0446	0.3667	0.006	0.3038	0.5198	1.2802
	Py	0.023	0.0343	0.0231	0.0255	0.0337	0.0337	0.0255	0.0225	0.0255	0.0225
	Cor	0.000	0.000	0.000	0.000	0.000	0.000	0.000	0.000	0.000	0.000
	Chr	0.000	0.000	0.000	0.000	0.000	0.000	0.000	0.000	0.000	0.000
	Ol	0.000	0.000	0.000	0.000	0.000	0.000	0.000	0.000	0.000	0.000
	Neph	0.000	0.000	0.000	0.000	0.000	0.000	0.000	0.000	0.000	0.000
	ap	0.000	0.000	0.000	0.000	0.000	0.000	0.000	0.000	0.000	0.019
LILE	Ba	440	410	410	425	550	600	550	550	600	600
	Rb	195	180	185	185	195	200	200	200	205	200
	Sr	15	14	13.5	13.5	18.5	20	18	21	19.5	21
	Cs	0.1	0.1	0.1	0.1	0.1	0.1	bd	bd	bd	bd
	Pb	37.5	36.5	38	38	38.5	40	37	37.5	39	37.5
Incompatible. E.	Ni	bd	bd	bd	bd	bd	bd	bd	bd	bd	bd
	Co	145	120	115	75	120	120	180	115	75	110
	Cr	bd	bd	bd	bd	bd	bd	bd	bd	bd	bd
	Cu	9.5	5	4.5	3.5	2	2	3.5	1	3	2.5
	Zn	55	50	55	55	50	46	50	47.5	44.5	55
	V	bd	bd	bd	bd	bd	bd	bd	bd	bd	bd
Rare Earth Elements	La	85	85	70	85	60	85	90	125	100	105
	Ce	155	165	150	160	120	170	165	220	205	205
	Pr	16	17.5	15	17	12	17	18.5	25	23	22
	Nd	55	60	50	60	41.5	60	70	85	80	80
	Sm	10.5	12	11	12.5	8.5	12	15	17.5	16	15.5
	Eu	0.76	0.76	0.72	0.8	0.76	0.96	1.15	1.3	1.3	1.25
	Gd	10	12	11	12.5	8.5	12	15.5	16.5	15.5	14.5
	Tb	1.55	2	1.9	2.2	1.5	2.1	2.6	2.7	2.5	2.4
	Dy	9	12.5	12	13.5	9.5	13.5	18	18	17.5	16
	Ho	1.65	2.4	2.3	2.6	1.9	2.7	3.3	3.3	3.1	2.9
	Er	4.4	6.5	6.5	7.5	5.5	8	11.5	11	10	9.5
	Mo	1.6	1.5	1.5	1.2	1.7	1.7	2.2	1.8	2.4	1.8
	Tm	0.6	0.9	0.9	1	0.8	1.2	1.4	1.35	1.2	1.15
	Yb	3.9	5.5	5.5	6.5	5.5	8	10	9.5	8.5	8
	Lu	0.54	0.74	0.76	0.82	0.74	1.05	1.25	1.15	1.05	1
HFSE	Zr	215	220	165	160	230	275	215	245	205	300
	Th	44	43	37.5	43.5	35	47	55	55	55	50
	Nb	12.5	16	21.5	22.5	26.5	34.5	35	28	25	18
	U	5.5	3.7	3.3	3.4	4.2	5.5	9.5	6	8	8
	Y	40.5	60	60	65	48	70	75	75	65	65
	Sc	bd	bd	bd	bd	bd	bd	bd	bd	bd	bd
	Tl	0.6	0.6	0.6	0.6	0.6	0.7	0.6	0.6	0.7	0.6
Incompatible. E.	Ga	20.5	19.5	19	18.5	18	18.5	17.5	17.5	18	18
	Ag	0.1	bd	0.1	0.1	0.1	0.1	0.4	0.2	0.2	0.2
	As	bd	0.5	bd	bd	bd	bd	1	bd	1	1
	Bi	bd	bd	bd	bd	bd	bd	bd	bd	bd	bd
	Cd	bd	bd	bd	bd	bd	bd	bd	bd	bd	bd
	In	bd	bd	bd	bd	bd	bd	bd	bd	bd	bd
	Sb	bd	bd	bd	bd	bd	bd	bd	bd	bd	bd
	Se	bd	bd	bd	bd	bd	bd	bd	bd	bd	bd
	Te	bd	bd	bd	bd	bd	bd	bd	bd	bd	bd
	W	1100	1000	1300	850	1900	1900	2000	1400	900	1000
	S	0.02	0.03	0.02	0.02	0.03	0.03	0.02	0.02	0.02	0.02
Ratios	Rb/Ba	0.443	0.439	0.451	0.435	0.355	0.333	0.364	0.364	0.342	0.333
	Rb/Sr	13.000	12.857	13.704	13.704	10.541	10.000	11.111	9.524	10.513	9.524
	Nb/Zr	0.058	0.073	0.130	0.141	0.115	0.125	0.163	0.114	0.122	0.060
	Ce/Zr	0.721	0.750	0.909	1.000	0.522	0.618	0.767	0.898	1.000	0.683
	La_N/Yb_N	14.73	10.44	8.60	8.84	7.37	7.18	6.08	8.89	7.95	8.87
	Eu/Eu*	0.07	0.06	0.07	0.06	0.09	0.08	0.08	0.08	0.08	0.08
	Eu/Sm	0.07	0.06	0.07	0.06	0.09	0.08	0.08	0.07	0.08	0.08
	Eu/Gd	0.08	0.06	0.07	0.06	0.09	0.08	0.07	0.08	0.08	0.09
	Nd/Th	1.25	1.40	1.33	1.38	1.19	1.28	1.27	1.55	1.45	1.60
	Nb/Ce	0.08	0.10	0.14	0.14	0.22	0.20	0.21	0.13	0.12	0.09
	Ce/Yb	39.74	30.00	27.27	24.62	21.82	21.25	16.50	23.16	24.12	25.63
	La/Lu	157.41	114.86	92.11	103.66	81.08	80.95	72.00	108.70	95.24	105.00
	Ba/La	5.18	4.82	5.86	5.00	9.17	7.06	6.11	4.40	6.00	5.71
	Sr/Y	0.37	0.23	0.23	0.21	0.39	0.29	0.24	0.28	0.30	0.32

Table 3a. Sm-Nd isotopic data from Ayyarmalai and other locations

Sample/ Locality	Rock Type	Nd (ppm)	Sm (ppm)	Sm/Nd	147Sm/ 144Nd	143Nd/ 144Nd	2σ	εNd(0)	T(Ga)	εNd(T)	143Nd/ 144Nd (T)	εNd (2.65Ga)	143Nd/ 144Nd	TDM (Ga)
Ayyarmalai														
SR-1	Charnockite	38.206	6.832	0.1788	0.1081	0.510939	0.000008	-33.14	2.5	-4.7	0.509156	-2.97	0.509047981	2.89
SR-57	Charnockite	71.804	13.991	0.1948	0.1179	0.511027	0.000055	-31.42	2.5	-6.11	0.50908	-4.57	0.508966827	3.03
SR-84	Charnockite	84.644	18.745	0.2215	0.134	0.5113488	0.000006	-25.15	2.5	-5	0.509141	-3.78	0.509006961	3.04
SR-68H	Alkali Granite	49.212	9.390	0.1908	0.11535	0.511024	0.000006	-25.15	2.5	-5.39	0.509121	-3.8	0.509005933	2.97
SR-861	Alkali Granite	54.459	10.547	0.1937	0.1171	0.510977	0.000006	-32.4	2.5	-6.86	0.509046	-5.31	0.508929015	3.09

Sample/ Locality	Rock Type	Nd (ppm)	Sm (ppm)	Sm/Nd	147Sm/ 144Nd	143Nd/ 144Nd	εNd(0)	T(Ga)	εNd(T)	TDM (Ga)	Reference
Palghat-Cauvery Shear System											
SLM 99/10	Charnockite	10.8	1.5	0.1389	0.0844	0.51066	-38.5	2.5	-2.36	2.83	Tomson *et.al* , 2006
SLM 99/61	Charnockite	27.3	3.4	0.1245	0.0741	0.51056	-40.5	2.5	-1.56	2.73	Tomson *et.al* , 2006
TNT-99/27	Charnockite	42.2	6.7	0.1588	0.0962	0.51075	-36.8	2.5	-4.49	3	Tomson *et.al* , 2006
TNT 99/55	Charnockite	11.5	2.3	0.2000	0.1223	0.51068	-38.84	0.55	-13.93	3.75	Tomson *et.al* , 2006
99 SLM - 61	Charnockite	27.270	3.350	0.1228	0.0741	0.51056	-40.54	2.73	2.56	2.79	Bhaskar Rao et.al, 2003
99 SLM-62	Charnockite	15.930	2.140	0.1343	0.081	0.510646	-38.86	2.77	2.42	2.42	Bhaskar Rao et.al, 2003
PS - 1 118A	Charnockite	61.200	13.800	0.2255	0.1366	0.511518	-21.85	3.01	1.47	3.17	Meißner et.al, 2002
Southern Granulite Terrain											
TNT-00/130 (MB)	Charnockite	25.5	4.8	0.1882	0.1139	0.51128	-26	2.5	0.15	2.57	Tomson *et.al* , 2006
SLM-00/28 (MB)	Charnockite	29.5	7.1	0.2407	0.1444	0.51153	-21.5	0.55	0.16	2.35	Tomson *et.al* , 2006
33 (MB)	Charnockite	25.06	3.92	0.1564	0.946	0.511002	-30.7	0.55	-25.42	3.08	Harris et.al, 1994
327 (MB)	Charnockite	12.24	2.27	0.1855	0.1122	0.511364	-24.85	0.55	-18.94	2.42	Harris et.al, 1994
PE5 (MB)	Charnockite	42.53	7.29	0.1714	0.1035	0.511068	-30.63	0.55	-24.12	2.62	Harris et.al, 1994
Northern Granulite Terrain											
JB 10 (BH)	Felsic Granulites	32.98	6.87	0.2083	0.1269	0.511094	-30.1	3.46	1.5	3.51	Bhaskar Rao et.al, 2003
JB 11 (BH)	Felsic Granulites	8.89	1.23	0.1384	0.1259	0.5110476	-42.2	3.46	1.52	3.03	Bhaskar Rao et.al, 2003
ND4A (NH)	Charnockite	38.67	8.15	0.2108	0.1274	0.511518	-21.8	2.7	2.25	2.7	Bhaskar Rao et.al, 2003
NTA5A (NH)	Charnockite	58.6	10.27	0.1753	0.1059	0.51113	-29.4	2.67	2.26	2.71	Bhaskar Rao et.al, 2003
NTA5B (NH)	Charnockite	59.02	10.52	0.1782	0.1078	0.511187	-28.3	2.67	2.26	2.67	Bhaskar Rao et.al, 2003
NTA5C (NH)	Charnockite	66.98	12.49	0.1865	0.1127	0.511224	-27.6	2.67	2.26	2.75	Bhaskar Rao et.al, 2003
MS-12 B	hbl-bt-gneiss	10.6	1.61	0.1519	0.0921	0.51099	-35.15	2.59	2.73	2.67	Meißner et.al, 2002
MS-12 C	gt-px-pl- granulite	9.94	2.72	0.2736	0.1657	0.512086	-10.77	2.5	-0.38	3.04	Meißner et.al, 2002
Dharwar Craton											
PG2 (BAN)	TTG Gneiss	43.6	8.51	0.1952	0.118	0.510922	-34	2.54	-8	3.364	Jayananda et.al, 2000
PG 20 (BAN)	TTG Gneiss	25.5	4.92	0.1929	0.117	0.511068	-31	2.54	-5	3.095	Jayananda et.al, 2000
ARK 1 (AB Suite)	Late Archaen K-Granite	60.9	10.1	0.1658	0.1003	0.510772	-36.4	2.6	-4.5	3.173	Jayananda et.al, 2006
ARK 2 (AB Suite)	Late Archaen K-Granite	46.8	7.98	0.1705	0.1031	0.510794	-35.97	2.6	-5	3.084	Jayananda et.al, 2006
ARK 3 (AB Suite)	TTG Gneiss	72.6	10.9	0.1501	0.0911	0.510519	-41.36	2.6	-6.3	3.247	Jayananda et.al, 2006
CH5 (EG)	Charnockite	26	5.5	0.2115	0.12691	0.511564	-20.95	0.985	-12.32	2.59	Paul et.al, 1990
CH9 (EG)	Charnockite	56.9	11.8	0.2074	0.12521	0.511526	-21.69	0.985	-12.74	2.61	Paul et.al, 1990
CH13 (EG)	Charnockite	53.4	9.5	0.1779	0.1076	0.511401	-24.13	0.985	-12.93	2.35	Paul et.al, 1990
PG18A	Pyroxene Granulite	161.7	26.5	0.1639	0.16502	0.511681	-18	0.985	-6.4	2.1	Paul et.al, 1990
KT 10	Charnockite	19.19	4.52	0.2355	0.1425	0.511622	-19.82	2.89	0.35	3.21	Drury et.al, 1983
KT14	Charnockite	12.45	3.12	0.2506	0.1515	0.511801	-16.33	2.86	0.31	3.24	Drury et.al, 1983
KT19	Charnockite	6.22	1.55	0.2492	0.1506	0.511786	-16.62	2.85	0.29	3.23	Drury et.al, 1983
KR 421 (EG)	Granite	78.29	10.42	0.1331	0.0804	0.510622	-39.33	2.5	-1.9	2.9	Rickers et. al, 2001
112	Granite	33.64	10.43	0.3100	0.1874	0.512212	-8.31	2.5	-5.4	3.2	Rickers et. al, 2001
KR47-1	Granite	29.29	4.159	0.1420	0.0858	0.510933	-33.26	2.5	2.4	3.5	Rickers et. al, 2001
Sri Lanka											
SL 137 (HC)	Charnockite	73.58	16.72	0.2272	0.1373	0.511302	-26.06	0.6	-21.5	3.4	Melisenda et.al, 1996
SL 110 (HC)	Gt Charnockite	35.04	9.86	0.2814	0.1702	0.511933	-13.75	0.6	-11.7	2.2	Melisenda et.al, 1996
SL 125 (HC)	Gt Charnockite	29.61	5.43	0.1834	0.1109	0.511195	-28.14	0.6	-21.5	2.7	Melisenda et.al, 1996
SL 359 (VC)	gt-hbl-bio-gneiss	20.18	4.26	0.2111	0.127	0.511261	-26.86	1	1.6	1.5	Melisenda et.al, 1996
SL 359-3a (VC)	gt-hbl-bio-gneiss	25.15	3.96	0.1575	0.0953	0.512222	-8.11	1	4.9	1.1	Melisenda et.al, 1996
SL 359-3b (WC)	gt-hbl-bio-gneiss	33.66	4.48	0.1331	0.0804	0.51219	-8.74	1	6.1	1.1	Melisenda et.al, 1996
SL 29 (WC)	Charnockite	20.1	2.96	0.1473	0.0891	0.511795	-16.4	0.77	-5.8	1.6	Melisenda et.al, 1996
SL 30 (WC)	Charnockite	38.08	5.46	0.1434	0.0867	0.511738	-17.56	0.77	-6.7	1.6	Melisenda et.al, 1996
SL 348 (WC)	Charnockite	20.34	4.87	0.2394	0.1448	0.512395	-4.74	1.1	2.6	1.3	Melisenda et.al, 1996
SL 2.1	Pink Granite	64.72	13.43	0.2075	0.1254	0.512273	-7.12	0.55	-2.1	1.4	Melisenda et.al, 1996
SL 2.2	Pink Granite	90.98	17.73	0.1949	0.1178	0.512207	-8.41	0.55	-2.9	1.4	Melisenda et.al, 1996
Antarctica											
410429-2	Insel Massif Charnockite	44	8.97	0.2039	0.1206	0.512442	-3.82	0.5	0.87	1.04	Mikhalsky et.al, 2006; Mikhalsky et.al, 1997
78285007-A (EL)	Tonalitic Orthogneiss	24.42	3.49	0.1429	0.0846	0.50901	-60	3.4	-22.61	3.87	Black & McCullouch, 1987
78285007-B (EL)	Mafic Granulite	26.87	6.66	0.2479	0.1499	0.51057	-40.43	3.4	-20	-	Black & McCullouch, 1987
M (EL)	Charnockite	15.72	1.81	0.1151	0.0694	0.50913	-68.43	3.1	-17.81	3.37	Black & McCullouch, 1984
N (EL)	Charnockite	6.11	0.82	0.1342	0.081	0.50936	-63.9	3.1	-17.93	3.4	Black & McCullouch, 1984
J1 (EL)	Charnockite	10.37	1.7	0.1639	0.0991	0.50979	-55.56	3.1	-16.72	3.37	Black & McCullouch, 1984
J5 (EL)	Charnockite	4.65	0.53	0.1140	0.0692	0.50917	-67.65	3.1	-16.74	3.32	Black & McCullouch, 1984

AYMB = Ayyarmalai , MB=Madurai Block, WC = Wanni Complex, HC= Highland Complex, RC = Rayner Complex, BH= Biligiririangan Hills, BAN=Bangalore, NH= Nilgiri Hills, EG = Eastern Ghats, EL= Enderby Land
gt = garnet, hbl=hornblende, bio=biotite, px = pyroxene, pl= plagioclase

2σ error on 143Nd/144Nd
Depleted Mantle Nd model ages calculated as in Goldstein et.al, (1984). Measured εNd values calculated with present day CHUR 143Nd/144Nd and 147Sm.144Nd ratios of 0.512638 and 0.1966

Table 3b. Rb-Sr isotope data from Ayyarmalai

Sample	Rock Type	Sr ppm	Rb ppm	Rb/Sr	Sr87/86	2σ	87Rb/86Sr	87/86(2.5)	87/86(2.65)	I/C_{Sr}
Ayyarmalai										
SR-1	Charnockite	70.1000	140.5000	2.0043	0.9158	0.0001	5.9170	0.7019	0.6889	0.0143
SR-57	Charnockite	92.7000	126.7000	1.3668	0.8797	0.0001	3.9230	0.7344	0.7255	0.0108
SR-84	Charnockite	162.6000	68.1000	0.4188	0.7534	0.0003	1.2170	0.7094	0.7067	0.0062
SR-68H	Alkali Granite	14.4000	181.7000	12.6181	2.0526	0.0454	41.3110	0.5598	0.4685	0.0694
SR-861	Alkali Granite	18.8000	197.2000	10.4894	1.9073	0.0008	34.0750	0.7068	0.6069	0.0532
Sample	**Rock Type**	**Sr ppm**	**Rb ppm**	**Rb/Sr**	**Sr87/86**	**87Rb/86Sr**	**T (Ga)**	**87Sr/86Sr(T)**	**Reference**	
Palghat-Cauvery Shear System										
SLM 99/10	Charnockite	367.0000	5.0000	0.0136	-	0.0380	0.5500	0.7037	Tomson *et.al* , 2006	
SLM 99/61	Charnockite	421.0000	153.0000	0.3634	-	1.0570	0.5500	0.7388	Tomson *et.al* , 2006	
TNT-99/11	Charnockite	397.0000	8.0000	0.0202	-	0.0550	0.5500	0.7053	Tomson *et.al* , 2006	
TNT 99/55	Charnockite	268.0000	45.0000	0.1679	-	0.4860	0.5500	0.7284	Tomson *et.al* , 2006	
99 SLM - 61	Charnockite	412.0000	153.3400	2.6868	-	1.0570	2.7300	0.7388	Bhaskar Rao et.al, 2003	
99 SLM-62	Charnockite	634.4000	163.1500	3.8884	-	0.7470	2.7700	0.7546	Bhaskar Rao et.al, 2003	
PS - 1 171 A	Bt-gt-Gneiss	207.0000	79.2000	2.6136		1.1100	-	0.7456	Meiβner et.al, 2002	
Southern Granulite Terrain										
TNT-00/130 (MB)	Charnockite	444.0000	162.0000	0.3649	-	1.0600	0.5500	0.7394	Tomson *et.al* , 2006	
SLM-00/28 (MB)	Charnockite	327.0000	35.0000	0.1070	-	0.3090	0.5500	0.7191	Tomson *et.al* , 2006	
Northern Granulite Terrain										
JB 10 (BH)	Felsic Granulites	329.3000	5.8000	0.0176	-	0.0510	3.4600	0.7076	Bhaskar Rao et.al, 2003	
JB 11 (BH)	Felsic Granulites	525.5000	43.8000	0.0833	-	0.2410	3.4600	0.7136	Bhaskar Rao et.al, 2003	
ND4A (NH)	Charnockite	128.9000	27.1000	0.2102	-	0.6090	2.7000	0.7219	Bhaskar Rao et.al, 2003	
NTA5A (NH)	Charnockite	1208.8000	21.6000	0.0179	-	0.0517	2.6700	0.7042	Bhaskar Rao et.al, 2003	
NTA5B (NH)	Charnockite	1402.0000	12.8000	0.0091	-	0.0264	2.6700	0.7031	Bhaskar Rao et.al, 2003	
NTA5C (NH)	Charnockite	1325.9000	22.5000	0.0170	-	0.0491	2.6700	0.7038	Bhaskar Rao et.al, 2003	
MS-12 B	hbl-bt-gneiss	630.0000	1.1100	0.0018	-	0.0051	2.5900	0.7027	Meiβner et.al, 2002	
MS-12 E	hbl-bt-gneiss	575.0000	4.6500	0.0081	-	0.0236	2.5000	0.7033	Meiβner et.al, 2002	
Dharwar Craton										
PG2 (BAN)	TTG Gneiss	238.0000	110.0000	2.1636	0.7189	1.3400	2.5400	0.6697	Jayananda et.al, 2000	
PG 20 (BAN)	TTG Gneiss	193.0000	72.0000	0.3731	0.7427	1.0800	2.5400	0.7029	Jayananda et.al, 2000	
Ind 61A	Late Archaen K-Granite	267.0000	134.0000	0.5019	0.7544	1.4500	2.5400	0.7011	Jayananda et.al, 2000	
Ind 61b	Late Archaen K-Granite	206.0000	150.0000	0.7282	0.7769	2.1300	2.5400	0.6986	Jayananda et.al, 2000	
Ind 61d	Late Archaen K-Granite	292.0000	110.0000	0.3767	0.7399	1.0700	2.5400	0.7006	Jayananda et.al, 2000	
KR 421 (EG)	Granite	330.2000	55.5000	0.1681	0.7222	0.4867	2.5000	0.7050	Rickers et. al, 2001	
KR78-1	Tonalitic Gneiss	46.6900	200.0000	4.2836	1.2572	13.0300	2.5000	0.7860	Rickers et. al, 2001	
KR47-1	Granite	216.4000	194.0000	0.8965	0.7660	2.6100	2.5000	0.6720	Rickers et. al, 2001	

Table 3c. Pb-Pb isotope data from Ayyarmalai

Sample	Rock Type	Pb ppm	U ppm	Th ppm	Measured			At 2.5Ga		
					206/204Pb	207/204 Pb	208/204 Pb	*I* (206/204Pb)	*I* (207/204 Pb)	*I* (208/204 Pb)
SR-57	Charnockite	34.5	6.5	34	22.8267	17.3980	44.6398	15.3198	16.1649	34.2548
SR-84	Charnockite	18.5	0.5	9	22.6738	15.9205	38.3312	20.1349	15.5034	34.5488
SR-68H	Alkali Granite	36	2.2	44.5	20.6806	16.9530	46.7797	19.6660	16.7707	41.5800
SR-861	Alkali Granite	38.50	4.20	35	24.3542	17.7484	49.2899	20.1888	17.0841	37.2930

Table 3d. Oxygen Isotope data from Ayyarmalai

Sample	Rock Type	δO^{18}wr(SMOW)	Duplicate	δO^{18} Qtz
SR-6	Gt-rich Charnockite	5.4	4.99	5.83
SR-57	Hbl-rich Charnockite	-0.11	-0.1	-
SR-84	Gt-rich Charnockite	4.56	-	-
SR-87	Dehydration Vein	1.79	-	-
SR-68H	Alkali Granite	2.96	-	2.89
SR-861	Alkali di-Granite	0.73	-	0.79

Table 4. LA-ICP-MS U-Pb zircon geochronology data

Grain Spot	$^{232}Th/^{238}U$	Cores v. Rims	Radiogenic Ratios						Age (Ma)						Discord.
			$^{207}Pb/^{206}Pb$	1σ	$^{207}Pb/^{235}U$	1σ	$^{206}Pb/^{238}U$	1σ	$^{207}Pb/^{206}Pb$	1σ	$^{207}Pb/^{235}U$	1σ	$^{206}Pb/^{238}U$	1σ	
Sample SR - 68H Ayyarmalai Pink Granite															
5801	0.54	Core	0.18407	0.00184	12.46391	0.15926	0.49146	0.00632	2689.9	16.39	2640	12.01	2577	27.31	96%
5802	0.43	Rim	0.16127	0.00162	9.62222	0.12911	0.43293	0.00587	2469	16.85	2399.3	12.34	2318.9	26.4	94%
5803	0.17	Rim	0.1594	0.00157	8.92075	0.11976	0.4062	0.00556	2449.3	16.6	2329.9	12.26	2197.5	25.47	90%
5804	0.27	Rim	0.15967	0.00159	9.43564	0.12717	0.42869	0.00584	2452.1	16.77	2381.3	12.37	2299.8	26.33	94%
5805	0.36	Rim	0.17163	0.00174	11.00668	0.13697	0.46557	0.00578	2573.6	16.84	2523.7	11.58	2464.1	25.44	96%
5806	0.28	Rim	0.18166	0.00182	11.79921	0.15132	0.47133	0.00608	2668.1	16.49	2588.6	12	2489.4	26.62	93%
5807	0.38	Core	0.18096	0.00181	11.84891	0.15027	0.47528	0.00605	2661.7	16.51	2592.5	11.87	2506.7	26.45	94%
5808	0.17	Rim	0.15624	0.00156	6.70158	0.09171	0.31109	0.0043	2415.4	16.83	2072.8	12.09	1746.1	21.16	72%
5809	0.20	Rim	0.15892	0.00158	7.83932	0.10473	0.35793	0.00483	2444.2	16.77	2212.7	12.03	1972.4	22.92	81%
5810	0.65	Core	0.17332	0.00174	6.90272	0.08834	0.28902	0.00372	2589.9	16.63	2099	11.35	1636.6	18.62	63%
5811	0.19	Rim	0.1569	0.00154	8.74516	0.11825	0.40428	0.00559	2422.5	16.6	2311.8	12.32	2188.7	25.66	90%
5812	0.15	rim	0.15979	0.00158	9.80493	0.13019	0.44509	0.00602	2453.5	16.62	2416.6	12.23	2373.4	26.84	97%
5813	0.45	Core	0.17877	0.00177	11.1716	0.14543	0.45331	0.00599	2641.5	16.36	2537.5	12.13	2410	26.56	91%
5814	0.37	Rim	0.16646	0.00165	9.87631	0.12843	0.43038	0.00568	2522.4	16.55	2423.3	11.99	2307.4	25.59	91%
5815	0.59	Core	0.18151	0.00179	11.83955	0.15887	0.47315	0.00647	2666.7	16.28	2591.8	12.56	2497.4	28.31	94%
5816	0.86	Core	0.34875	0.00348	2.35931	0.0307	0.04907	0.00065	3701.6	15.1	1230.4	9.28	308.8	3.98	8%
5817	0.39	Core	0.1781	0.00176	11.90564	0.15577	0.48487	0.00646	2635.3	16.3	2597	12.26	2548.4	28.06	97%
5818	0.74	Rim	0.18103	0.00179	11.61758	0.15333	0.46548	0.00626	2662.3	16.29	2574.1	12.34	2463.7	27.53	93%
5819	0.52	Rim	0.18075	0.00181	9.32622	0.11834	0.37438	0.00478	2659.8	16.5	2370.6	11.64	2050	22.4	77%
5820	0.18	Rim	0.15766	0.00156	7.79452	0.10115	0.3586	0.00473	2430.7	16.67	2207.6	11.68	1975.6	22.44	81%
5821	0.18	Rim	0.15337	0.00153	5.70598	0.07352	0.26987	0.00352	2383.9	16.86	1932.3	11.13	1540.1	17.85	65%
5822	0.38	Core	0.1753	0.00177	11.68578	0.14897	0.48359	0.00619	2608.9	16.68	2579.6	11.92	2542.9	26.91	97%
5823	0.14	Rim	0.16345	0.00161	9.12315	0.11976	0.40488	0.00541	2491.6	16.5	2350.4	12.01	2191.5	24.83	88%
5824	0.53	Core	0.19986	0.00202	5.88581	0.07743	0.21362	0.00282	2825.1	16.36	1959.1	11.42	1248.1	15	44%
5825	0.36	Rim	0.15733	0.00152	9.35367	0.12807	0.43109	0.00616	2427.2	16.3	2373.3	12.56	2310.6	27.76	95%
5826	0.51	Rim	0.17887	0.00183	11.46012	0.14961	0.46464	0.00607	2642.4	16.92	2561.3	12.19	2460	26.73	93%
5827	0.24	Rim	0.15683	0.00154	9.06752	0.12624	0.41921	0.00605	2421.8	16.55	2344.8	12.73	2256.9	27.47	93%
5828	0.24	Rim	0.16518	0.00165	8.61093	0.1098	0.37812	0.00486	2509.4	16.67	2297.7	11.6	2067.5	22.75	82%
5829	0.45	Core	0.18066	0.00181	12.51296	0.16627	0.50241	0.00676	2658.9	16.47	2643.7	12.49	2624.2	29.02	99%
5830	0.42	Core	0.17721	0.00177	12.20669	0.15975	0.49959	0.0066	2626.9	16.54	2620.4	12.28	2612.1	28.37	99%
5831	0.65	Rim	0.17127	0.00169	9.88907	0.12679	0.41885	0.00549	2570.1	16.37	2424.5	11.82	2255.2	24.96	88%
5832	0.48	Rim	0.16258	0.0016	8.55273	0.11121	0.38161	0.00508	2482.7	16.52	2291.5	11.82	2083.8	23.72	84%
5833	0.32	Rim	0.16681	0.00164	9.84658	0.12704	0.42822	0.00567	2525.9	16.43	2420.5	11.89	2297.7	25.57	91%
5834	0.85	core	0.199	0.00196	7.27604	0.093	0.26523	0.00347	2818	15.99	2145.9	11.41	1516.5	17.68	54%
5835	0.26	Rim	0.16609	0.00163	8.73981	0.11181	0.38172	0.005	2518.6	16.4	2311.2	11.66	2084.3	23.35	83%
5836	0.45	Rim	0.17344	0.0017	9.48251	0.12197	0.3966	0.00522	2591.2	16.28	2385.9	11.82	2153.4	24.11	83%
5837	0.08	rim	0.11918	0.00117	3.07397	0.03953	0.1871	0.00246	1944	17.48	1426.2	9.85	1105.7	13.38	57%
5838	0.55	Rim	0.18069	0.00178	10.44769	0.14095	0.41945	0.00579	2659.2	16.24	2475.3	12.5	2258	26.32	85%
5839	0.23	Rim	0.15591	0.00154	9.1604	0.12429	0.42621	0.00594	2411.8	16.62	2354.2	12.42	2288.6	26.85	95%
5840	0.45	Rim	0.18081	0.00179	10.33033	0.14024	0.41446	0.00574	2660.4	16.35	2464.8	12.57	2235.3	26.14	84%
5841	0.16	Rim	0.15229	0.00149	7.6026	0.09807	0.36212	0.00478	2371.8	16.64	2185.2	11.58	1992.2	22.63	84%
5842	0.51	Core	0.17692	0.00174	11.52931	0.1495	0.47272	0.00627	2624.2	16.26	2567	12.12	2495.5	27.44	95%
5843	0.13	Rim	0.14019	0.00138	5.10056	0.06565	0.26391	0.00347	2229.6	16.92	1836.2	10.93	1509.8	17.71	68%
5844	0.12	Core	0.55059	0.00839	31.8689	0.50872	0.41986	0.00692	4382.7	22.1	3546.3	15.72	2259.9	31.42	52%
5845	0.43	Rim	0.17106	0.00169	10.85285	0.14128	0.46022	0.00612	2568	16.41	2510.6	12.1	2440.5	27.02	95%
5846	0.50	Rim	0.17587	0.00174	10.58225	0.13842	0.43647	0.00583	2614.3	16.36	2487.2	12.14	2334.8	26.16	89%
5847	0.53	Rim	0.1951	0.00193	10.97911	0.14854	0.4082	0.00565	2785.7	16.1	2521.4	12.59	2206.7	25.87	79%
5848	0.54	Rim	0.17024	0.00169	9.44914	0.12559	0.40263	0.00546	2560	16.51	2382.6	12.2	2181.1	25.09	85%
5849	0.40	Core	0.17454	0.00171	11.90518	0.15418	0.49476	0.00656	2601.7	16.25	2597	12.13	2591.2	28.29	100%
5850	0.19	Rim	0.15699	0.00154	9.07588	0.11752	0.41935	0.00556	2423.5	16.55	2345.7	11.84	2257.5	25.23	93%

Table 4 (Cont.) - U-Pb zircon geochronology data

Grain Spot	$^{232}Th/^{238}U$	Cores v. Rims	Radiogenic Ratios						Age (Ma)						Discord.
			$^{207}Pb/^{206}Pb$	1σ	$^{207}Pb/^{235}U$	1σ	$^{206}Pb/^{238}U$	1σ	$^{207}Pb/^{206}Pb$	1σ	$^{207}Pb/^{235}U$	1σ	$^{206}Pb/^{238}U$	1σ	
Sample SR-63 Ayyarmalai Grey Granite															
s1	0.16	rim	0.14585	0.00254	8.03431	0.14485	0.39736	0.0066	2297.8	29.6	2234.9	16.28	2156.9	30.46	94%
s2	0.46	core	0.16098	0.00198	7.82253	0.10991	0.35758	0.00503	2466	20.68	2210.8	12.65	1970.7	23.9	80%
s3	0.84	core	0.17169	0.00262	11.17707	0.18578	0.46601	0.00684	2574.2	25.31	2538	15.49	2466.1	30.06	96%
s4	0.19	rim	0.14794	0.00195	7.5276	0.11036	0.37773	0.00541	2322.2	22.43	2176.3	13.14	2065.7	25.31	89%
s5	0.35	core	0.18005	0.0021	11.73638	0.17279	0.47139	0.00676	2653.3	19.25	2583.6	13.77	2489.7	29.61	94%
s6	0.20	core	0.15846	0.00188	6.97033	0.10145	0.31809	0.00448	2439.3	19.93	2107.7	12.92	1780.4	21.91	73%
s7	0.33	rim	0.16704	0.00249	10.7251	0.17435	0.46368	0.00679	2528.2	24.82	2499.6	15.1	2455.8	29.88	97%
s8	0.37	core	0.18115	0.00228	12.06153	0.1779	0.48132	0.00671	2663.5	20.74	2609.2	13.83	2533	29.21	95%
s9	0.21	rim	0.17203	0.0019	11.38741	0.15932	0.47611	0.00641	2577.5	18.32	2555.4	13.06	2510.3	27.97	97%
s10	0.35	core	0.17529	0.0021	11.60045	0.16231	0.47751	0.00649	2608.8	19.81	2572.7	13.08	2516.4	28.31	96%
s11	0.18	rim	0.15321	0.00207	8.9545	0.13937	0.42382	0.0062	2382	22.88	2333.4	14.22	2277.8	28.07	96%
s12	0.47	core	0.17261	0.00409	10.94326	0.25403	0.45871	0.0084	2583.2	39.07	2518.3	21.6	2433.8	37.12	94%
s13	0.13	rim	0.15048	0.00175	8.54282	0.11059	0.41361	0.00524	2351.3	19.73	2290.5	11.77	2231.4	23.89	95%
s14	0.37	core	0.17433	0.00181	11.4992	0.14916	0.4773	0.00619	2599.7	17.2	2564.5	12.12	2515.5	27.03	97%
s15	0.16	core	0.17099	0.00188	11.77373	0.15988	0.49823	0.00658	2567.4	18.22	2586.6	12.71	2606.2	28.3	102%
s16	0.18	rim	0.15423	0.00218	8.82745	0.13523	0.41599	0.00588	2393.4	23.86	2320.3	13.97	2242.3	26.78	94%
s17	0.20	rim	0.15784	0.00223	9.39439	0.13157	0.43373	0.00565	2432.7	23.8	2377.3	12.85	2322.5	25.39	95%
s18	0.42	core	0.17412	0.00205	11.29704	0.15161	0.47014	0.00604	2597.7	19.46	2548	12.52	2484.2	26.5	96%
s19	0.37	core	0.18485	0.00383	12.83204	0.26023	0.50229	0.00805	2696.8	33.83	2667.4	19.1	2623.6	34.55	97%
s20	0.16	rim	0.15538	0.00185	6.95611	0.09715	0.32477	0.00427	2406	20.09	2105.8	12.4	1813	20.78	75%
S21	0.31	core	0.17479	0.00211	11.46798	0.15044	0.47601	0.00623	2562	12.25	2562	12.25	2509.9	27.2	98%
S22	0.13	rim	0.16537	0.00502	10.6273	0.14279	0.46574	0.00593	2491.1	12.47	2491.1	12.47	2464.9	26.06	99%
S23	0.20	rim	0.16419	0.00191	9.8059	0.12576	0.43338	0.00553	2416.7	11.82	2416.7	11.82	2320.9	24.88	96%
S24	1.13	core	0.10743	0.00183	1.30793	0.03088	0.08844	0.00143	849.2	13.58	849.2	13.58	546.3	8.47	64%
S25	0.82	rim	0.18971	0.00196	2.15716	0.03104	0.08247	0.00114	1167.4	9.98	1167.4	9.98	510.8	6.79	44%
S26	0.14	rim	0.15794	0.00222	8.8272	0.11424	0.40552	0.00525	2320.3	11.8	2320.3	11.8	2194.4	24.09	95%
S27	0.30	rim	0.17367	0.00284	10.73086	0.14153	0.44828	0.00591	2500.1	12.25	2500.1	12.25	2387.6	26.3	96%
S28	0.15	rim	0.15058	0.00239	7.4168	0.09538	0.35748	0.0046	2163	11.51	2163	11.51	1970.2	21.83	91%
S29	0.35	core	0.17366	0.00435	10.53323	0.17575	0.44002	0.00655	2482.8	15.47	2482.8	15.47	2350.7	29.34	95%
S30	0.28	core	0.16275	0.00191	9.38393	0.12153	0.41839	0.00544	2376.3	11.88	2376.3	11.88	2253.2	24.72	95%
S31	0.35	rim	0.17549	0.00199	11.37978	0.15009	0.47069	0.00602	2610.7	18.8	2554.8	12.31	2486.6	26.37	95%
S32	0.31	core	0.16726	0.00188	10.87468	0.15046	0.47148	0.00643	2530.4	18.77	2512.5	12.87	2490.1	28.17	98%
S33	0.11	core	0.17249	0.00273	10.57504	0.17051	0.44428	0.00627	2582	26.2	2486.5	14.96	2369.8	27.98	92%
S34	0.35	core	0.17903	0.00442	10.37048	0.24219	0.42064	0.00744	2643.9	40.36	2468.4	21.63	2263.4	33.77	86%
S35	0.17	rim	0.17717	0.0028	10.62148	0.17217	0.43476	0.00605	2626.6	26.05	2490.6	15.04	2327.1	27.18	89%
S36	0.17	rim	0.16627	0.00258	9.20836	0.14571	0.4023	0.00549	2520.4	25.85	2358.9	14.49	2179.6	25.24	86%
S37	0.26	core	0.18264	0.00218	11.05813	0.15256	0.43912	0.0059	2677	19.62	2528	12.85	2346.7	26.44	88%
S38	0.33	rim	0.17463	0.00262	10.28408	0.16647	0.4265	0.00622	2602.6	24.81	2460.7	14.98	2289.9	28.13	88%
S39	0.16	core	0.16169	0.00345	7.1613	0.14693	0.32176	0.00513	2473.4	35.53	2131.7	18.28	1798.3	25.02	73%
S40	0.25	core	0.15991	0.00182	8.83014	0.11395	0.40089	0.00505	2454.7	19.13	2320.6	11.77	2173.1	23.24	89%

Table 4 (Cont.) - U-Pb zircon geochronology data

Grain Spot	$^{232}Th/^{238}U$	Cores v. Rims	Radiogenic Ratios						Age (Ma)						Discord.
			$^{207}Pb/^{206}Pb$	1σ	$^{207}Pb/^{235}U$	1σ	$^{206}Pb/^{238}U$	1σ	$^{207}Pb/^{206}Pb$	1σ	$^{207}Pb/^{235}U$	1σ	$^{206}Pb/^{238}U$	1σ	
Sample SR -57 Ayyarmalai Hornblende rich Charnockite															
5701	0.36	Core	0.18033	0.00189	12.54251	0.16549	0.50474	0.00663	2655.9	17.25	2645.9	12.41	2634.1	28.4	99%
5702	0.34	Rim	0.15379	0.00169	7.32117	0.10207	0.34552	0.00473	2388.5	18.55	2151.4	12.46	1913.2	22.67	80%
5703	0.18	Rim	0.15783	0.0016	9.37879	0.13332	0.43123	0.00632	2432.5	17.04	2375.8	13.04	2311.3	28.47	95%
5704	0.09	Core	0.17229	0.00172	11.24567	0.15445	0.47362	0.00659	2580	16.61	2543.7	12.81	2499.4	28.83	97%
5705	0.18	Rim	0.16261	0.00163	9.74911	0.12793	0.43517	0.00576	2483	16.85	2411.4	12.08	2329	25.88	94%
5706	0.35	Rim	0.16259	0.00191	8.43282	0.12796	0.37632	0.00556	2482.8	19.71	2278.7	13.77	2059.1	26.04	83%
5707	0.17	Rim	0.16385	0.00164	10.36747	0.14346	0.45908	0.00644	2495.8	16.79	2468.1	12.81	2435.5	28.46	98%
5708	0.48	Rim	0.16168	0.00164	9.69156	0.13282	0.43493	0.006	2473.3	17.02	2405.9	12.61	2327.9	26.97	94%
5709	0.10	Rim	0.16118	0.0016	9.89251	0.13927	0.44524	0.00638	2468.1	16.72	2424.8	12.98	2374.1	28.45	96%
5710	0.20	Rim	0.16231	0.00163	9.41967	0.12492	0.42106	0.00562	2479.9	16.84	2379.7	12.17	2265.3	25.49	91%
5711	0.40	Core	0.16797	0.00181	9.9691	0.14522	0.43052	0.00633	2537.5	17.95	2431.9	13.44	2308.1	28.54	91%
5712	0.23	Rim	0.15847	0.00158	9.34651	0.12475	0.42781	0.00577	2439.4	16.8	2372.6	12.24	2295.8	26.05	94%
5713	0.52	Core	0.16884	0.00183	10.17533	0.14669	0.43731	0.00629	2546.2	18.05	2450.8	13.33	2338.6	28.2	92%
5714	0.25	Rim	0.15659	0.00157	8.60851	0.11368	0.39874	0.00531	2419.1	16.96	2297.5	12.01	2163.2	24.46	89%
5716	0.02	Rim	0.17462	0.00177	0.94214	0.13964	0.13065	0.00518	324.4	317.44	674	73.01	791.5	29.51	244%
5715	0.35	Core	0.0529	0.00818	11.48164	0.15433	0.47689	0.00645	2602.4	16.83	2563.1	12.55	2513.7	28.17	97%
5717	0.42	Core	0.17859	0.0018	12.45941	0.16856	0.506	0.00693	2639.8	16.68	2639.7	12.72	2639.5	29.65	100%
5718	0.38	core	0.15959	0.00164	8.74037	0.12248	0.39715	0.00566	2451.3	17.33	2311.3	12.77	2155.9	26.12	88%
5719	0.14	Rim	0.15826	0.00156	9.34736	0.12522	0.42835	0.00586	2437.1	16.6	2372.7	12.29	2298.3	26.46	94%
5720	0.14	Rim	0.15649	0.00154	9.53111	0.12737	0.44168	0.00604	2418.1	16.55	2390.6	12.28	2358.1	27.03	98%
5721	0.43	Core	0.16863	0.0017	10.22283	0.13829	0.43981	0.00605	2544.1	16.81	2455.1	12.51	2349.8	27.11	92%
5722	0.21	Rim	0.16216	0.00161	10.25566	0.1384	0.45877	0.00636	2478.3	16.6	2458.1	12.49	2434.1	28.09	98%
5723	0.09	Rim	0.15362	0.0015	8.8192	0.11765	0.41646	0.00571	2386.7	16.52	2319.5	12.17	2244.4	26	94%
5724	0.36	Core	0.16458	0.00166	10.04036	0.13861	0.44264	0.00624	2503.2	16.88	2438.5	12.75	2362.5	27.89	94%
5725	0.38	Core	0.17944	0.00185	11.21301	0.15364	0.45328	0.0062	2647.7	16.98	2541	12.77	2409.8	27.49	91%
5726	0.35	Core	0.17366	0.00184	10.48103	0.14717	0.43775	0.00609	2593.3	17.56	2478.2	13.02	2340.6	27.3	90%
5727	0.11	Rim	0.15665	0.00156	8.94281	0.12105	0.41413	0.00565	2419.8	16.83	2332.2	12.36	2233.8	25.73	92%
5728	0.37	Core	0.17368	0.00182	11.44419	0.1596	0.47796	0.00662	2593.4	17.41	2560	13.02	2518.4	28.86	97%
5729	0.03	Rim	0.07972	0.00094	1.1443	0.01772	0.10412	0.00153	1190.1	23.18	774.5	8.39	638.5	8.91	54%
5730	0.22	Rim	0.15862	0.00159	9.35559	0.12926	0.42782	0.00596	2441	16.84	2373.5	12.67	2295.9	26.93	94%
5731	0.29	Rim	0.15856	0.00159	9.21307	0.12571	0.42152	0.00581	2440.3	16.92	2359.4	12.5	2267.4	26.34	93%
5732	0.38	Core	0.18242	0.00191	12.67014	0.17631	0.50386	0.00701	2675	17.26	2655.4	13.1	2630.3	30.04	98%
5733	0.12	Core	0.16547	0.00165	11.29492	0.15369	0.49518	0.00682	2512.4	16.7	2547.8	12.69	2593	29.39	103%
5734	0.12	Rim	0.15928	0.00162	9.09879	0.12468	0.41441	0.00572	2448	17.07	2348	12.54	2235.1	26.06	91%
5735	0.34	Core	0.16888	0.00178	10.13223	0.14144	0.43524	0.00605	2546.6	17.6	2446.9	12.9	2329.3	27.18	91%
5736	0.11	Core	0.17181	0.00172	10.92497	0.14884	0.4613	0.00635	2575.4	16.66	2516.8	12.67	2445.3	28.01	95%
5737	0.12	Rim	0.16382	0.00166	9.54373	0.13075	0.42264	0.00583	2495.5	17	2391.8	12.59	2272.4	26.41	91%
5738	0.35	Core	0.17361	0.00182	10.51787	0.14638	0.43951	0.0061	2592.7	17.42	2481.5	12.9	2348.5	27.33	91%
5739	0.36	Core	0.17345	0.00186	11.0285	0.15498	0.46126	0.00643	2591.3	17.78	2525.5	13.08	2445.1	28.36	94%
5740	0.11	Core	0.17261	0.00173	10.73702	0.1463	0.45127	0.00621	2583.1	16.66	2500.6	12.66	2400.9	27.58	93%
5741	0.11	Rim	0.16363	0.00163	9.02421	0.12695	0.40034	0.00578	2493.6	16.66	2340.5	12.86	2170.6	26.61	87%
5744	0.42	Core	0.17113	0.00173	10.6659	0.14511	0.45205	0.00621	2568.7	16.81	2494.5	12.63	2404.4	27.57	94%
5745	0.47	Rim	0.15749	0.0016	8.6881	0.12104	0.40016	0.00563	2428.9	17.09	2305.8	12.69	2169.8	25.94	89%
5746	0.19	Rim	0.16171	0.00164	10.1206	0.13846	0.45406	0.00626	2473.7	16.96	2445.9	12.64	2413.3	27.76	98%
5747	0.08	Rim	0.15953	0.00157	9.55168	0.12891	0.43426	0.00596	2450.7	16.6	2392.5	12.41	2324.9	26.8	95%
5748	0.52	Rim	0.15605	0.00161	8.43055	0.12009	0.39205	0.0056	2413.3	17.37	2278.5	12.93	2132.3	25.94	88%
5749	0.18	Rim	0.165	0.00168	10.59037	0.14544	0.46556	0.00644	2507.5	17.04	2487.9	12.74	2464.1	28.32	98%
5750	0.09	Rim	0.15996	0.00161	9.03338	0.12807	0.40973	0.00586	2455.3	16.89	2341.4	12.96	2213.7	26.79	90%

Table 4 (Cont.) - U-Pb zircon geochronology data

Grain Spot	$^{232}Th/^{238}U$	Cores v. Rims	Radiogenic Ratios						Age (Ma)						Discord.
			$^{207}Pb/^{206}Pb$	1σ	$^{207}Pb/^{235}U$	1σ	$^{206}Pb/^{238}U$	1σ	$^{207}Pb/^{206}Pb$	1σ	$^{207}Pb/^{235}U$	1σ	$^{206}Pb/^{238}U$	1σ	
Sample SR - 6 Ayyarmalai Garnet rich Charnockite															
SR6.1	0.14	Rim	0.17801	0.00206	11.08643	0.17117	0.45977	0.00637	2634.4	19.06	2530.4	14.38	2438.5	28.14	93%
SR6.2	0.32	Core	0.14746	0.00431	8.11201	0.22175	0.39475	0.0079	2316.6	49.26	2243.6	24.71	2144.8	36.53	93%
SR6.3	0.12	Core	0.19917	0.00284	12.02318	0.21135	0.46571	0.00699	2819.4	23.08	2606.2	16.48	2464.7	30.75	87%
SR6.5	0.32	Rim	0.13351	0.00107	6.62514	0.0571	0.3401	0.00355	2144.7	13.88	2062.7	7.6	1887.1	17.07	88%
SR6.6	0.37	Core	0.12436	0.00113	6.14619	0.05706	0.318	0.00316	2019.6	16.07	1996.8	8.11	1780	15.46	88%
SR6.7	0.32	Rim	0.11757	0.0014	5.02217	0.05836	0.29744	0.0035	1919.7	21.19	1823.1	9.84	1678.6	17.37	87%
SR6.8	0.46	Rim	0.0784	0.00143	1.01484	0.01784	0.08875	0.00109	1157.1	35.88	711.3	8.99	548.1	6.45	47%
SR6.9	0.14	Core	0.19319	0.0036	12.15344	0.21585	0.47273	0.00665	2769.5	30.23	2616.3	16.66	2495.5	29.09	90%
SR6.10	0.46	Rim	0.1488	0.0018	7.41209	0.09774	0.36507	0.0047	2332.1	20.53	2162.4	11.8	2006.1	22.19	86%
SR6.11	0.28	Rim	0.17227	0.0017	12.34254	0.16028	0.51956	0.00705	2579.9	16.36	2630.8	12.2	2697.3	29.9	105%
SR6.12	0.50	Rim	0.17776	0.00184	12.74457	0.17251	0.52119	0.00719	2632.1	17.14	2661	12.74	2704.2	30.46	103%
SR6.13	0.21	Rim	0.17608	0.0019	12.02064	0.16302	0.49738	0.00678	2616.3	17.84	2606	12.71	2602.5	29.19	99%
SR6.14	0.36	core	0.16789	0.0035	10.98384	0.22964	0.47155	0.00797	2536.8	34.58	2521.8	19.46	2490.4	34.9	98%
SR6.15	0.14	rim	0.15505	0.00212	8.26593	0.13527	0.38639	0.00595	2402.4	23.04	2260.6	14.82	2106.1	27.65	88%
SR6.16	0.07	Core	0.17923	0.002	11.72493	0.16811	0.47487	0.00677	2645.8	18.38	2582.7	13.41	2504.9	29.58	95%
SR6.17	0.54	Rim	0.28329	0.00288	21.54768	0.29734	0.55373	0.00778	3381.2	15.78	3163.6	13.39	2840.7	32.29	84%
SR6.18	0.14	Core	0.17922	0.0018	11.84725	0.14986	0.48435	0.00626	2645.7	16.58	2592.4	11.84	2546.2	27.2	96%
SR6.19	0.40	Rim	0.15057	0.00237	7.15905	0.12555	0.34463	0.00549	2352.4	26.62	2131.4	15.62	1908.9	26.31	81%
SR6.20	0.45	core	0.14732	0.00456	6.69016	0.19534	0.33043	0.00691	2315	52.16	2071.3	25.79	1840.5	33.49	80%
SR6.21	0.60	rim	0.16221	0.00206	9.96952	0.14292	0.4463	0.0059	2478.8	21.32	2432	13.23	2378.8	26.3	96%
SR6.22	0.12	rim	0.13031	0.00209	4.53833	0.07777	0.25419	0.00386	2102.1	27.92	1738	14.26	1460	19.84	69%
SR6.23	0.41	Core	0.18101	0.00194	12.43769	0.17373	0.49847	0.0068	2662.1	17.68	2638	13.13	2607.2	29.24	98%
SR6.24	0.30	Rim	0.15902	0.00191	8.26807	0.12493	0.37743	0.00547	2445.2	20.17	2260.8	13.69	2064.3	25.62	84%
SR6.25	0.08	Core	0.18466	0.00199	12.98243	0.1819	0.50997	0.00697	2695.2	17.71	2678.4	13.21	2656.5	29.75	99%
SR6.26	0.38	Core	0.18602	0.00197	13.91408	0.19391	0.54265	0.00744	2707.3	17.33	2743.9	13.2	2794.6	31.07	103%
SR6.27	0.48	Core	0.1764	0.00185	11.79947	0.15845	0.4853	0.00643	2619.3	17.37	2588.6	12.57	2550.3	27.91	97%
SR6.28	0.08	Rim	0.15229	0.00201	8.34917	0.13176	0.39878	0.00613	2371.8	22.35	2269.7	14.31	2163.4	28.27	91%
SR6.29	1.41	Core	0.18216	0.00195	12.71613	0.18061	0.50642	0.00705	2672.6	17.64	2658.9	13.37	2641.3	30.18	99%
SR6.30	0.21	Core	0.17873	0.00185	12.23658	0.16736	0.49668	0.00673	2641.1	17.1	2622.7	12.84	2599.5	28.98	98%
Sample SR - 55 Charnockite Gneiss															
SR55.1	1.120	core	0.1596	0.00159	9.89681	0.12312	0.44984	0.00568	2451.4	16.79	2425.2	11.47	2394.5	25.24	98%
SR55.2	0.312	core	0.17036	0.00171	10.08992	0.12563	0.42963	0.00541	2561.2	16.68	2443	11.5	2304.1	24.4	90%
SR55.3	0.239	rim	0.16434	0.00165	8.35653	0.10445	0.36891	0.00467	2500.8	16.79	2270.5	11.34	2024.3	21.99	81%
SR55.4	0.038	rim	0.15507	0.00159	7.3197	0.09962	0.3427	0.00472	2402.6	17.36	2151.2	12.16	1899.6	22.67	79%
SR55.5	0.381	core	0.16777	0.00184	8.81523	0.12321	0.38157	0.00527	2535.6	18.26	2319.1	12.75	2083.6	24.6	82%
SR55.6	0.485	rim	0.15717	0.00157	8.12842	0.10212	0.37529	0.00478	2425.4	16.86	2245.4	11.36	2054.2	22.39	85%
SR55.7	0.296	core	0.16048	0.00165	6.98577	0.09377	0.3159	0.00425	2460.7	17.3	2109.6	11.92	1769.7	20.83	72%
SR55.8	0.239	rim	0.16325	0.00163	8.03537	0.10056	0.35718	0.00453	2489.6	16.68	2235	11.3	1968.8	21.51	79%
SR55.9	0.228	rim	0.15572	0.00155	7.67531	0.09637	0.35765	0.00456	2409.7	16.78	2193.7	11.28	1971	21.63	82%
SR55.10	0.229	core	0.14897	0.00155	5.95945	0.07334	0.29032	0.00356	2334.1	17.75	1969.9	10.7	1643.1	17.77	70%
SR55.11	0.150	rim	0.15408	0.00161	8.119	0.10952	0.38225	0.0051	2391.7	17.72	2244.4	12.19	2086.8	23.8	87%
SR55.12	0.284	core	0.17159	0.00188	10.87829	0.14752	0.4599	0.00603	2573.2	18.19	2512.8	12.61	2439.1	26.64	95%
SR55.13	1.165	core	0.15354	0.00164	7.85391	0.1093	0.37103	0.00511	2385.7	18.03	2214.4	12.54	2034.3	24.04	85%
SR55.14	0.372	core	0.17755	0.00182	11.21357	0.14876	0.45813	0.00609	2630.1	16.92	2541	12.37	2431.3	26.92	92%
SR55.15	0.372	core	0.2126	0.00225	11.31802	0.15484	0.38618	0.00526	2925.4	17.02	2549.7	12.76	2105.1	24.48	72%
SR55.16	0.354	rim	0.17457	0.00184	11.23853	0.15793	0.46698	0.0065	2601.9	17.5	2543.1	13.1	2470.3	28.57	95%
SR55.17	0.288	rim	0.17621	0.00177	11.13626	0.15003	0.45845	0.00623	2617.5	16.66	2534.6	12.55	2432.7	27.53	93%
SR55.18	0.611	core	0.15893	0.00162	9.03066	0.12405	0.41217	0.00567	2444.3	17.17	2341.1	12.56	2224.8	25.88	91%
SR55.19	0.407	core	0.16852	0.0018	9.61546	0.13773	0.41383	0.00586	2543	17.83	2398.7	13.17	2232.4	26.73	88%
SR55.20	0.249	rim	0.16963	0.00175	9.80025	0.1387	0.41903	0.00594	2554	17.15	2416.2	13.04	2256.1	26.97	88%
SR55.21	0.234	core	0.1702	0.00173	11.19087	0.14544	0.47699	0.00621	2559.6	16.96	2539.2	12.11	2514.2	27.11	98%
SR55.22	0.107	rim	0.16456	0.00163	9.04931	0.11971	0.39891	0.00534	2503	16.61	2343	12.1	2164	24.62	86%
SR55.23	1.056	core	0.15246	0.00176	7.24321	0.10603	0.34468	0.00487	2373.7	19.57	2141.8	13.06	1909.1	23.35	80%

Note: Uncertainties are given at 1σ level, 100% denotes a concordant analysis.

Table 5a: Representative Compositions of hornblendes

Rock Type	Hornblende Rich Charnockite						Garnet Rich Charnockites				Pink Granite			
Sample No.	SR - 57	SR - 57	SR - 57	SR - 57	SR - 57	SR-57	SR - 84	SR - 84	SR - 84	SR - 84	SR- 71	SR - 71	SR- 71	SR - 71
Oxides %	Core	Rim	Core	Rim	Core	Rim	Core	Rim	Core	Rim	Core	Rim	Core	Rim
SiO_2	39.195	38.610	39.587	39.129	39.770	39.857	39.525	33.598	40.164	39.486	42.477	42.113	41.903	40.201
TiO_2	2.394	2.520	2.478	2.253	2.272	2.169	1.970	4.101	1.538	2.090	1.842	1.723	1.582	1.644
Al_2O_3	10.559	10.543	10.788	10.727	10.820	10.765	10.933	13.013	10.831	10.408	8.495	8.132	7.872	8.277
FeO	27.067	26.363	27.388	26.403	27.973	27.644	26.946	29.303	27.970	27.685	21.639	21.464	21.690	22.030
MnO	0.305	0.320	0.291	0.371	0.305	0.333	0.145	0.089	0.208	0.075	0.471	0.549	0.492	0.515
MgO	2.619	2.708	2.758	2.791	2.728	2.681	3.566	4.347	3.553	3.586	8.129	8.304	8.156	7.609
CaO	10.274	10.485	10.631	10.449	10.661	10.399	10.948	0.096	11.097	10.780	10.884	10.911	10.782	10.880
Na_2O	1.665	1.659	1.816	1.733	1.646	1.652	1.482	0.453	1.487	1.770	2.128	2.007	2.187	2.023
K_2O	1.551	1.448	1.622	1.570	1.652	1.593	1.471	8.720	1.357	1.485	1.348	1.272	1.245	1.329
P_2O_3	0.007	0.010	0.001	0.000	0.013	0.013	0.011	0.016	0.009	0.007	0.017	0.000	0.000	0.000
Cl	0.286	0.281	0.250	0.277	0.261	0.258	0.327	0.458	0.316	0.375	0.279	0.223	0.291	0.263
F	0.202	0.324	0.427	0.339	0.290	0.282	0.215	0.379	0.230	0.193	0.740	0.652	0.694	0.531
Total	96.122	95.271	98.035	96.041	98.392	97.646	97.539	94.572	98.759	97.940	98.449	97.349	96.892	95.303
	Formula unit on 23 Oxygen basis													
Si	5.121	5.103	5.077	5.124	5.071	5.122	6.025	5.290	6.055	5.995	6.241	6.255	6.257	6.112
Ti	0.235	0.251	0.239	0.222	0.218	0.210	0.226	0.486	0.174	0.239	0.204	0.193	0.178	0.188
Al	1.626	1.642	1.630	1.655	1.626	1.630	1.964	2.415	1.924	1.862	1.471	1.423	1.385	1.483
Fe^{3+}	6.196	6.122	4.228	4.154	4.299	4.209	4.045	5.594	4.103	4.249	4.084	4.138	4.215	4.449
Fe^{2+}	-0.876	-0.881	1.056	1.047	1.067	1.134	-0.611	-1.736	-0.577	-0.734	-1.426	-1.472	-1.507	-1.648
Mn^{2+}	0.070	0.075	0.066	0.086	0.069	0.076	0.019	0.012	0.026	0.010	0.059	0.069	0.062	0.066
Mg	0.510	0.534	0.527	0.545	0.518	0.514	0.810	1.020	0.799	0.812	1.781	1.839	1.815	1.725
Ca	1.438	1.485	1.461	1.466	1.456	1.432	1.788	0.016	1.792	1.753	1.713	1.736	1.725	1.772
Na	0.422	0.425	0.451	0.440	0.407	0.412	0.438	0.138	0.435	0.521	0.606	0.578	0.633	0.596
K	0.258	0.244	0.265	0.262	0.269	0.261	0.286	1.751	0.261	0.288	0.253	0.241	0.237	0.258
P	0.001	0.001	0.000	0.000	0.001	0.001	0.010	0.013	0.007	0.006	0.014	0.000	0.000	0.000
F	0.063	0.063	0.054	0.061	0.056	0.056	0.055	0.101	0.059	0.050	0.344	0.306	0.328	0.255
Cl	0.084	0.135	0.173	0.140	0.117	0.114	0.157	0.228	0.151	0.180	0.070	0.056	0.074	0.068
Cation	15.147	15.198	16.518	16.489	15.174	15.171	15.222	15.343	15.217	15.236	15.428	15.362	15.401	15.323
X_{Mg}	0.241	0.247	0.091	0.095	0.088	0.088	0.191	0.209	0.185	0.188	0.401	0.408	0.401	0.381

Table 5b: Representative Compositions of Orthopyroxenes

Rock Type	Hornblende Rich Charnockite						Garnet Rich Charnockites			
Sample No.	SR - 57	SR - 57	SR - 57	SR - 57	SR - 57	SR-57	SR - 84	SR - 84	SR - 84	SR - 84
Oxides %	Core	Rim	Core	Rim	Core	Rim	Core	Rim	Core	Rim
SiO_2	47.737	47.238	46.882	47.389	46.237	46.860	47.559	46.222	45.426	45.830
TiO_2	0.097	0.090	0.037	0.086	0.041	0.012	0.099	0.118	0.117	0.112
Al_2O_3	0.300	0.288	0.252	0.323	0.486	0.398	0.389	0.405	0.473	0.402
FeO	42.894	43.596	44.690	43.880	42.240	42.958	42.910	42.385	43.351	44.974
MnO	1.179	1.117	1.317	1.454	1.229	1.203	0.771	0.853	0.605	0.611
MgO	5.296	5.376	4.072	4.204	5.102	5.204	6.409	6.192	6.044	5.899
CaO	0.642	0.830	0.672	0.829	0.930	0.960	0.962	0.892	0.815	0.853
Na_2O	0.011	0.000	0.057	0.035	0.037	0.036	0.000	0.108	0.001	0.016
K_2O	0.000	0.008	0.012	0.004	0.008	0.016	0.021	0.006	0.004	0.000
P_2O_3	0.017	0.000	0.000	0.000	0.000	0.004	0.000	0.006	0.009	0.004
Cl	0.024	0.006	0.017	0.002	0.006	0.023	0.441	0.415	0.291	0.418
F	0.345	0.363	0.236	0.288	0.365	0.330	0.000	0.020	0.000	0.001
Total	98.543	98.911	98.244	98.493	96.680	98.004	99.561	97.621	97.135	99.121
	Formula unit on 6 Oxygen basis									
Si	1.522	1.527	1.516	1.533	1.526	1.524	1.997	1.980	1.959	1.945
Ti	0.002	0.002	0.001	0.002	0.001	0.000	0.003	0.004	0.004	0.004
Al	0.011	0.020	0.010	0.012	0.019	0.015	0.019	0.020	0.024	0.020
Fe^{3+}	0.903	0.881	0.935	0.890	0.892	0.903	0.000	0.000	0.012	0.029
Fe^{2+}	1.211	1.228	1.239	1.246	1.204	1.199	1.507	1.518	1.551	1.567
Mn^{2+}	0.064	0.065	0.075	0.083	0.072	0.069	0.027	0.031	0.022	0.022
Mg	0.258	0.248	0.196	0.203	0.251	0.252	0.401	0.395	0.388	0.373
Ca	0.029	0.027	0.023	0.029	0.033	0.033	0.043	0.041	0.038	0.039
Na	0.000	0.000	0.004	0.002	0.002	0.002	0.000	0.009	0.000	0.001
K	0.000	0.000	0.000	0.000	0.000	0.001	0.001	0.000	0.000	0.000
P	0.000	0.000	0.000	0.000	0.000	0.000	0.000	0.001	0.002	0.001
F	0.000	0.000	0.001	0.000	0.000	0.001	0.000	0.001	0.000	0.000
Cl	0.037	0.039	0.024	0.029	0.038	0.034	0.059	0.056	0.040	0.056
Cation	4.306	4.325	4.025	4.030	4.038	4.035	4.059	4.059	4.042	4.057
X_{Mg}	0.109	0.109	0.083	0.087	0.107	0.107	0.210	0.207	0.199	0.190

Table 5c: Representative Compositions of Clinopyroxenes

Rock Type	Hornblende rich Charnockite				Garnet rich Charnockite				Grey Granites					
Sample No.	SR - 57	SR - 57	SR - 57	SR - 57	SR - 84	SR - 84	SR - 84	SR - 84	SR 85	SR85	SR 85	SR85	SR85	SR85
Oxides %	Core	Rim	Core	Rim	Core	Rim	Core	Rim	Core	Rim	Core	Rim	Core	Rim
SiO_2	48.878	48.700	48.450	49.321	46.151	43.964	44.720	39.660	48.7324	39.068	48.1712	46.3624	48.6089	47.4133
TiO_2	0.142	0.165	0.182	0.152	0.067	0.179	0.225	0.182	0.2401	0.1183	0.1301	0.1536	0.1483	0.1117
Al_2O_3	0.946	0.994	1.271	0.962	0.382	3.252	3.504	2.549	1.2123	21.7941	1.1089	1.0439	1.2202	0.8873
FeO	23.525	23.448	28.052	24.444	42.256	31.955	31.562	37.737	20.9347	23.4364	20.1456	20.2339	20.6276	20.3329
MnO	0.491	0.639	0.784	0.717	0.790	0.695	0.584	0.379	1.1924	0.4656	1.2136	1.252	1.1892	1.2289
MgO	4.581	4.468	4.282	4.264	6.233	2.296	2.874	1.888	5.3238	10.7375	5.4688	5.5161	5.45	5.4921
CaO	19.434	19.110	14.306	18.673	1.012	2.011	2.281	1.479	20.8341	4.3101	20.7748	20.4563	20.6323	20.9058
Na_2O	0.325	0.408	0.257	0.339	0.158	0.187	0.062	0.203	0.9733	0.0251	0.8361	0.797	0.9321	0.8095
K_2O	0.004	0.012	0.011	0.013	0.048	0.531	0.222	0.238	0.029	0.0001	0.0217	0.0001	0.0171	0.0169
P_2O_3	0.016	0.001	0.031	0.000	0.000	0.000	0.000	0.000	0.0322	0.0322	0.032	0.032	0.0322	0.0322
Cl	0.006	0.017	0.010	0.013	0.272	0.261	0.241	0.363	0.0147	0.0001	0.0109	0.0197	0.015	0.0001
F	0.250	0.305	0.239	0.274	0.046	0.158	0.074	0.024	0.2248	0.2248	0.2248	0.2248	0.2248	0.2248
Total	98.598	98.265	97.874	99.169	97.414	85.489	86.350	84.701	99.744	100.212	98.139	96.092	99.098	97.456
						Formula unit on 6 Oxygen basis								
Si	1.705	1.704	1.672	1.706	1.977	2.148	2.154	1.989	1.926	1.479	1.933	1.901	1.932	1.917
Ti	0.004	0.004	0.005	0.004	0.002	0.007	0.008	0.007	0.007	0.003	0.004	0.005	0.004	0.003
Al	0.039	0.041	0.052	0.039	0.019	0.187	0.199	0.151	0.056	0.972	0.052	0.050	0.057	0.042
Fe^{3+}	0.537	0.536	0.059	0.534	0.000	0.000	0.000	0.000	0.124	0.039	0.111	0.171	0.114	0.153
Fe^{2+}	0.697	0.698	0.870	0.738	1.513	1.306	1.271	1.582	0.567	0.703	0.565	0.523	0.572	0.535
Mn^{2+}	0.030	0.039	0.048	0.044	0.029	0.029	0.024	0.016	0.040	0.015	0.041	0.043	0.040	0.042
Mg	0.238	0.233	0.220	0.220	0.398	0.167	0.206	0.141	0.314	0.606	0.327	0.337	0.323	0.331
Ca	0.726	0.716	0.529	0.692	0.046	0.105	0.118	0.079	0.882	0.175	0.893	0.899	0.878	0.905
Na	0.022	0.028	0.017	0.023	0.013	0.018	0.006	0.020	0.075	0.002	0.065	0.063	0.072	0.063
K	0.000	0.001	0.000	0.001	0.003	0.033	0.014	0.015	0.001	0.000	0.001	0.000	0.001	0.001
P	0.000	0.000	0.001	0.000	0.000	0.000	0.000	0.000	0.007	0.007	0.007	0.007	0.007	0.007
Cl	0.028	0.034	0.026	0.030	0.003	0.013	0.006	0.002	0.001	0.000	0.001	0.001	0.001	0.000
F	0.000	0.001	0.001	0.001	0.037	0.040	0.037	0.058	0.028	0.027	0.029	0.029	0.028	0.029
Cation	4.028	4.035	4.027	4.031	4.040	4.053	4.043	4.060	4.000	4.034	4.000	4.000	4.000	4.000
X_{Fe}					0.792	0.886	0.860	0.918	0.644	0.537	0.686	0.680	0.674	0.673
X_{Mg}	0.162	0.159	0.131	0.147	0.208	0.114	0.140	0.082	0.312	0.450	0.326	0.327	0.320	0.325

Table 5d: Representative Compositions of Biotites

Rock Type	Hornblende Rich Charnockite				Garnet Rich Charnockites								Pink Granite		Grey Granites	
Sample No.	SR - 57	SR - 57	SR - 57	SR - 57	SR - 84	SR - 84	SR - 84	SR - 84	SR - 84	SR - 84	SR - 84	SR - 84	SR- 71	SR - 71	SR 85	SR85
Oxides %	Core	Rim	Core	Rim	Core	Rim	Core	Rim	Core	Rim	Core	Rim	Core	Rim	Core	Rim
SiO_2	34.075	34.485	33.816	39.559	33.568	38.886	39.151	39.492	33.866	33.715	33.411	33.517	42.062	39.642	30.358	32.865
TiO_2	5.694	5.177	5.942	1.806	5.211	2.518	2.490	2.476	4.646	4.552	4.700	4.544	2.859	7.560	3.536	3.652
Al_2O_3	13.436	13.753	13.597	11.016	12.810	10.288	10.592	10.414	13.269	12.676	12.298	12.443	15.054	13.726	13.582	13.445
FeO	29.015	29.126	29.792	28.311	30.260	26.728	27.225	27.858	30.183	29.985	30.249	30.208	18.123	16.308	31.266	28.530
MnO	0.187	0.131	0.262	0.374	0.096	0.260	0.217	0.231	0.144	0.066	0.084	0.096	0.136	0.150	0.520	0.416
MgO	2.609	2.530	2.650	2.132	3.765	3.488	3.405	3.522	4.261	4.065	4.213	4.226	6.011	5.031	4.871	4.487
CaO	0.028	0.050	0.002	10.566	0.251	10.863	10.857	10.764	0.028	0.007	0.000	0.001	0.374	1.068	0.230	0.054
Na_2O	0.104	0.084	0.077	1.558	0.211	1.747	1.689	1.824	0.083	0.270	0.229	0.160	0.052	0.051	1.036	0.187
K_2O	8.740	8.679	8.946	1.408	9.043	1.564	1.532	1.581	8.888	8.992	8.920	8.994	4.867	4.955	4.791	6.876
P_2O_3	0.006	0.022	0.015	0.000	0.024	0.003	0.000	0.017	0.000	0.006	0.001	0.000	0.018	0.025	0.032	0.032
Cl	0.039	0.036	0.033	0.036	0.340	0.313	0.410	0.267	0.390	0.416	0.373	0.359	0.052	0.033	0.225	0.225
F	0.277	0.342	0.434	0.218	0.261	0.228	0.226	0.220	0.177	0.229	0.203	0.183	0.569	0.409	0.548	0.226
Total	94.210	94.414	95.564	96.983	95.840	96.884	97.794	98.665	95.935	94.978	94.680	94.729	90.175	88.957	90.995	90.993
	Formula unit on 11 Oxygen basis															
Si	2.073	2.093	2.027	2.344	2.415	2.746	2.746	2.737	2.428	2.441	2.429	2.434	3.121	3.024	2.291	2.472
Ti	0.260	0.236	0.268	0.080	0.282	0.134	0.131	0.129	0.251	0.248	0.257	0.248	0.160	0.434	0.201	0.207
Al	0.963	0.984	0.960	0.769	1.086	0.856	0.875	0.851	1.121	1.082	1.054	1.065	1.316	1.234	1.208	1.192
Fe^{3+}	1.114	1.107	1.165	1.996	0.000	0.694	0.687	0.731	0.000	0.000	0.000	0.000	0.000	0.000	0.595	0.072
Fe^{2+}	1.540	1.552	1.522	0.527	1.820	0.885	0.909	0.884	1.809	1.815	1.839	1.834	1.124	1.040	1.378	1.723
Mn^{2+}	0.020	0.014	0.028	0.039	0.006	0.016	0.013	0.014	0.009	0.004	0.005	0.006	0.009	0.010	0.033	0.026
Mg	0.237	0.229	0.237	0.188	0.404	0.367	0.356	0.364	0.455	0.439	0.457	0.457	0.665	0.572	0.548	0.503
Ca	0.002	0.003	0.000	0.671	0.019	0.822	0.816	0.799	0.002	0.001	0.000	0.000	0.030	0.087	0.019	0.004
Na	0.012	0.010	0.009	0.179	0.029	0.239	0.230	0.245	0.012	0.038	0.032	0.023	0.007	0.008	0.152	0.027
K	0.678	0.672	0.684	0.106	0.830	0.141	0.137	0.140	0.813	0.830	0.827	0.833	0.461	0.482	0.461	0.660
P	0.000	0.001	0.001	0.000	0.009	0.001	0.000	0.007	0.000	0.002	0.001	0.000	0.007	0.010	0.013	0.013
F	0.004	0.004	0.003	0.004	0.032	0.027	0.027	0.026	0.021	0.028	0.025	0.022	0.133	0.099	0.070	0.029
Cl	0.053	0.066	0.082	0.041	0.077	0.070	0.091	0.058	0.089	0.095	0.086	0.082	0.007	0.004	0.054	0.053
Cation	6.957	6.969	6.968	6.944	7.019	6.998	7.018	6.991	7.010	7.026	7.011	7.005	7.047	7.013	7.783	7.688
X_{Mg}	0.082	0.079	0.081	0.069	0.182	0.189	0.182	0.184	0.201	0.195	0.199	0.200	0.372	0.355	0.217	0.219

Table 5e: Representative Compositions of Plagioclase Feldspars

Rock Type	Hornblende rich Charnockite			Garnet Rich Charnockites				Pink Granite				Dehyration Zones			Grey Granites			
Sample No.	SR - 57	SR - 57	SR - 57	SR - 84	SR - 84	SR - 84	SR - 84	SR- 71	SR - 71	SR- 71	SR - 71	SR 85	SR85	SR85	SR 85	SR85	SR85	SR85
Oxides %															Core	Rim	Core	Rim
SiO_2	62.847	62.847	62.266	37.044	60.418	61.035	59.751	63.310	62.942	62.782	62.456	65.991	64.930	66.468	47.187	63.342	65.216	64.746
TiO_2	0.034	0.034	0.000	0.078	0.009	0.006	0.000	0.003	0.015	0.035	0.029	0.010	0.014	0.024	0.182	0.018	0.000	0.005
Al_2O_3	23.537	23.537	23.784	20.280	24.295	24.380	23.963	21.052	20.789	20.776	19.931	18.681	20.710	21.171	1.343	20.509	21.227	20.911
FeO	0.083	0.083	0.627	33.076	0.247	0.121	0.108	0.110	0.083	0.114	0.035	0.067	0.983	0.132	20.423	0.050	0.155	0.143
MnO	0.000	0.000	0.045	1.602	0.000	0.056	0.010	0.017	0.010	0.002	0.000	0.000	0.000	0.009	1.285	0.000	0.000	0.000
MgO	0.000	0.000	0.074	1.305	0.011	0.000	0.000	0.005	0.000	0.020	0.000	0.005	0.060	0.001	5.220	0.000	0.000	0.000
CaO	5.243	5.243	5.222	6.830	6.652	6.855	6.936	3.743	3.684	3.766	3.372	0.315	2.604	2.124	20.702	2.769	2.636	2.913
Na_2O	8.822	8.822	8.904	0.043	8.264	7.920	7.975	9.656	9.883	9.715	9.724	11.878	10.477	10.968	0.868	10.310	10.203	10.070
K_2O	0.332	0.332	0.208	0.010	0.192	0.257	0.289	0.379	0.326	0.346	0.266	0.091	0.120	0.158	0.014	0.171	0.158	0.197
P_2O_3	0.000	0.003	0.010	0.007	0.008	0.000	0.000	0.000	0.003	0.006	0.011	0.032	0.032	0.032	0.032	0.032	0.032	0.032
Cl	0.001	0.001	0.007	0.262	0.109	0.038	0.093	0.000	0.016	0.020	0.000	0.225	0.225	0.225	0.225	0.225	0.225	0.225
F	0.063	0.063	0.111	0.000	0.016	0.000	0.010	0.033	0.041	0.045	0.000	0.000	0.034	0.002	0.000	0.018	0.001	0.022
Total	100.901	100.904	101.140	100.275	100.096	100.630	99.033	98.275	97.735	97.562	95.824	97.070	99.931	101.088	97.255	97.201	99.627	99.017
	Formula unit on 8 Oxygen basis																	
Si	2.763	2.763	2.733	1.233	2.011	2.032	1.989	2.108	2.095	2.090	2.079	2.197	2.161	2.213	1.571	2.109	2.171	2.155
Ti	0.001	0.001	0.000	0.002	0.000	0.000	0.000	0.000	0.000	0.001	0.001	0.000	0.000	0.001	0.005	0.000	0.000	0.000
Al	1.220	1.220	1.230	0.597	0.715	0.717	0.705	0.619	0.612	0.611	0.586	0.550	0.609	0.623	0.040	0.603	0.625	0.615
Fe	0.005	0.005	0.041	0.460	0.003	0.002	0.001	0.002	0.001	0.002	0.000	0.001	0.014	0.002	0.284	0.001	0.002	0.002
Mn	0.000	0.000	0.003	0.023	0.000	0.001	0.000	0.000	0.000	0.000	0.000	0.000	0.000	0.000	0.018	0.000	0.000	0.000
Mg	0.000	0.000	0.005	0.032	0.000	0.000	0.000	0.000	0.000	0.000	0.000	0.000	0.001	0.000	0.130	0.000	0.000	0.000
Ca	0.247	0.247	0.246	0.122	0.119	0.122	0.124	0.067	0.066	0.067	0.060	0.006	0.046	0.038	0.369	0.049	0.047	0.052
Na	0.752	0.752	0.758	0.001	0.133	0.128	0.129	0.156	0.159	0.157	0.157	0.192	0.169	0.177	0.014	0.166	0.165	0.162
K	0.019	0.019	0.012	0.000	0.002	0.003	0.003	0.004	0.003	0.004	0.003	0.001	0.001	0.002	0.000	0.002	0.002	0.002
P	0.000	0.000	0.000	0.001	0.001	0.000	0.000	0.000	0.000	0.001	0.001	0.003	0.003	0.003	0.003	0.003	0.003	0.003
Cl	0.009	0.009	0.015	0.014	0.006	0.002	0.005	0.002	0.002	0.002	0.000	0.000	0.001	0.000	0.000	0.000	0.000	0.001
F	0.000	0.000	0.000	0.000	0.000	0.000	0.000	0.000	0.000	0.001	0.000	0.012	0.012	0.012	0.012	0.012	0.012	0.012
Cation	5.007	5.007	5.028	5.023	5.344	5.004	5.020	5.020	5.033	5.027	5.020	5.035	5.025	5.019	5.400	5.024	4.998	5.000
X_{alb}	0.627	0.364	0.364	0.685	0.011	0.667	0.665	0.806	0.815	0.808	0.827	0.981	0.873	0.896	0.071	0.863	0.867	0.853
X_{An}	0.373	0.428	0.425	0.305	0.987	0.319	0.319	0.173	0.168	0.173	0.158	0.014	0.120	0.096	0.929	0.128	0.124	0.136

Table 5f: Representative Compositions of Garnet

Rock Type	Hornblende Rich Charnockite					Garnet Rich Charnockites							
Sample No.	SR - 57	SR - 57	SR - 57	SR - 57	SR - 57	SR - 84	SR - 84	SR - 84	SR - 84	SR - 84	SR - 84	SR - 84	SR - 84
Oxides %	Rim	Rim	Core	Core	Rim	Core	Rim	Core	Rim	Core	Rim	Core	Rim
SiO_2	37.7005	36.9332	37.6335	37.3892	37.7023	37.4832	37.752	36.859	35.6894	36.809	36.6885	37.1951	35.7832
TiO_2	0.0386	0.0325	0.0225	0.0273	0.0492	0.0394	0.0656	0.0372	0.1078	0.0506	0.0063	0.0002	0.0462
Al_2O_3	20.0589	19.5791	19.9363	19.8611	20.3793	19.8942	20.0682	19.6166	19.5332	19.867	20.1996	20.2915	20.1822
FeO	30.744	30.6253	30.363	30.5298	30.7128	33.5952	33.672	33.4328	32.286	33.22	32.8377	33.3738	33.3572
MnO	2.5061	2.7176	2.4574	3.0663	3.0133	1.2076	1.7288	1.6129	0.9277	1.4829	1.8744	1.482	1.5745
MgO	1.0312	0.9208	1.0072	0.8901	0.8846	1.5912	1.2317	1.2224	1.5099	1.4957	1.1672	1.5629	1.5035
CaO	7.4805	7.622	7.6073	7.8988	7.7628	7.2427	6.9078	6.9917	7.8236	7.0389	6.9357	7.0196	6.7432
Na_2O	0.0003	0.0201	0.032	0.0003	0.0405	0.0425	0.0366	0.0383	0.0027	0.0187	0.0488	0.1129	0.0003
K_2O	0.0034	0.0105	0.006	0.0001	0.0131	0.0001	0.0051	0.0002	0.0001	0.0069	0.0137	0.0001	0.0048
P_2O_3	0.0058	0.0043	0.0173	0.0001	0.0001	0.0001	0.0001	0.0188	0.0001	0.0014	0.0101	0.0043	0.0001
Cl	0.02	0.0001	0.0001	0.0114	0.0078	0.3114	0.166	0.2502	0.3831	0.2788	0.2948	0.212	0.2127
F	0.1858	0.2419	0.1576	0.1257	0.1881	0.0124	0.0001	0.0083	0.0001	0.0001	0.0001	0.052	0.0105
Total	99.7751	98.7074	99.2402	99.8002	100.7539	101.42	101.634	100.0884	98.2637	100.27	100.0769	101.3064	99.4184
	Formula unit on 12 Oxygen basis												
Si	2.937	2.504	2.740	2.453	2.452	3.004	2.990	2.984	3.068	2.971	2.968	2.965	2.912
Ti	0.072	0.001	0.091	0.001	0.002	0.003	0.002	0.002	0.003	0.003	0.000	0.000	0.003
Al	0.000	0.000	0.000	0.000	0.000	0.986	1.870	1.872	1.989	1.890	1.926	1.906	1.936
Fe3+	0.214	1.367	1.724	1.529	1.496	0.000	0.071	0.097	0.000	0.095	0.070	0.121	0.179
Fe2+	1.868	1.526	1.172	1.484	1.508	0.004	2.170	2.167	1.984	2.147	2.151	2.103	2.091
Mn2+	0.047	0.362	0.039	0.356	0.346	0.000	0.082	0.111	0.070	0.101	0.128	0.100	0.109
Mg	0.038	0.084	0.228	0.087	0.086	0.000	0.189	0.148	0.183	0.180	0.141	0.186	0.182
Ca	1.207	0.559	0.789	0.555	0.541	0.006	0.619	0.606	0.693	0.609	0.601	0.599	0.588
Na	0.006	0.005	0.188	0.000	0.005	0.198	0.007	0.006	0.002	0.003	0.008	0.017	0.000
K	0.000	0.000	0.128	0.000	0.001	0.799	0.000	0.000	0.001	0.001	0.001	0.000	0.000
P	0.000	0.000	0.000	0.000	0.000	0.000	0.000	0.008	0.006	0.001	0.004	0.002	0.000
Cl	0.002	0.000	0.010	0.001	0.001	0.001	0.002	0.001	0.000	0.000	0.000	0.007	0.001
F	0.161	0.037	0.019	0.026	0.039	0.008	0.079	0.064	0.074	0.071	0.075	0.053	0.055
Cations	8.163	8.037	8.028	8.027	8.040	8.024	8.021	8.032	7.933	8.032	8.024	8.041	8.060
X Fe^{2+} (Almandine)	59.113	60.272	52.611	59.790	60.788	70.917	70.741	71.478	67.701	70.698	71.194	70.379	70.409
X Mg (Pyrope)	1.201	3.329	10.243	3.508	3.456	6.185	6.246	4.867	6.253	5.925	4.659	6.215	6.142
X Mn (Spessartine)	1.501	14.301	1.730	14.330	13.960	2.667	2.994	3.648	2.395	3.337	4.251	3.348	3.654
X Fe^{3+} (Andradite)	4.304	10.215	22.476	11.158	10.655	0.742	0.646	0.982	0.000	0.955	0.702	1.199	1.672
X Ca (Grossular)	32.433	11.874	11.750	11.204	11.124	19.465	19.356	19.001	23.614	19.053	19.191	18.859	18.097
X Ti (Ca-Ti garnet)	1.446	0.009	1.195	0.010	0.017	0.025	0.017	0.023	0.038	0.031	0.004	0.000	0.026

Figure 1

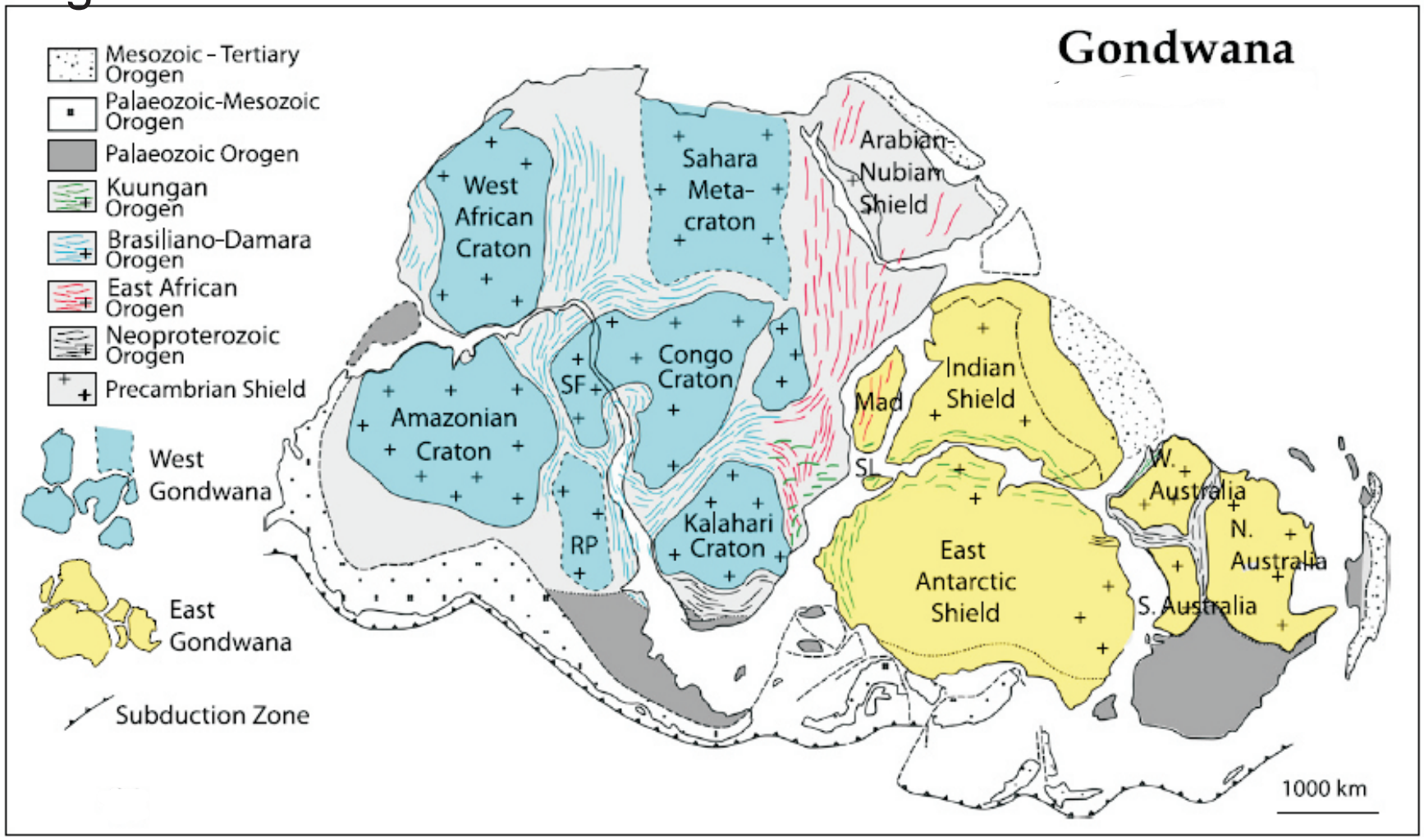
Gondwana
Mesozoic – Tertiary Orogen
Palaeozoic-Mesozoic Orogen
Palaeozoic Orogen
Kuungan Orogen
Brasiliano-Damara Orogen
East African Orogen
Neoproterozoic Orogen
Precambrian Shield
West Gondwana
East Gondwana
Subduction Zone
West African Craton
Sahara Meta-craton
Arabian-Nubian Shield
Amazonian Craton
SF
Congo Craton
Mad
Indian Shield
SL
RP
Kalahari Craton
East Antarctic Shield
W. Australia
N. Australia
S. Australia
1000 km

Figure 2a.

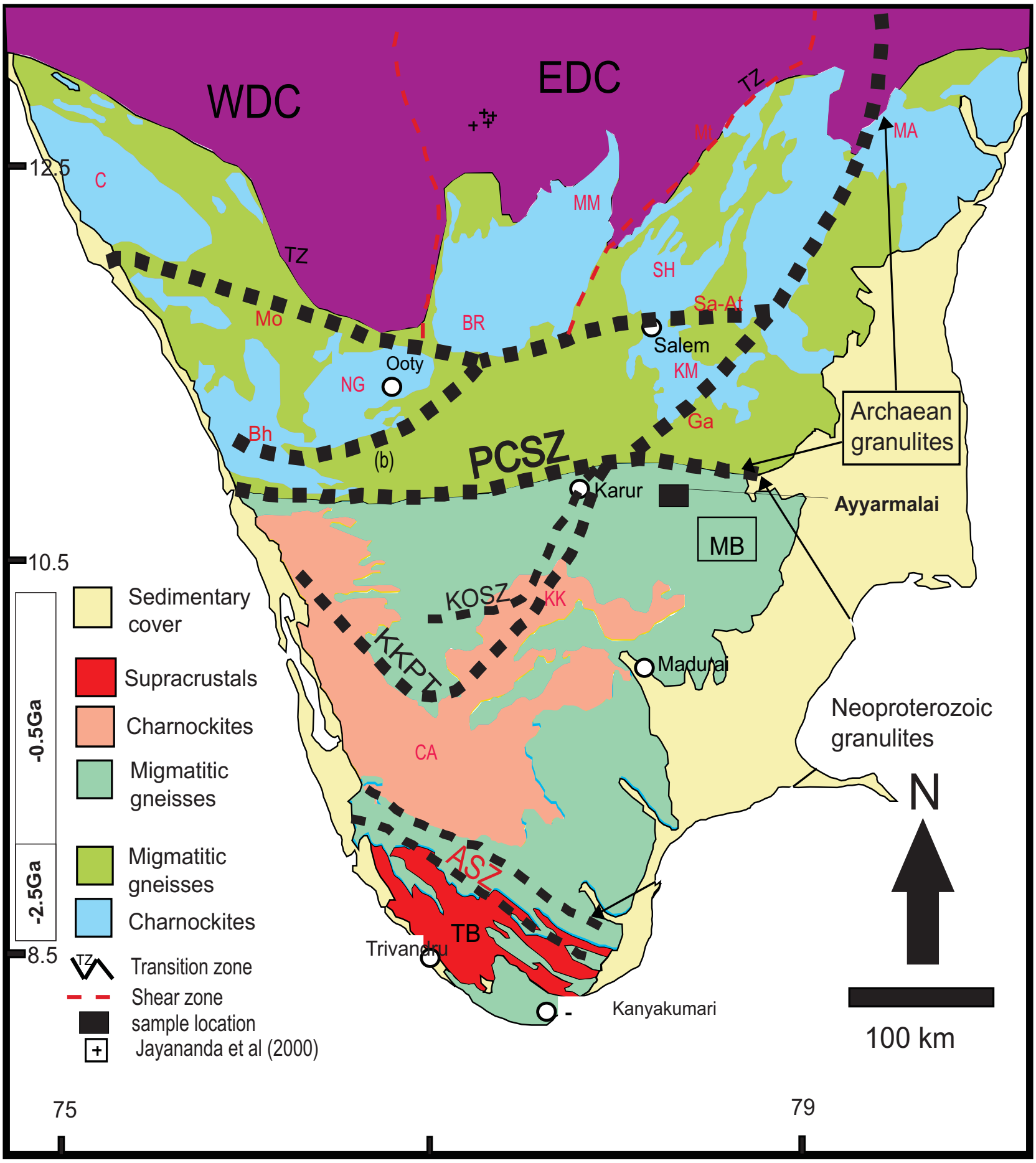

Figure 2c.

Figure 2b.

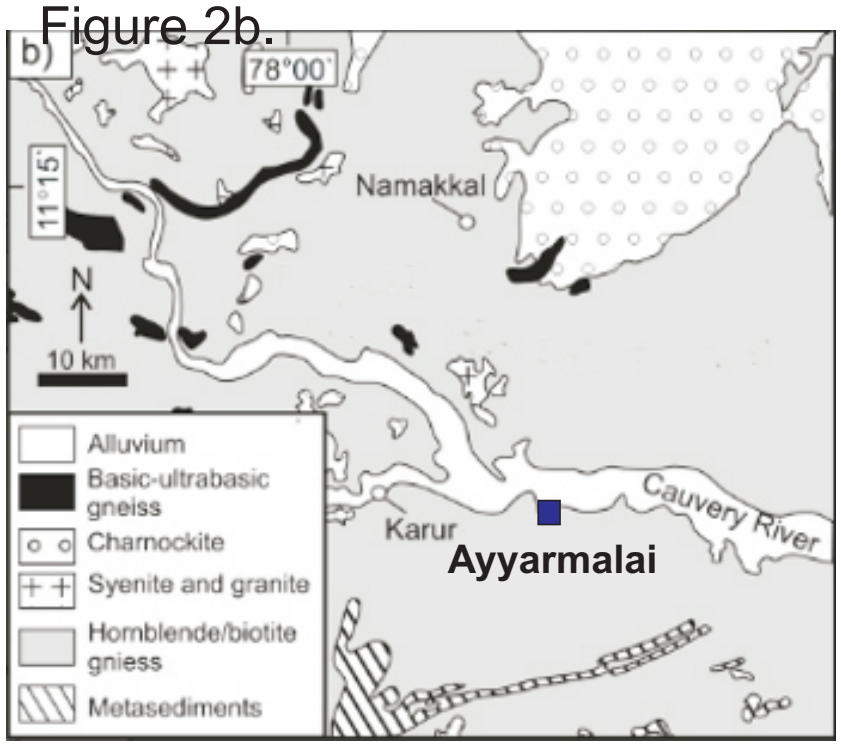

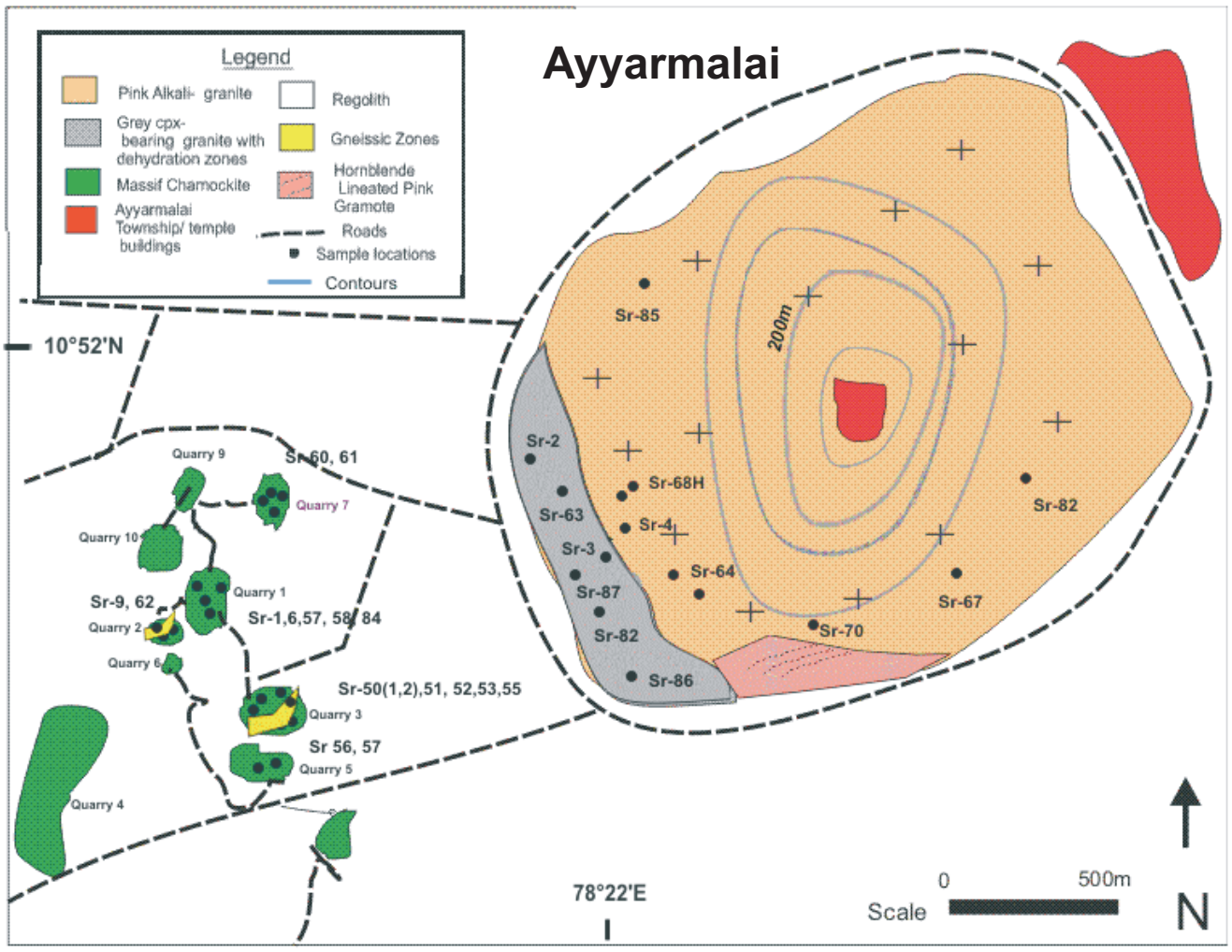

Figure 3a

Figure 3b

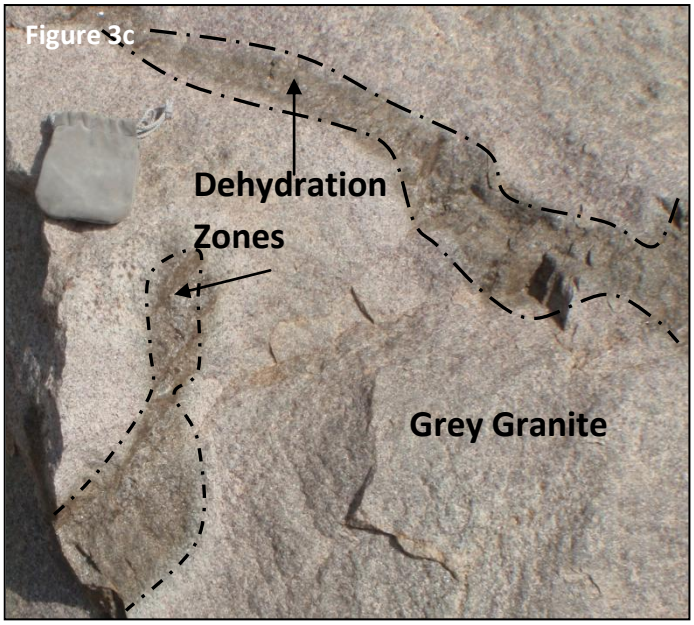
Figure 3c
Dehydration
Zones
Grey Granite

Figure 3d

Figure 3e

Figure 3f Pink Alkali Granite
Grey Granite

Figure 3g

Figure 3h

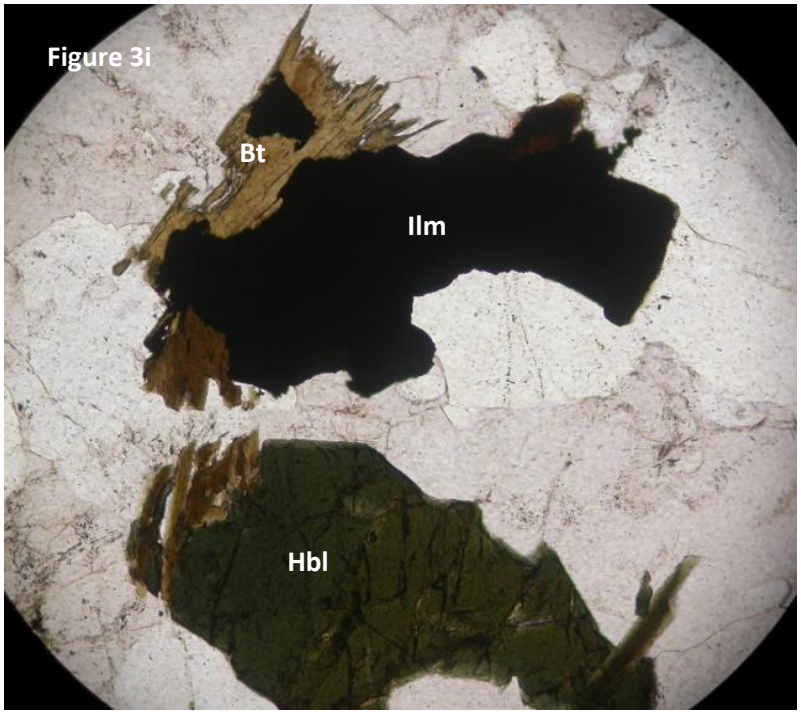
Figure 3i
Bt
Ilm
Hbl

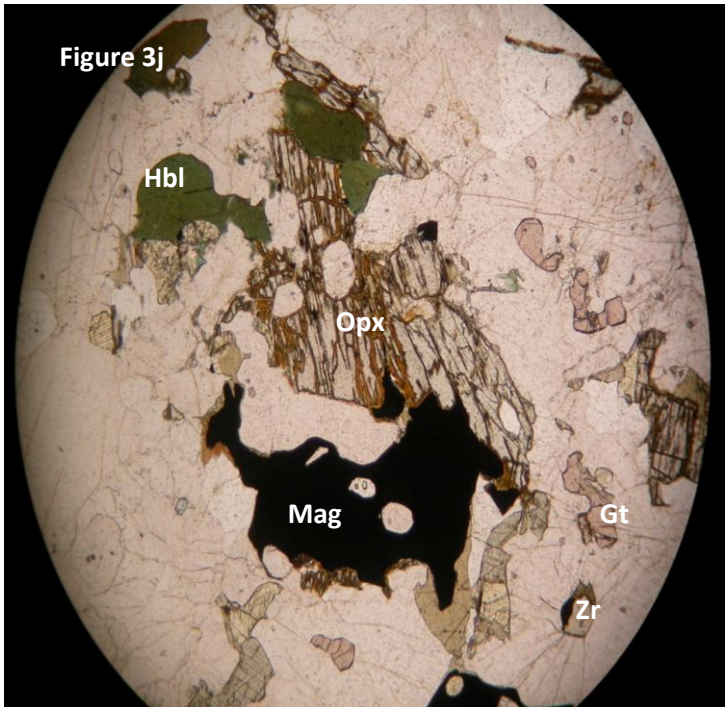
Figure 3j
Hbl
Opx
Mag
Gt
Zr

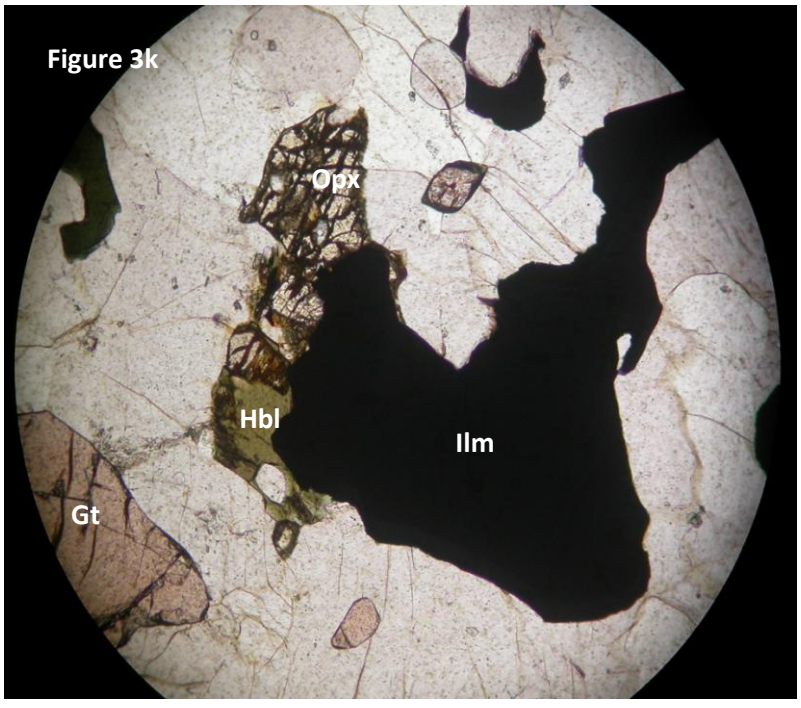
Figure 3k
Opx
Hbl
Ilm
Gt

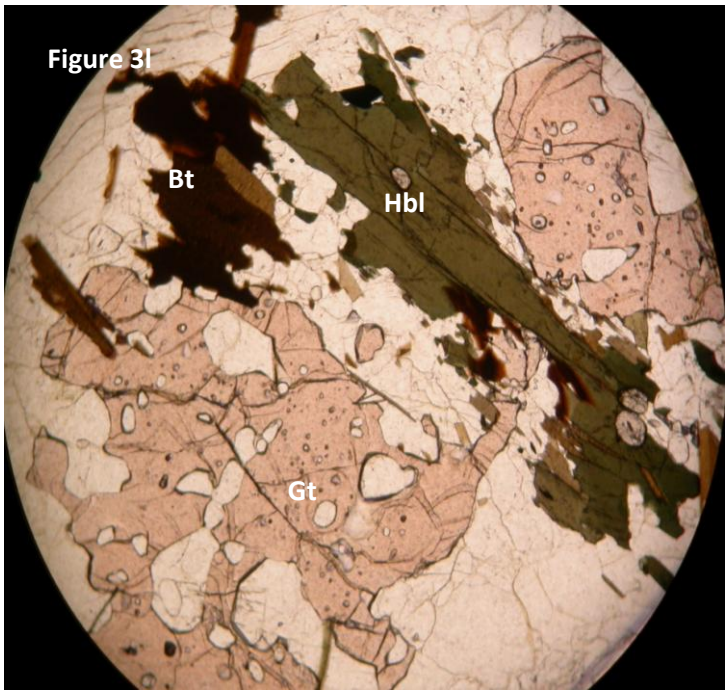
Figure 3l
Bt
Hbl
Gt

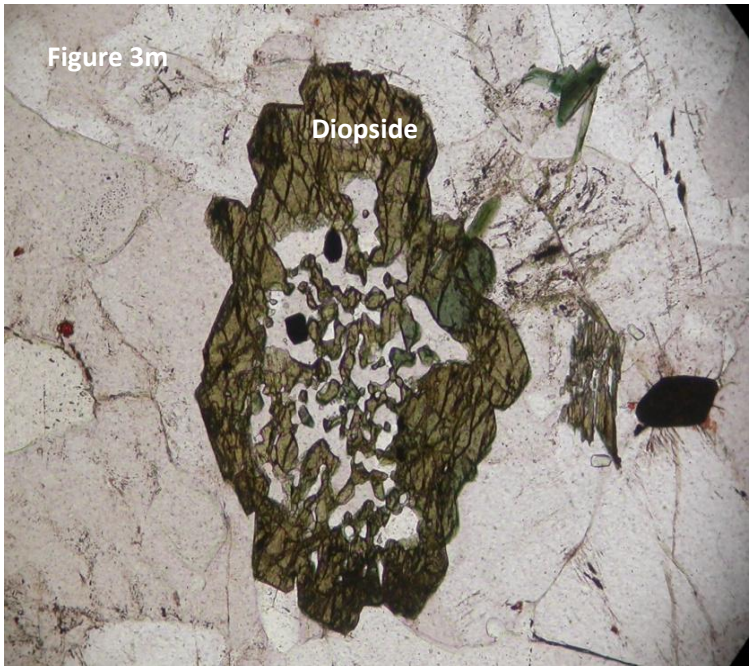
Figure 3m
Diopside

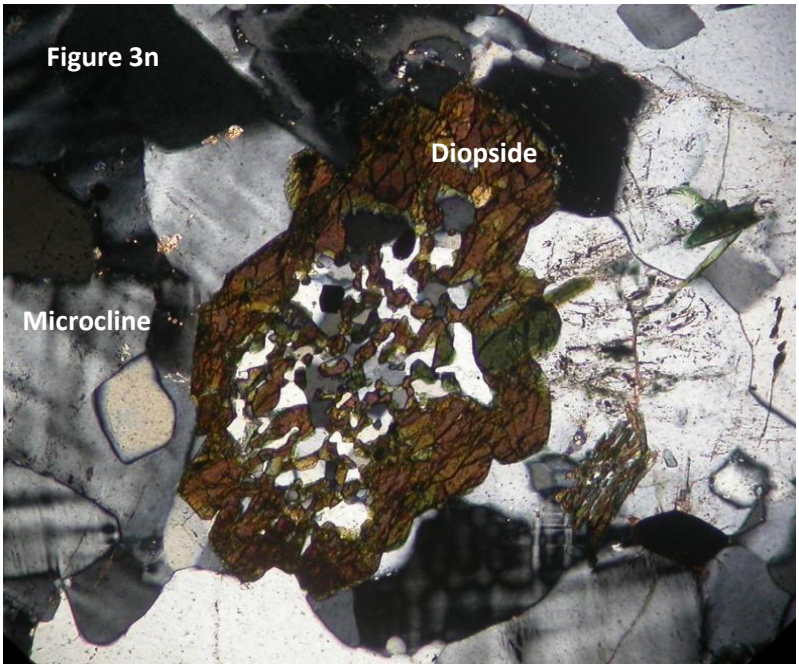
Figure 3n
Diopside
Microcline

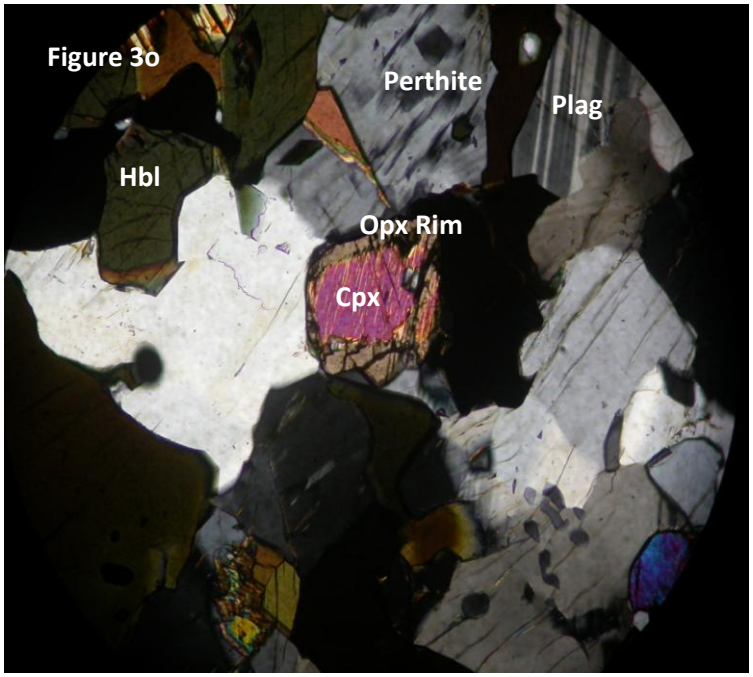
Figure 3o
Perthite
Plag
Hbl
Opx Rim
Cpx

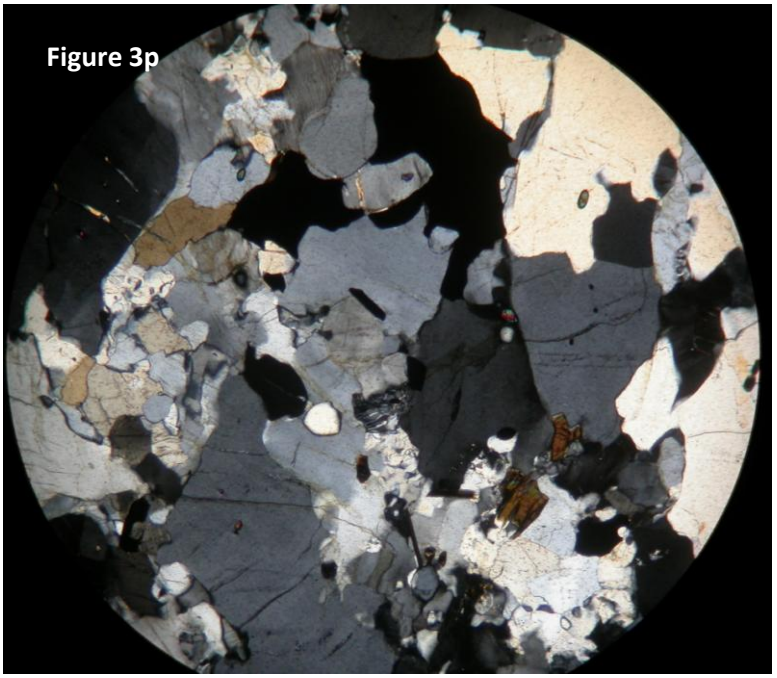
Figure 3p

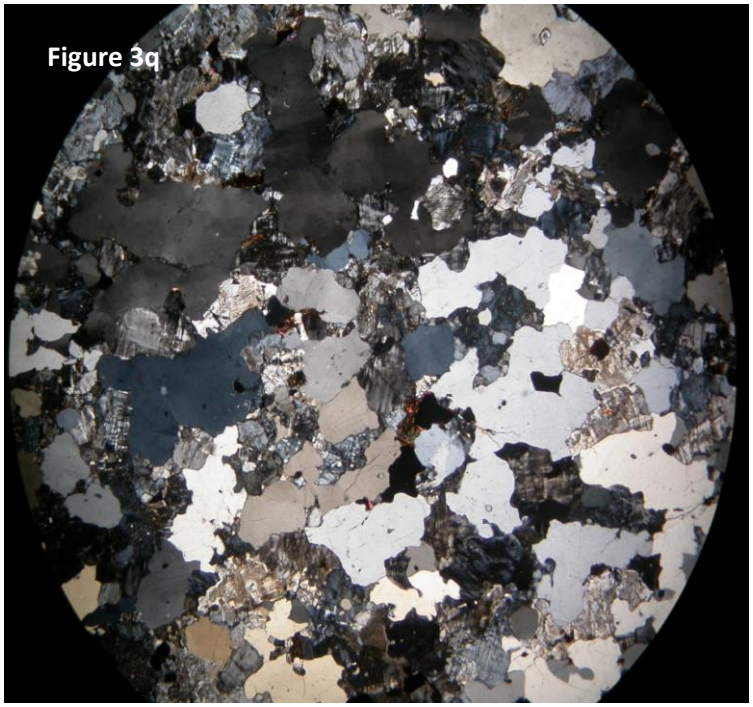
Figure 3q

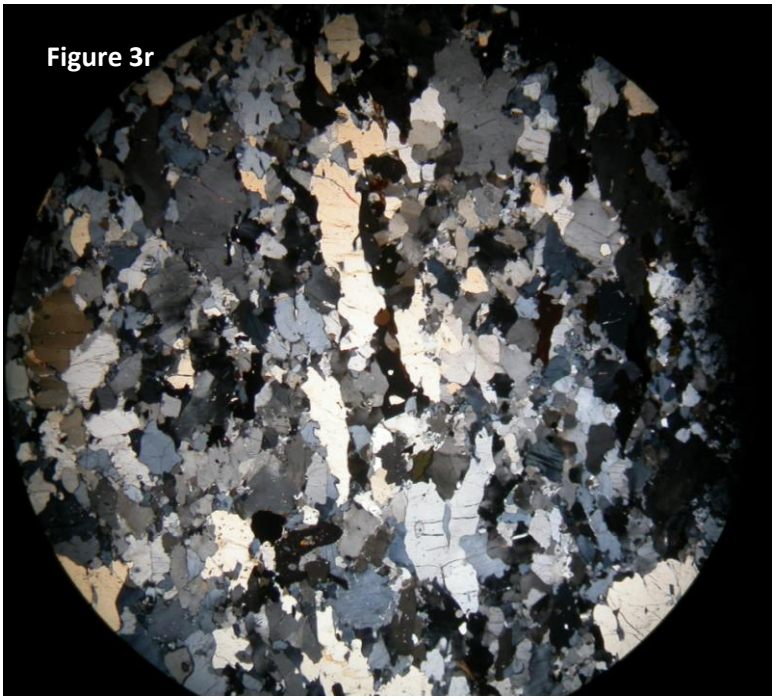
Figure 3r

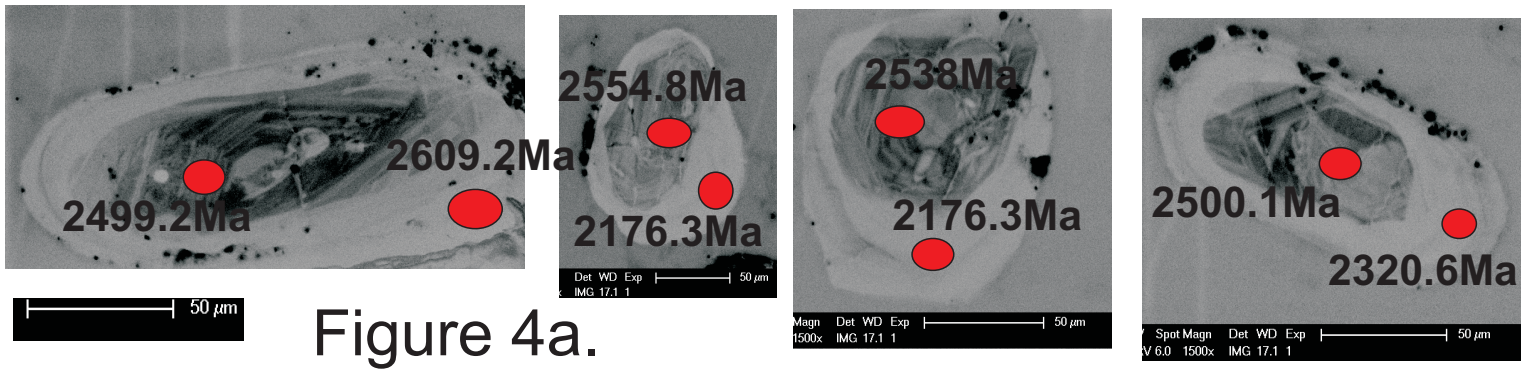
2499.2Ma
2609.2Ma
50 µm
2554.8Ma
2176.3Ma
Det WD Exp
IMG 17.1 1
50 µm
2538Ma
2176.3Ma
Magn Det WD Exp
1500x IMG 17.1 1
50 µm
2500.1Ma
2320.6Ma
Spot Magn Det WD Exp
V 6.0 1500x IMG 17.1 1
50 µm

Figure 4a.

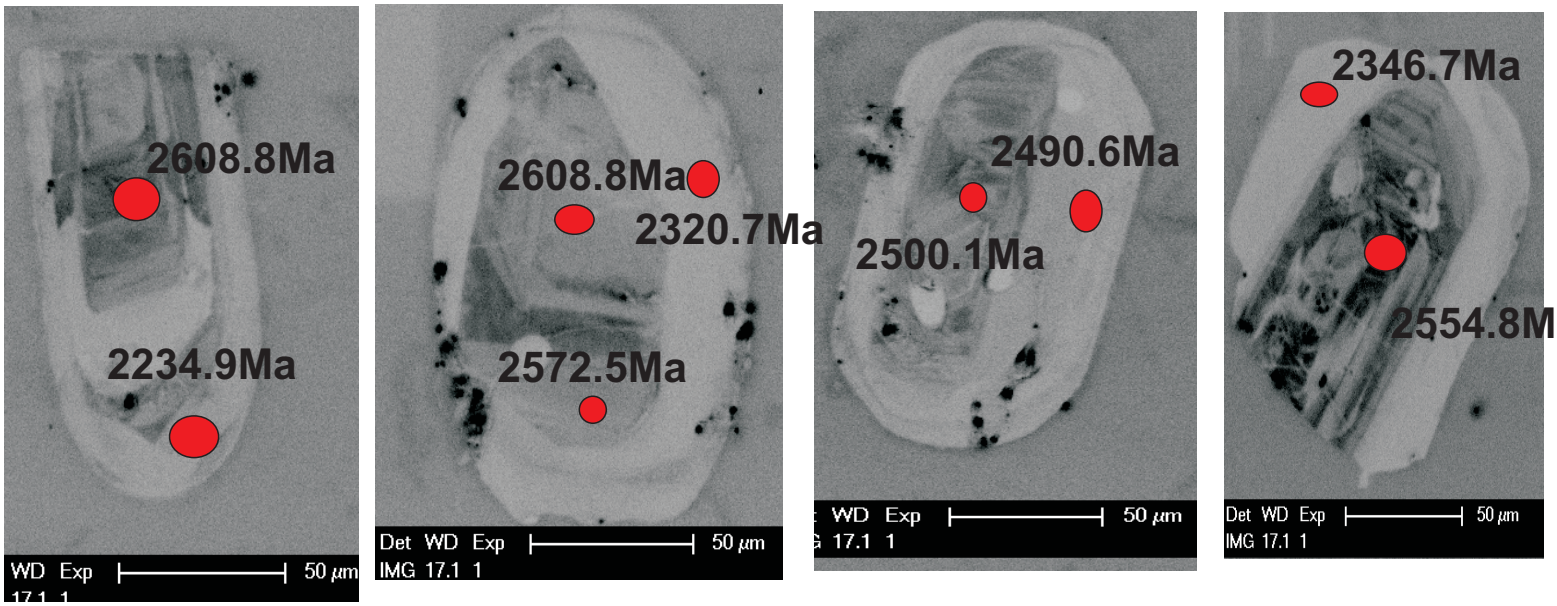
2608.8Ma
2234.9Ma
WD Exp
50 µm
2608.8Ma
2320.7Ma
2572.5Ma
Det WD Exp
50 µm
IMG 17.1 1
2490.6Ma
2500.1Ma
WD Exp
50 µm
17.1 1
2346.7Ma
2554.8Ma
Det WD Exp
50 µm
IMG 17.1 1

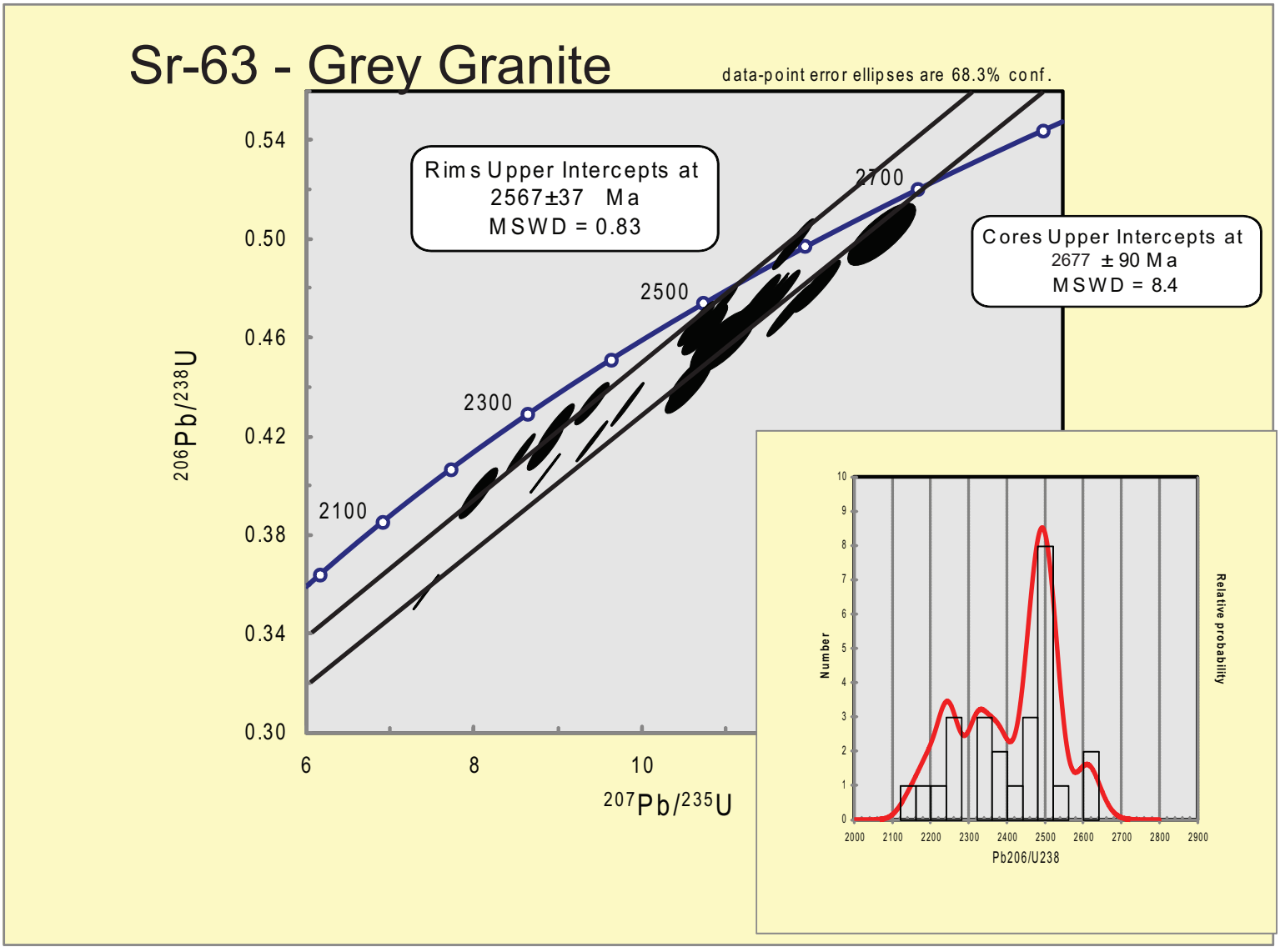
Sr-63 - Grey Granite
data-point error ellipses are 68.3% conf.
Rims Upper Intercepts at
2567±37 Ma
MSWD = 0.83
Cores Upper Intercepts at
2677 ± 90 Ma
MSWD = 8.4
2100
2300
2500
2700
0.54
0.50
0.46
0.42
0.38
0.34
0.30
6
8
10
206Pb/238U
207Pb/235U
Number
Relative probability
Pb206/U238
2000
2100
2200
2300
2400
2500
2600
2700
2800
2900

Figure 4b.

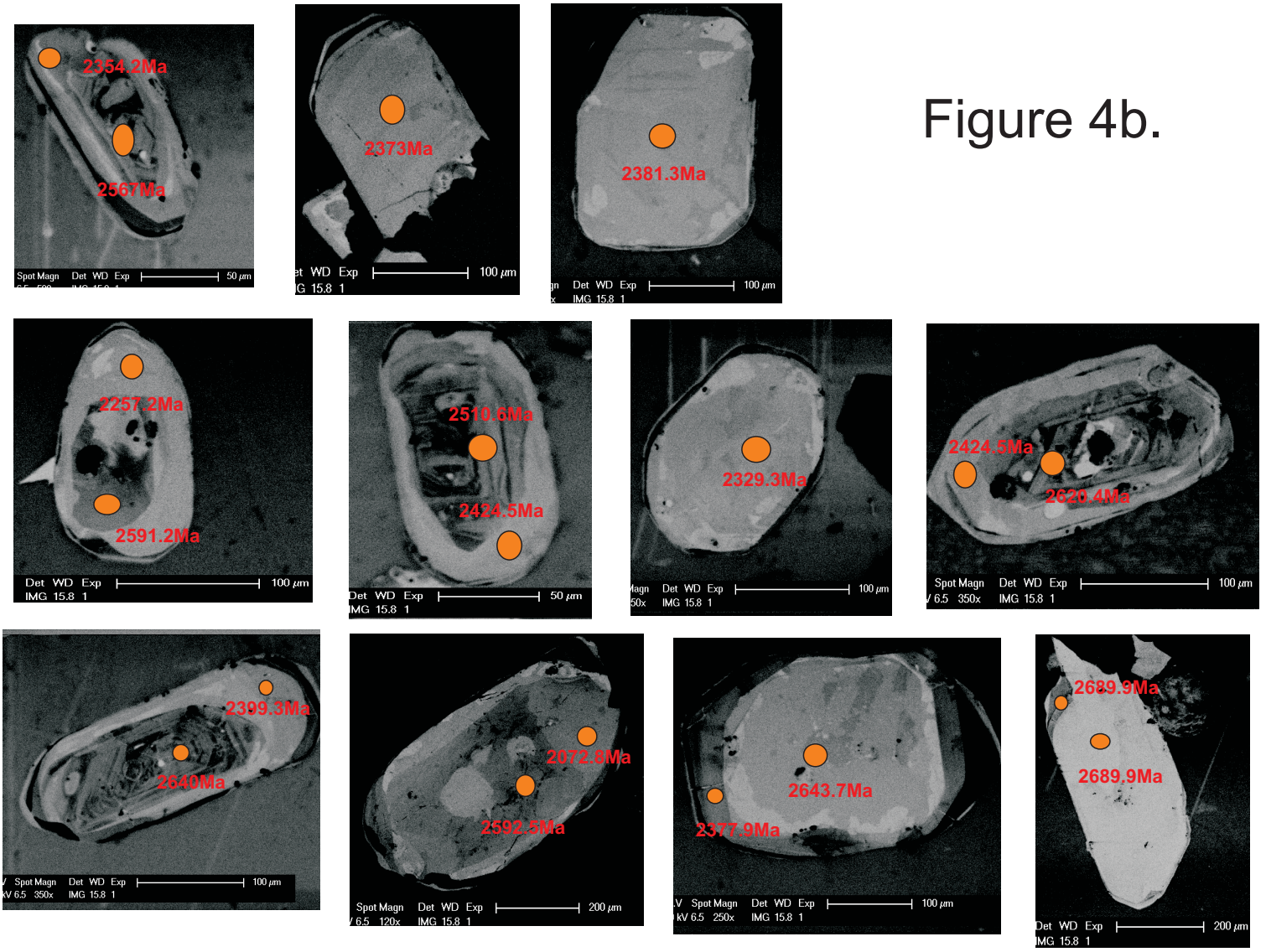

SR-68H Pink Alkali Granite

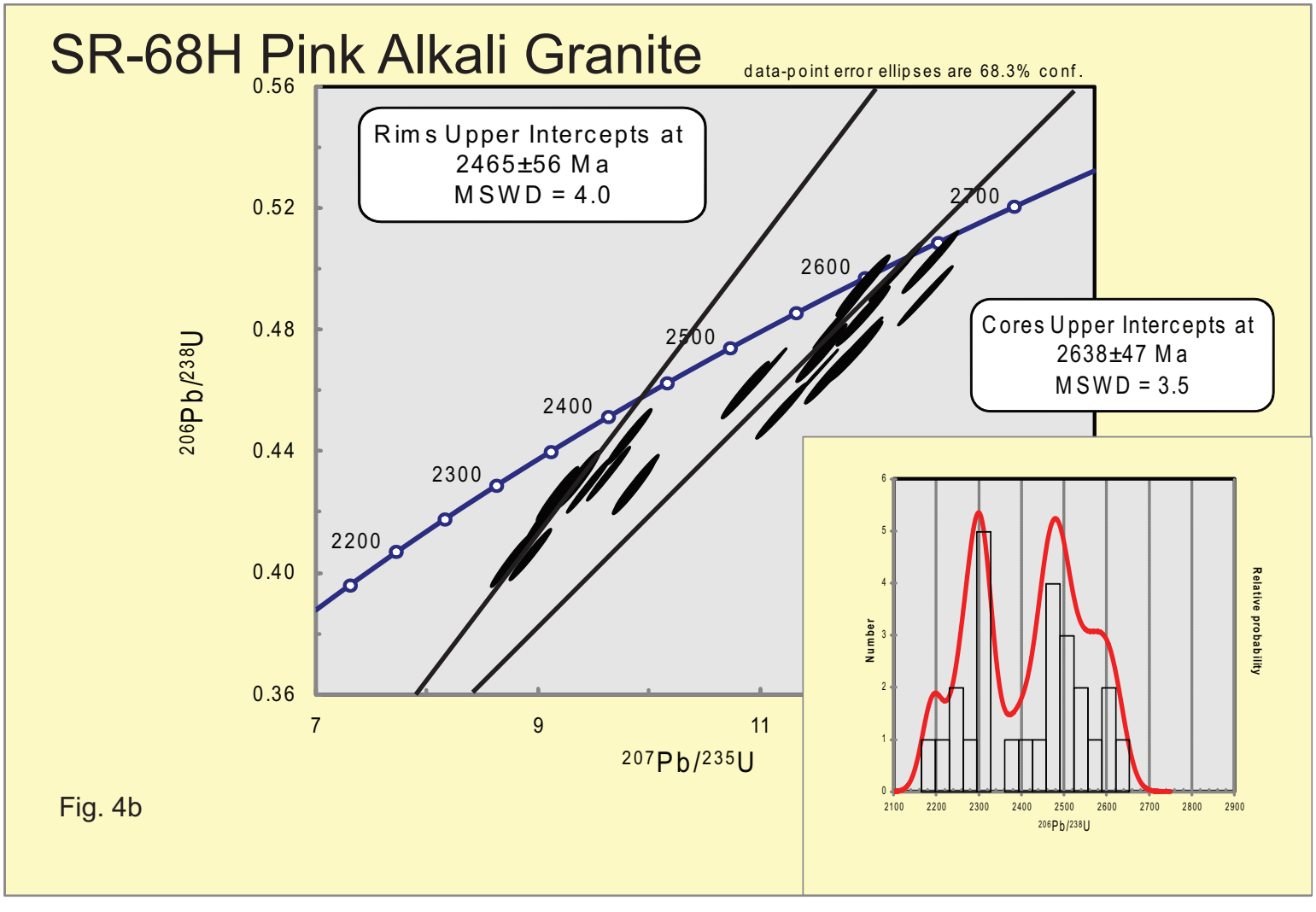

Fig. 4b

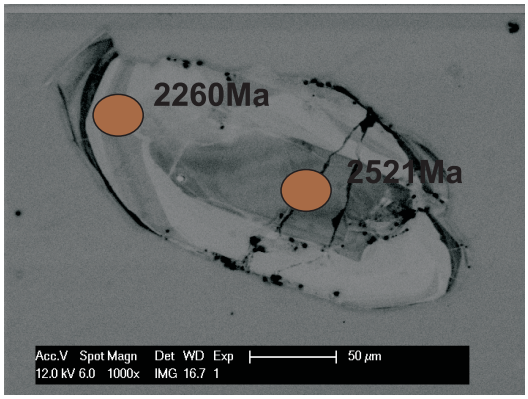

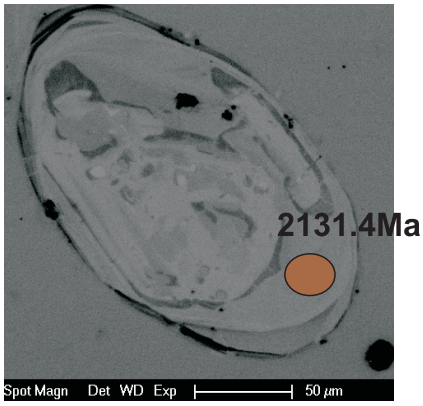

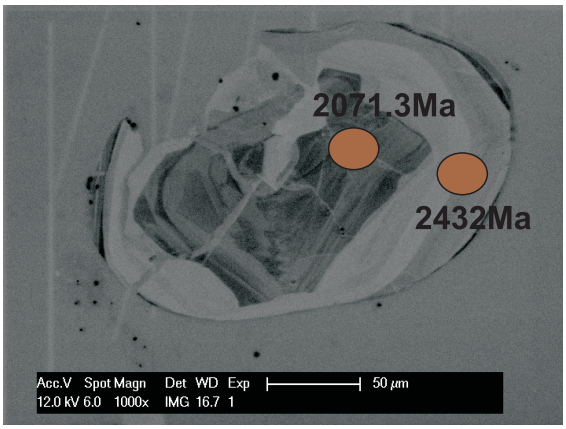

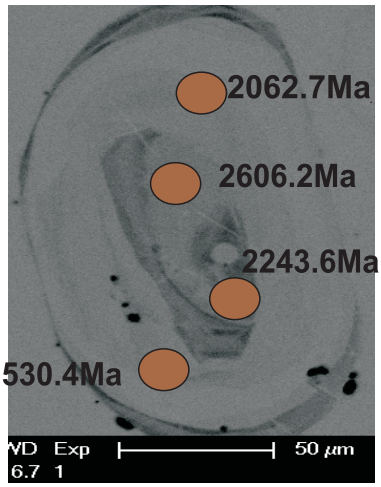

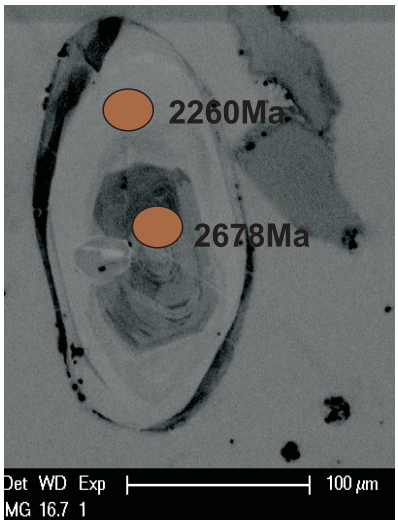

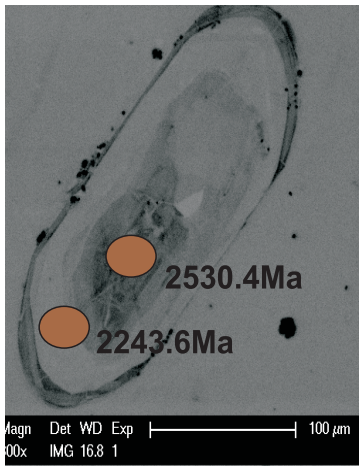

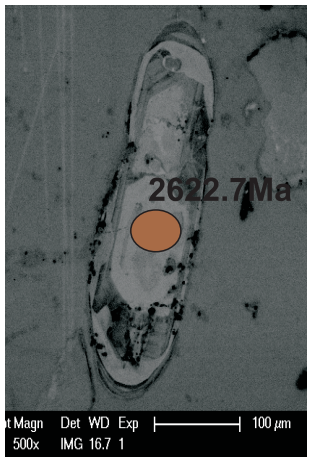

Garnet Rich Charnockite

Sr-6

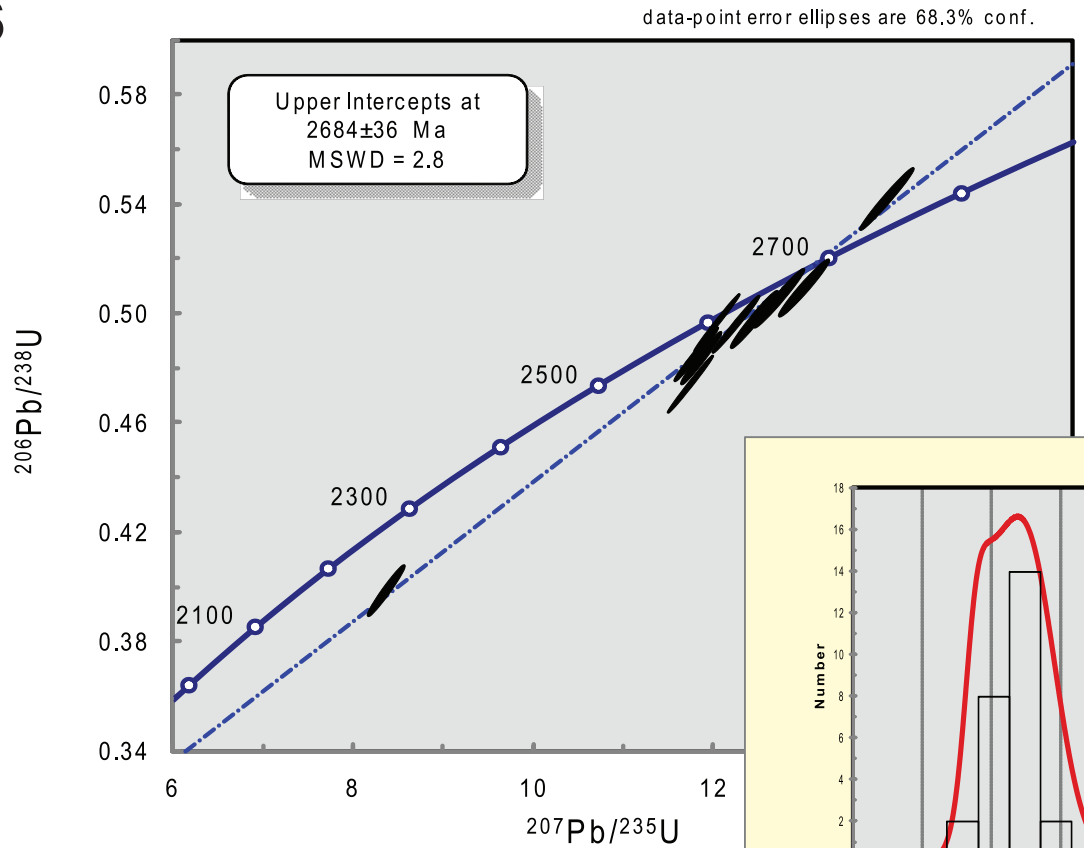

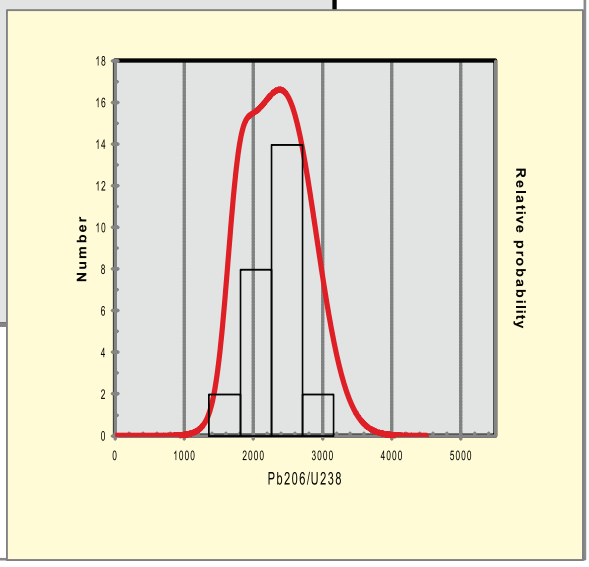

Fig. 4c.

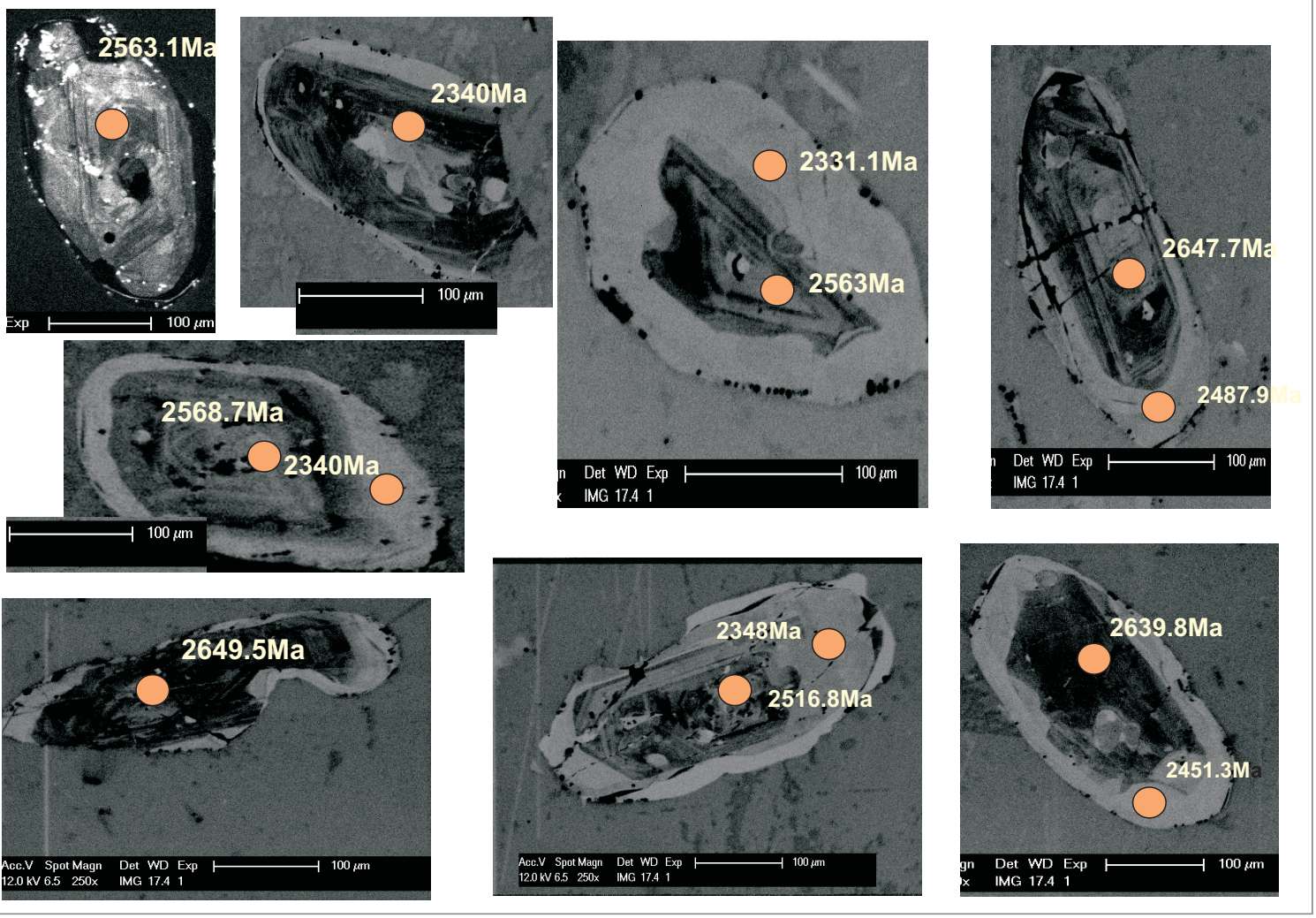

Sr-57Hornblende Rich Charnockite

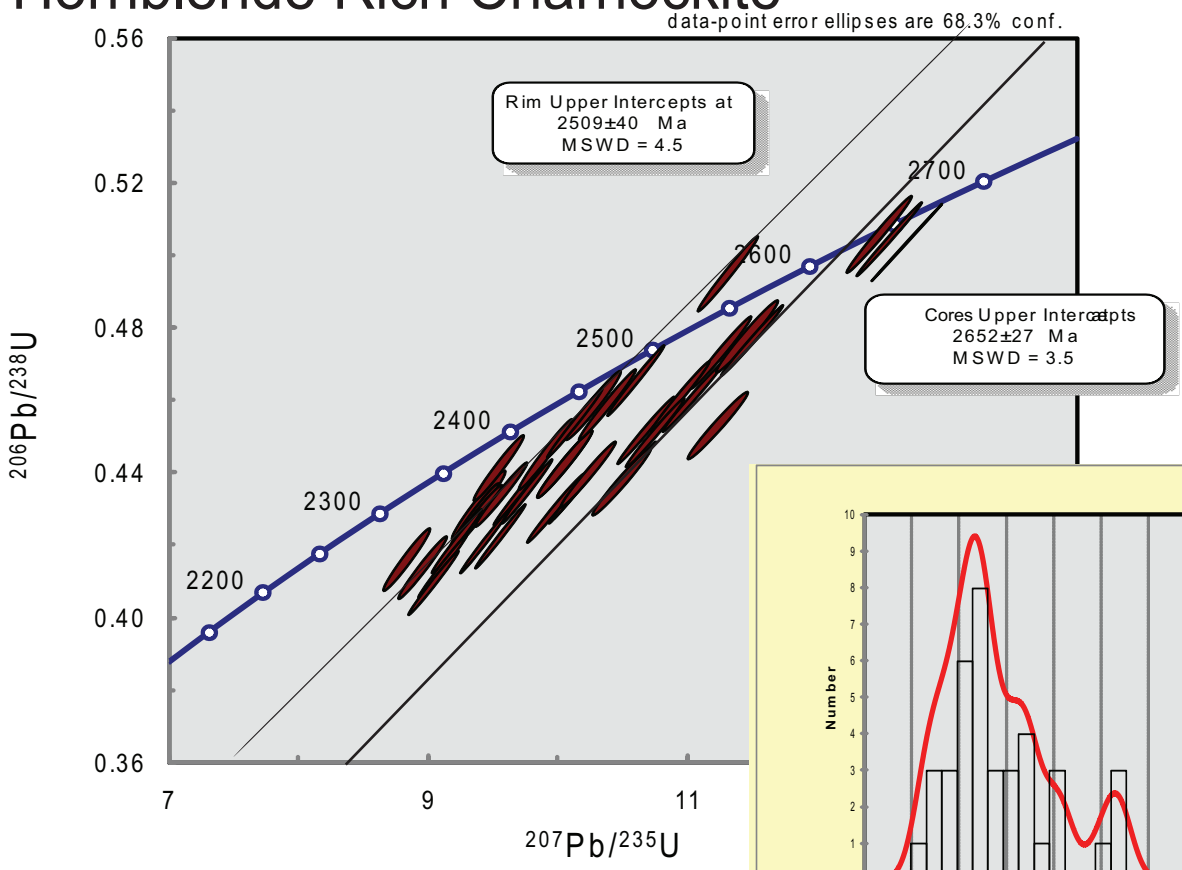

Fig.4d.

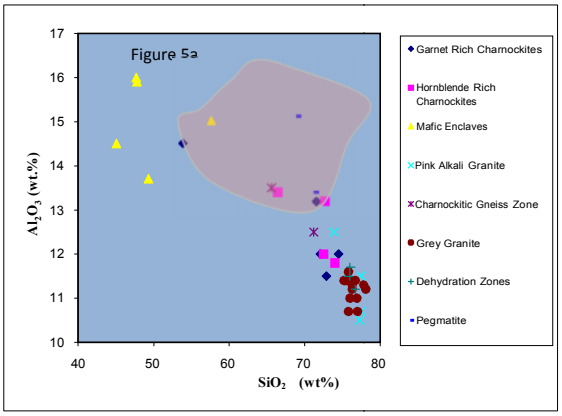
Figure 5a
Garnet Rich Charnockites
Hornblende Rich Charnockites
Mafic Enclaves
Pink Alkali Granite
Charnockitic Gneiss Zone
Grey Granite
Dehydration Zones
Pegmatite
Al_2O_3 (wt.%)
SiO_2 (wt%)

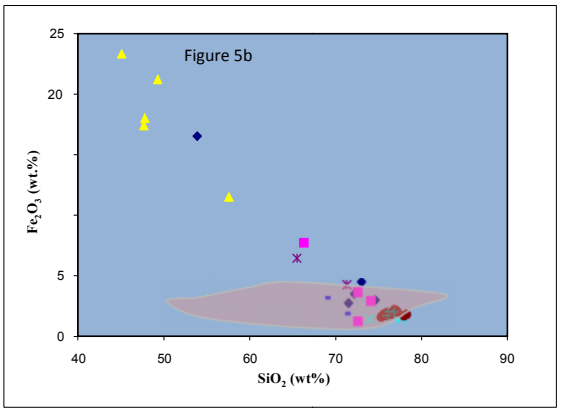
Figure 5b
Fe_2O_3 (wt.%)
SiO_2 (wt%)

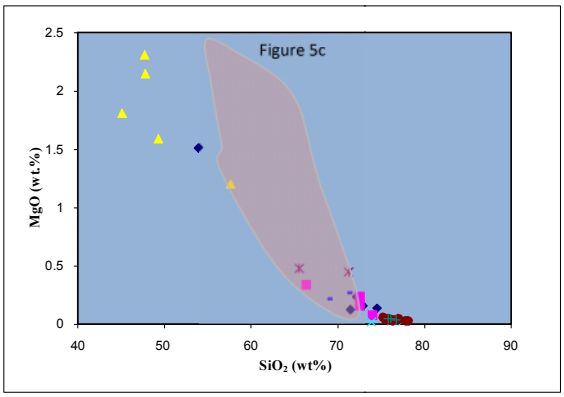
Figure 5c
MgO (wt.%)
SiO_2 (wt%)

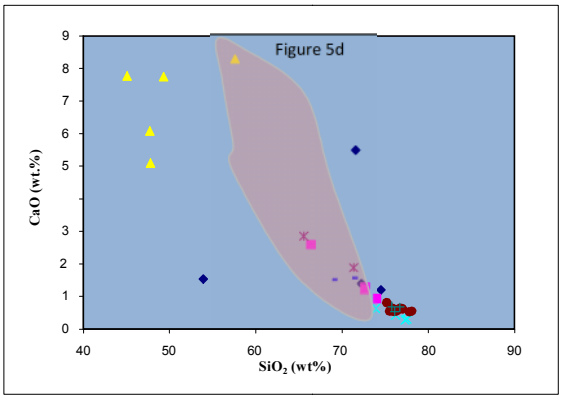
Figure 5d
CaO (wt.%)
SiO_2 (wt%)

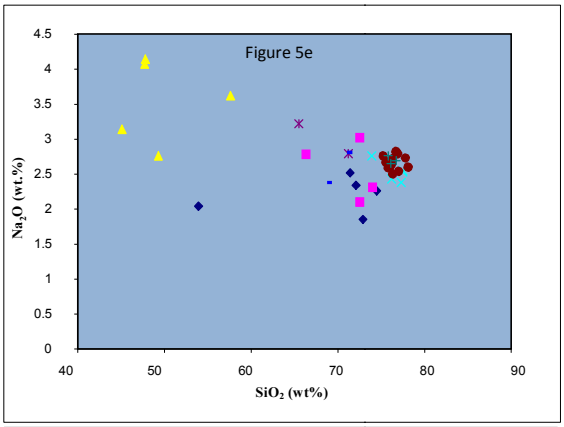
Figure 5e
Na_2O (wt.%)
SiO_2 (wt%)

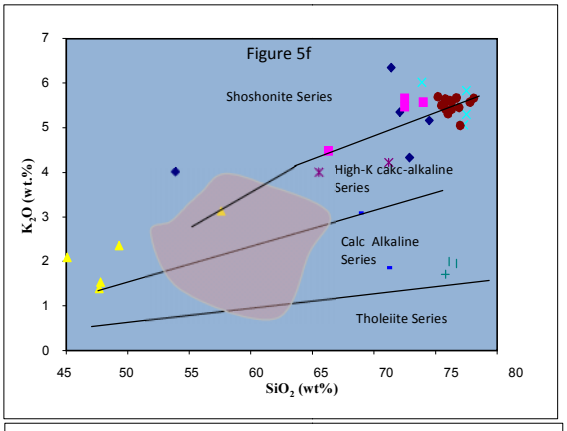
Figure 5f
Shoshonite Series
High-K calc-alkaline Series
Calc Alkaline Series
Tholeiite Series
K_2O (wt.%)
SiO_2 (wt%)

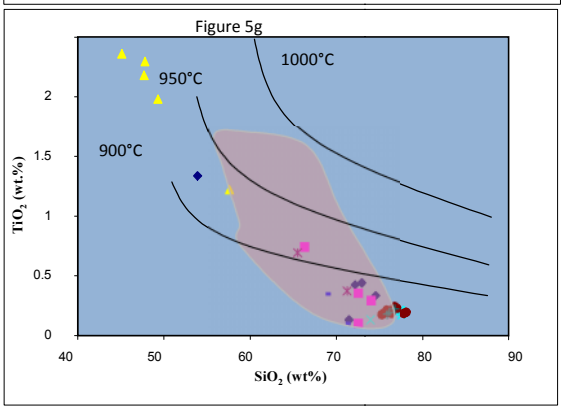
Figure 5g
1000°C
950°C
900°C
TiO_2 (wt.%)
SiO_2 (wt%)

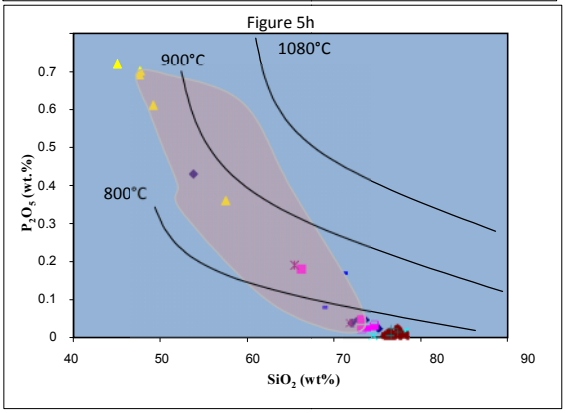
Figure 5h
1080°C
900°C
800°C
P_2O_5 (wt.%)
SiO_2 (wt%)

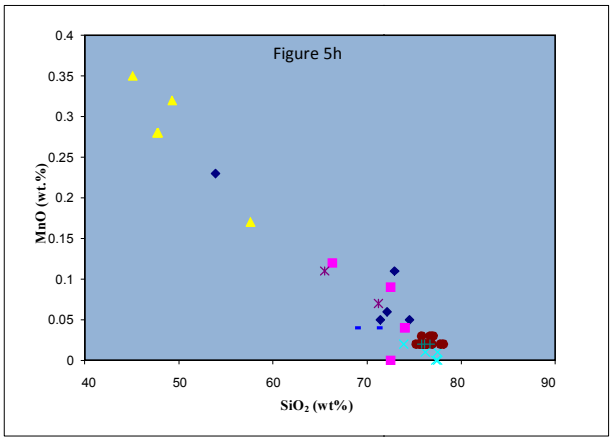
Figure 5h
MnO (wt.%)
SiO2 (wt%)

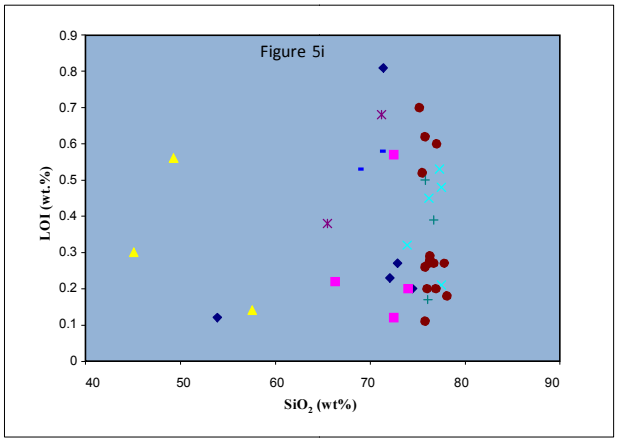
Figure 5i
LOI (wt.%)
SiO2 (wt%)

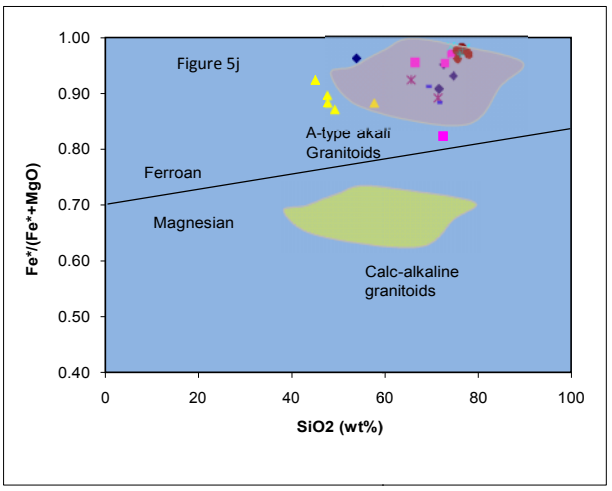
Figure 5j
A-type alkali Granitoids
Ferroan
Magnesian
Calc-alkaline granitoids
Fe*/(Fe*+MgO)
SiO2 (wt%)

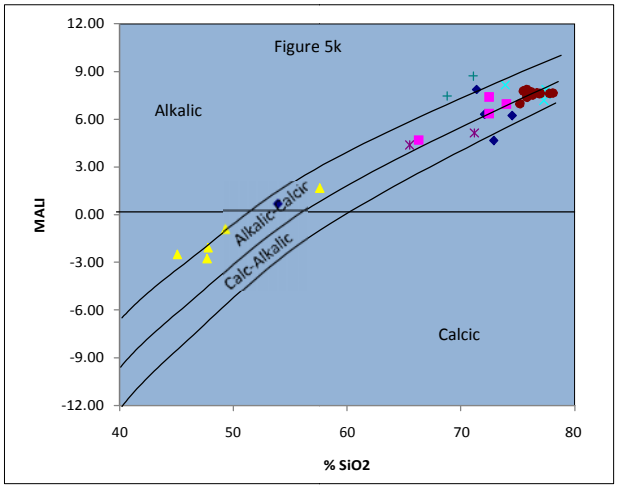
Figure 5k
Alkalic
Alkalic-calcic
Calc-Alkalic
Calcic
MALI
% SiO2

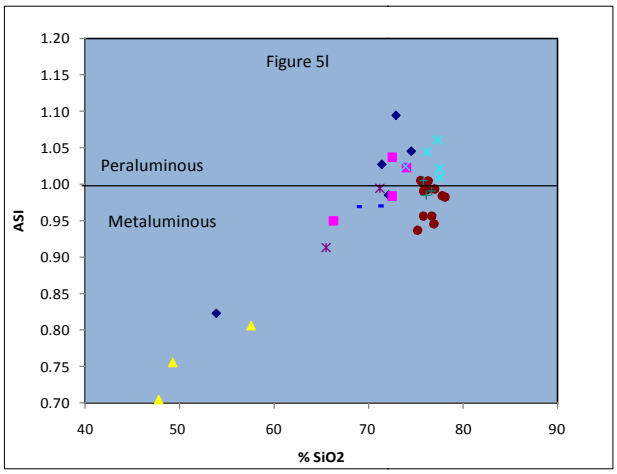
Figure 5l
Peraluminous
Metaluminous
ASI
% SiO2

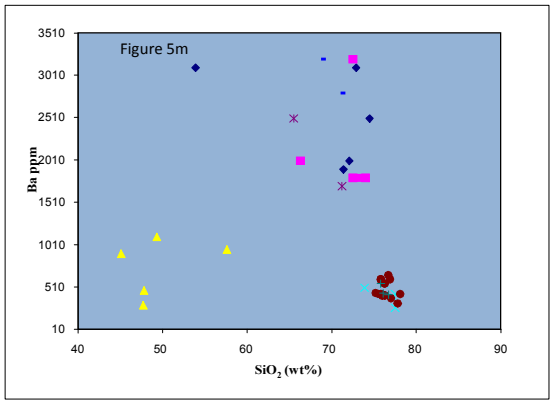
Figure 5m
Ba ppm
SiO2 (wt%)

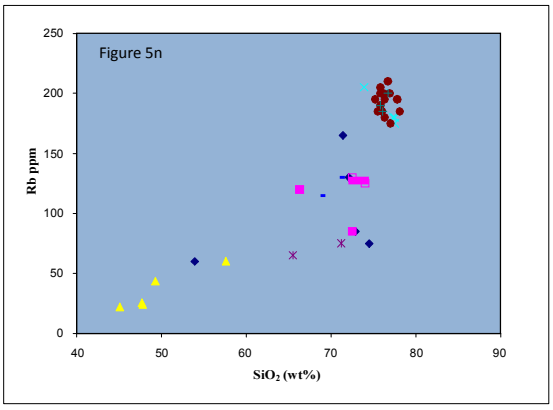
Figure 5n
Rb ppm
SiO2 (wt%)

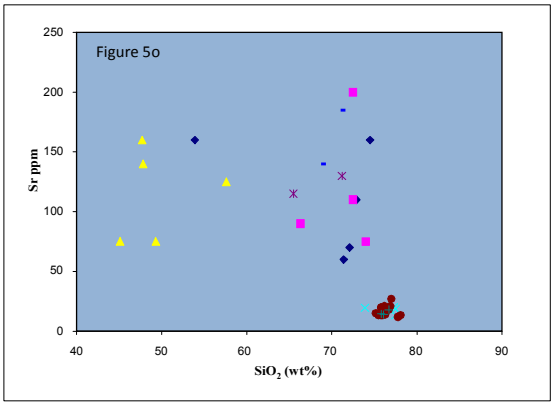
Figure 5o
Sr ppm
SiO2 (wt%)

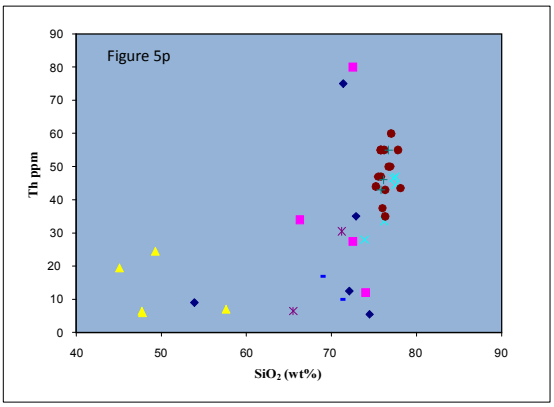
Figure 5p
Th ppm
SiO2 (wt%)

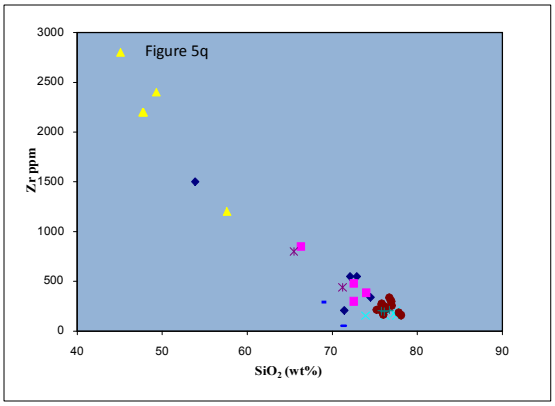
Figure 5q
Zr ppm
SiO2 (wt%)

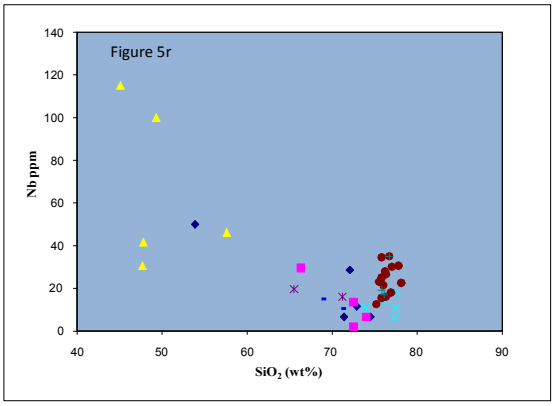
Figure 5r
Nb ppm
SiO2 (wt%)

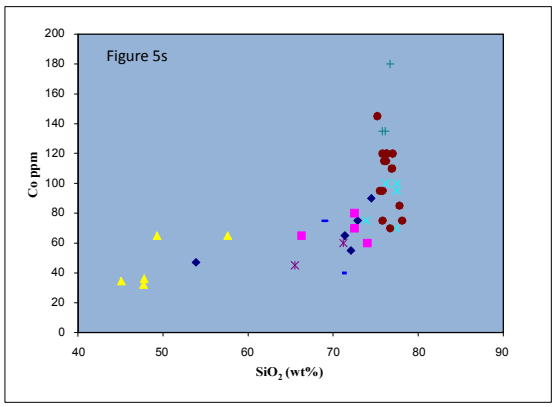
Figure 5s
Co ppm
SiO2 (wt%)

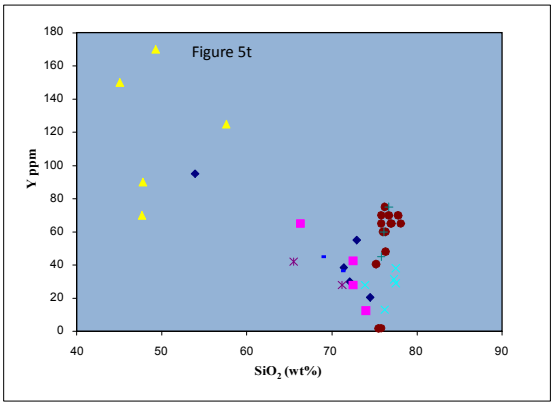
Figure 5t
Y ppm
SiO2 (wt%)

Figure 6a

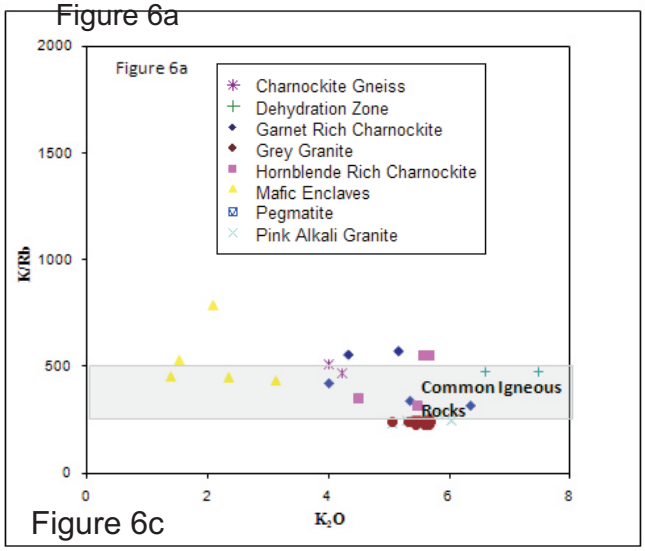

Figure 6b

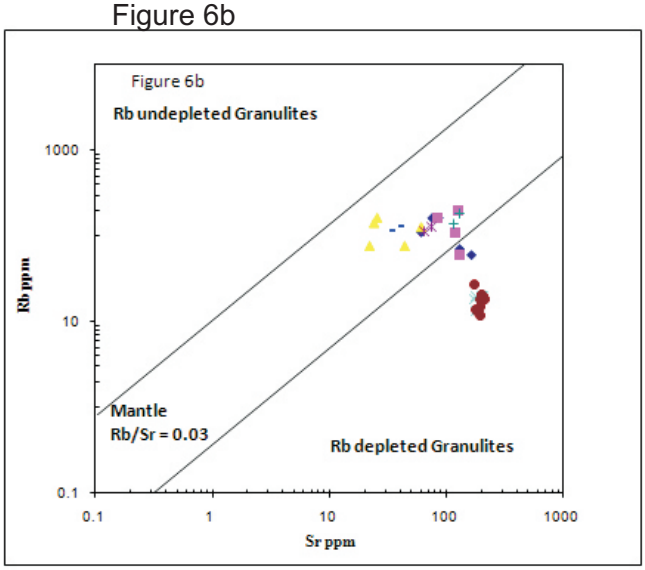

Figure 6c

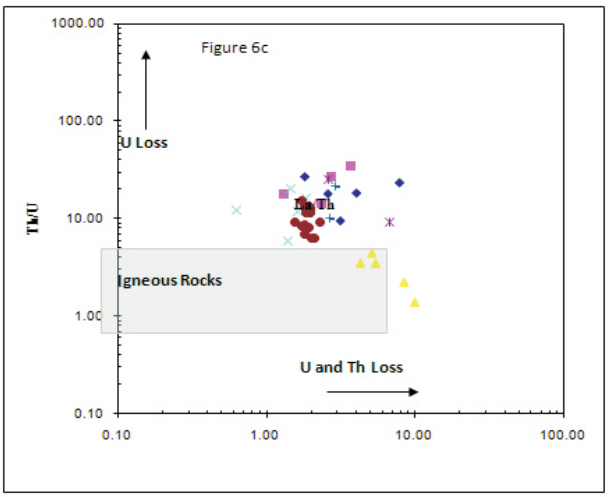

Figure 6d

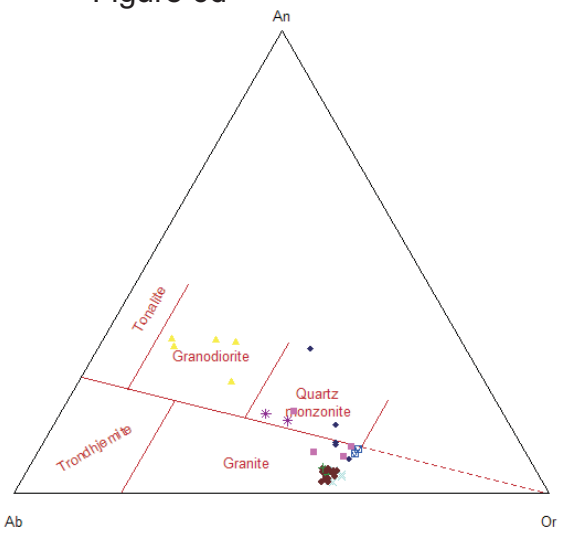

Figure 6e

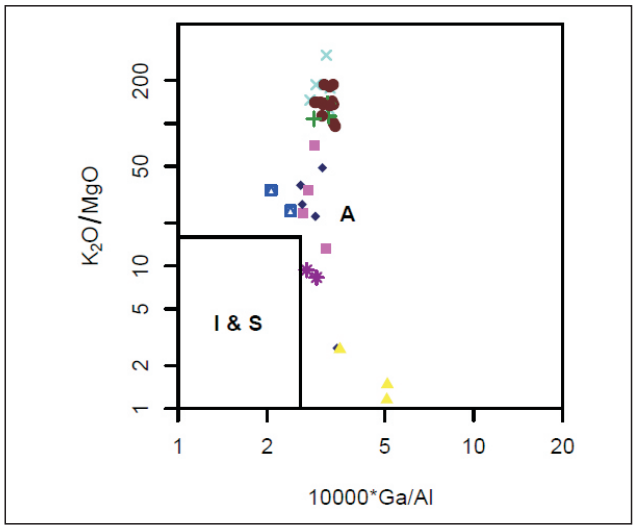

Figure 6f

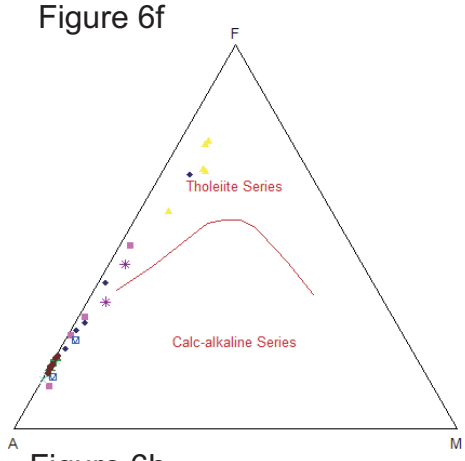

Figure 6g

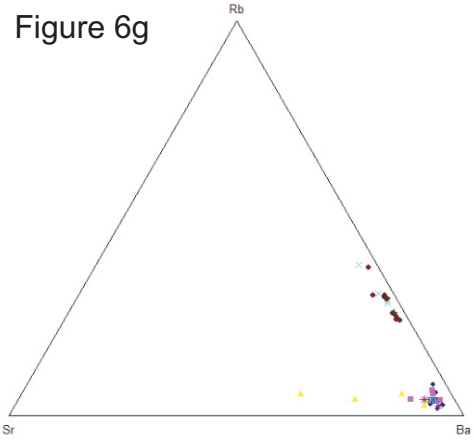

Figure 6h

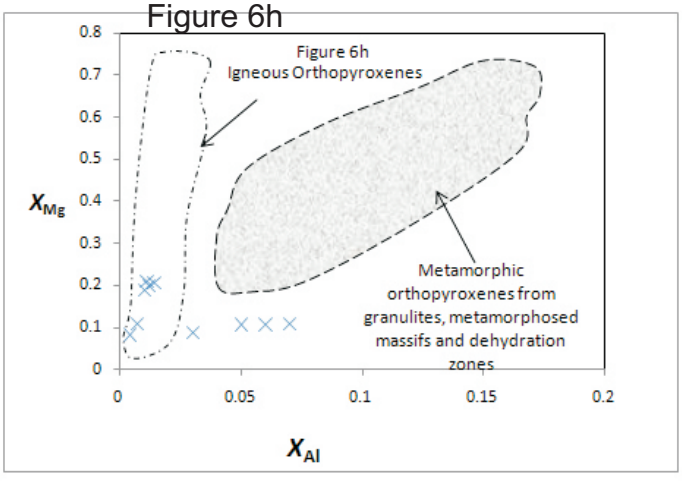

Figure 7a

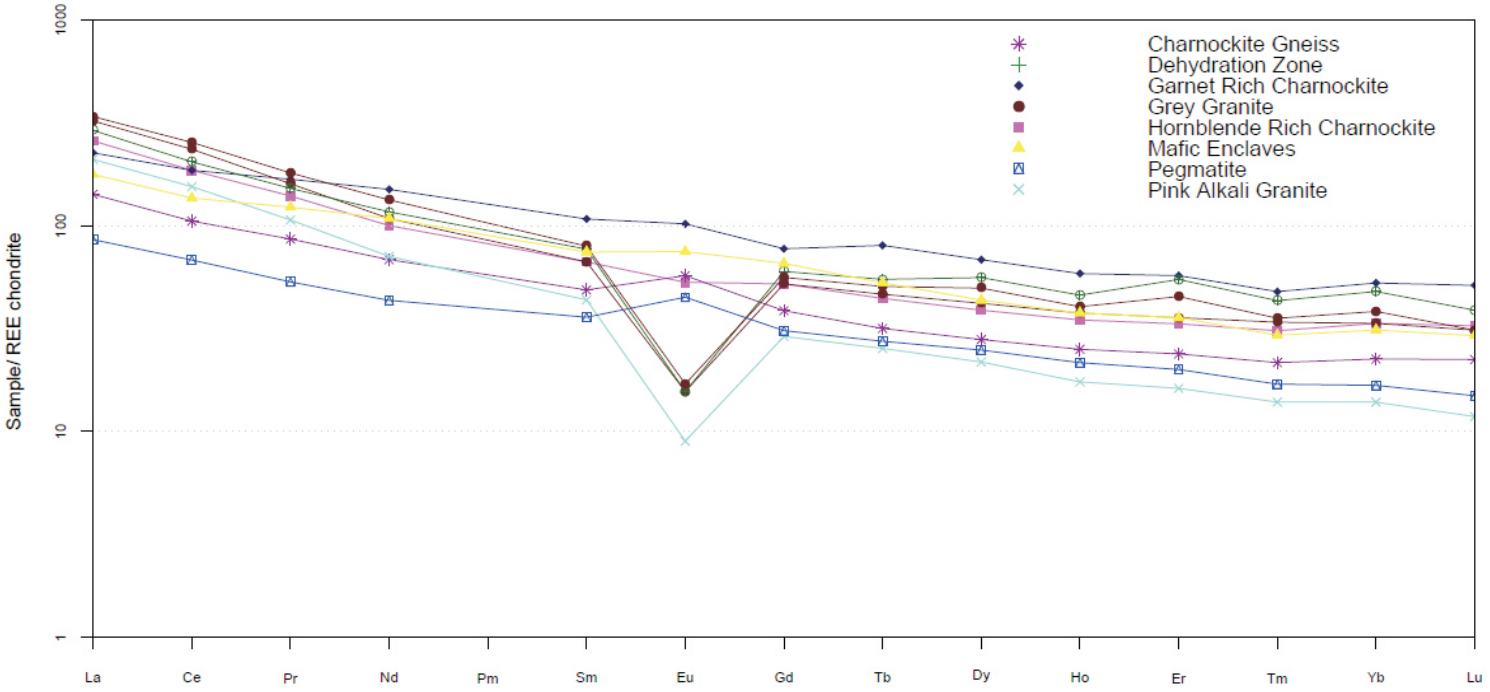

Figure 7b

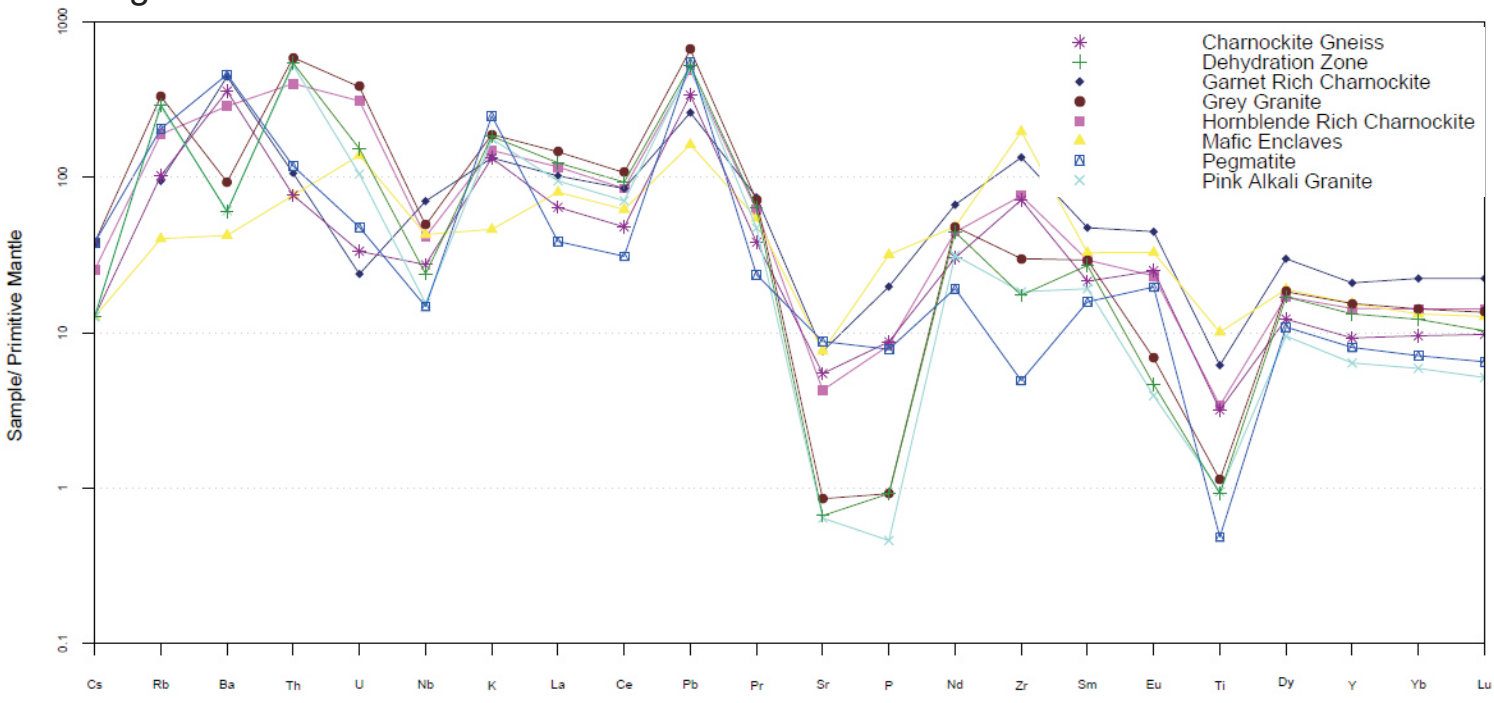

Figure 8.

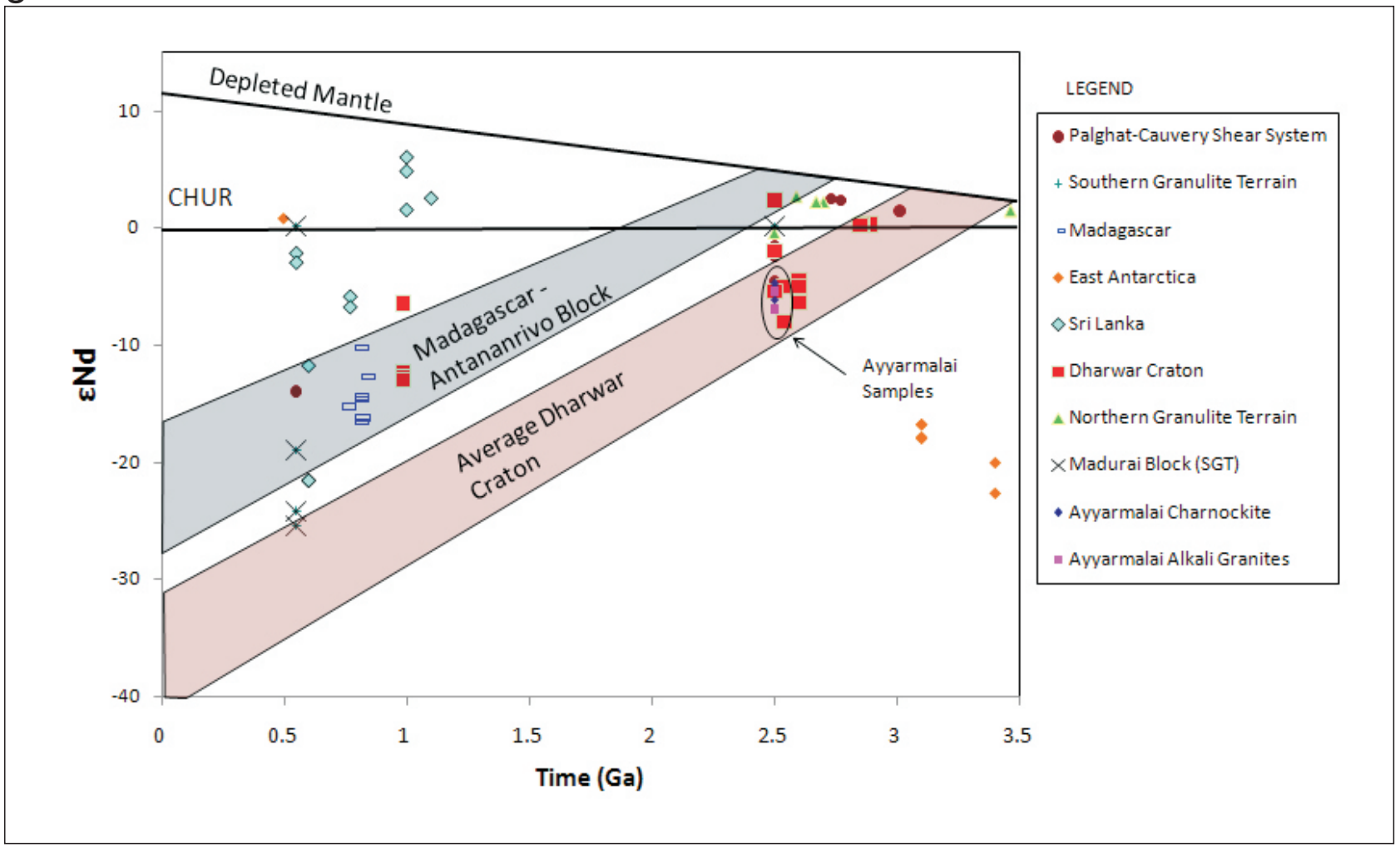
Depleted Mantle
CHUR
Madagascar - Antananrivo Block
Average Dharwar Craton
Ayyarmalai Samples
εNd
Time (Ga)
10
0
-10
-20
-30
-40
0
0.5
1
1.5
2
2.5
3
3.5
LEGEND
Palghat-Cauvery Shear System
Southern Granulite Terrain
Madagascar
East Antarctica
Sri Lanka
Dharwar Craton
Northern Granulite Terrain
Madurai Block (SGT)
Ayyarmalai Charnockite
Ayyarmalai Alkali Granites

Figure 9a

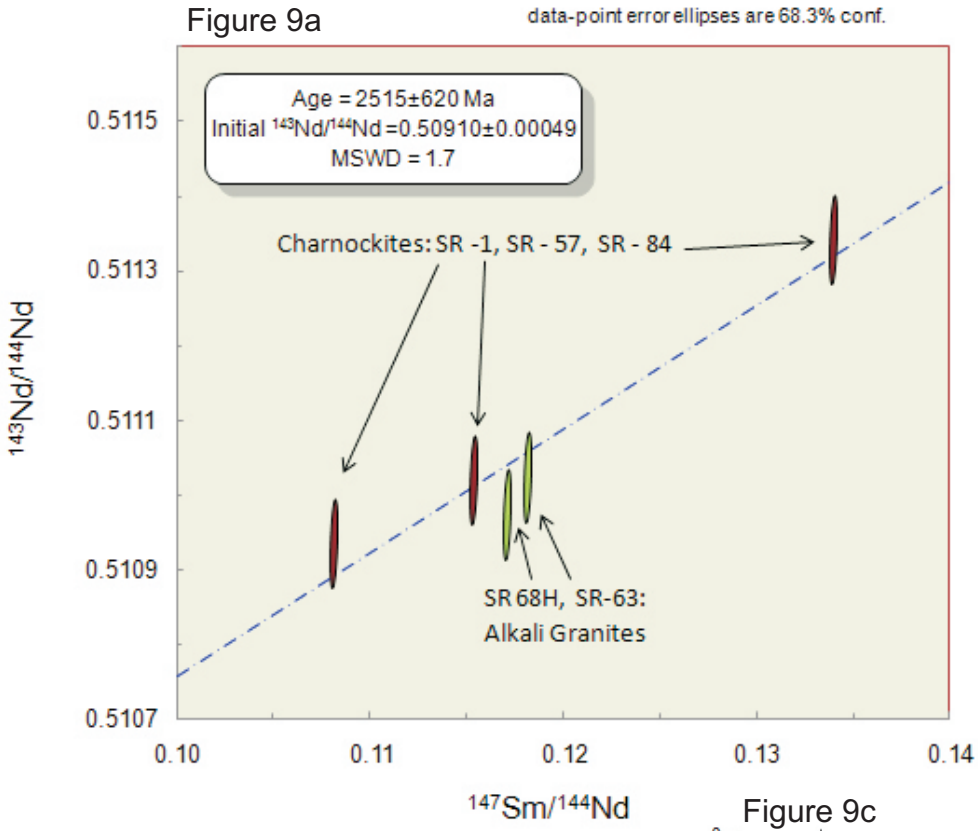

Figure 9b

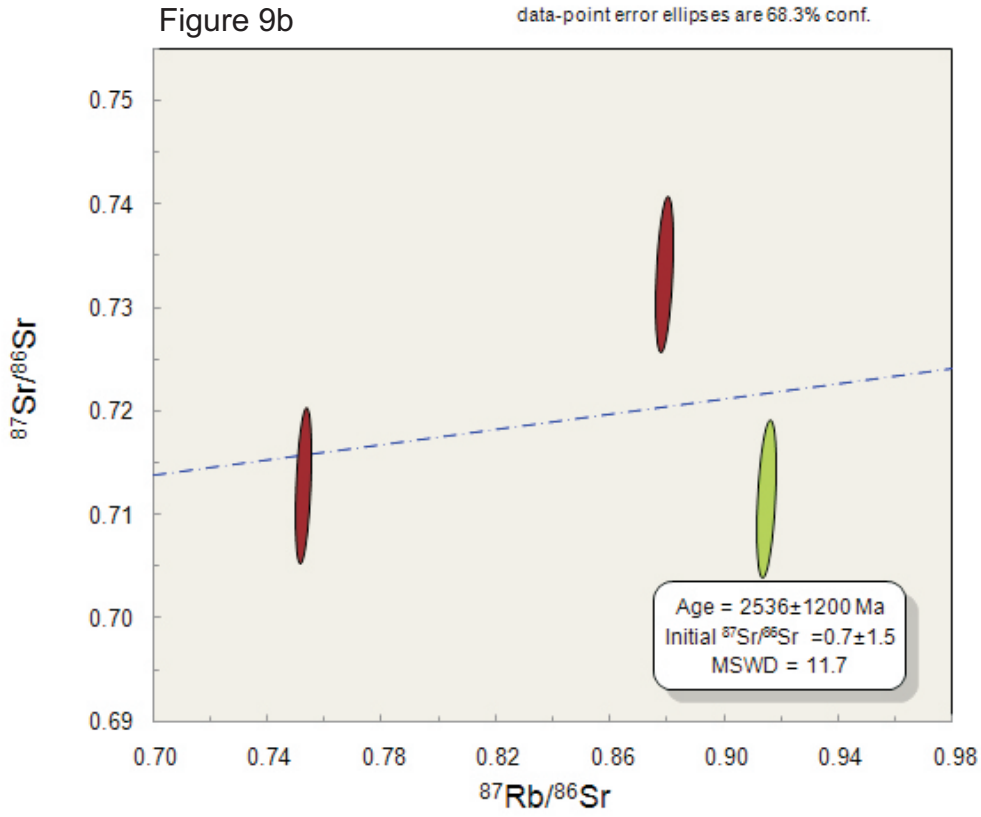

Figure 9c

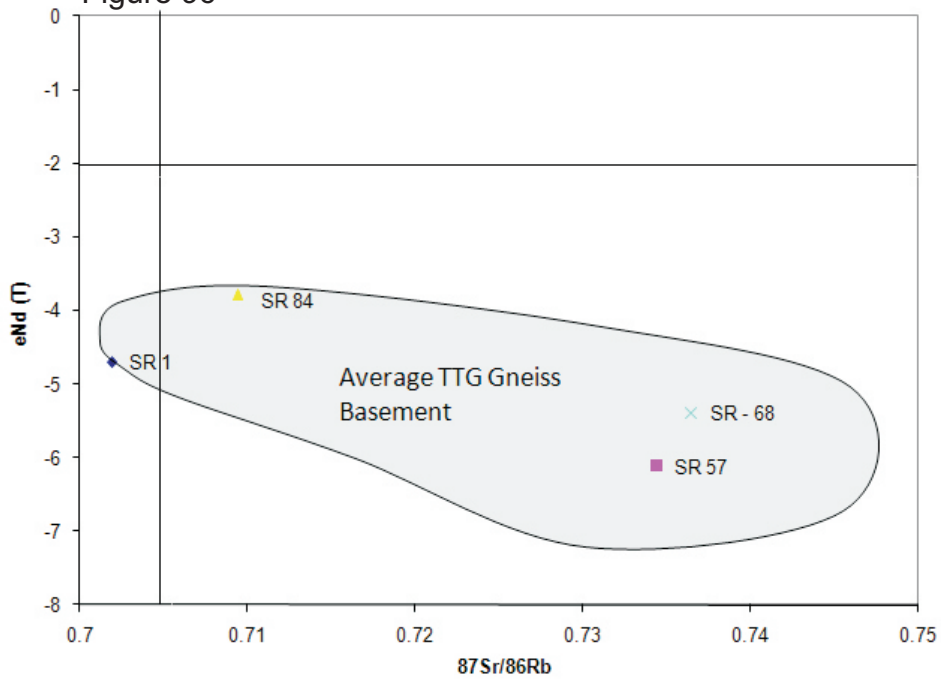

Figure 10

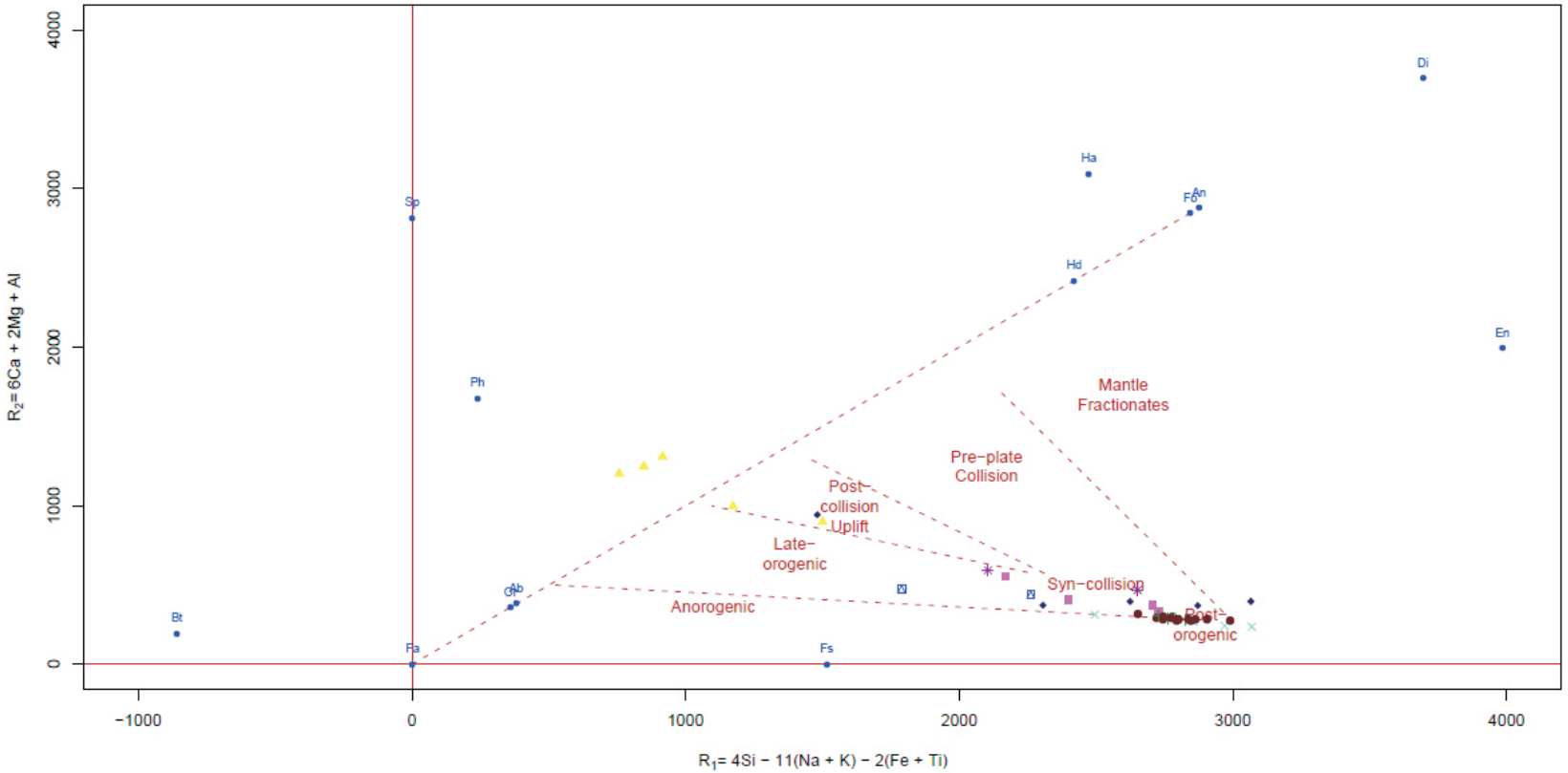
Di
Ha
Sp
An
Fo
Hd
En
Ph
Mantle
Fractionates
Pre-plate
Collision
Post-
collision
Uplift
Late-
orogenic
Syn-collision
Anorogenic
Post-
orogenic
Ab
Bt
Fa
Fs
4000
3000
2000
1000
0
−1000
0
1000
2000
3000
4000
R2= 6Ca + 2Mg + Al
R1= 4Si − 11(Na + K) − 2(Fe + Ti)

Figure 11

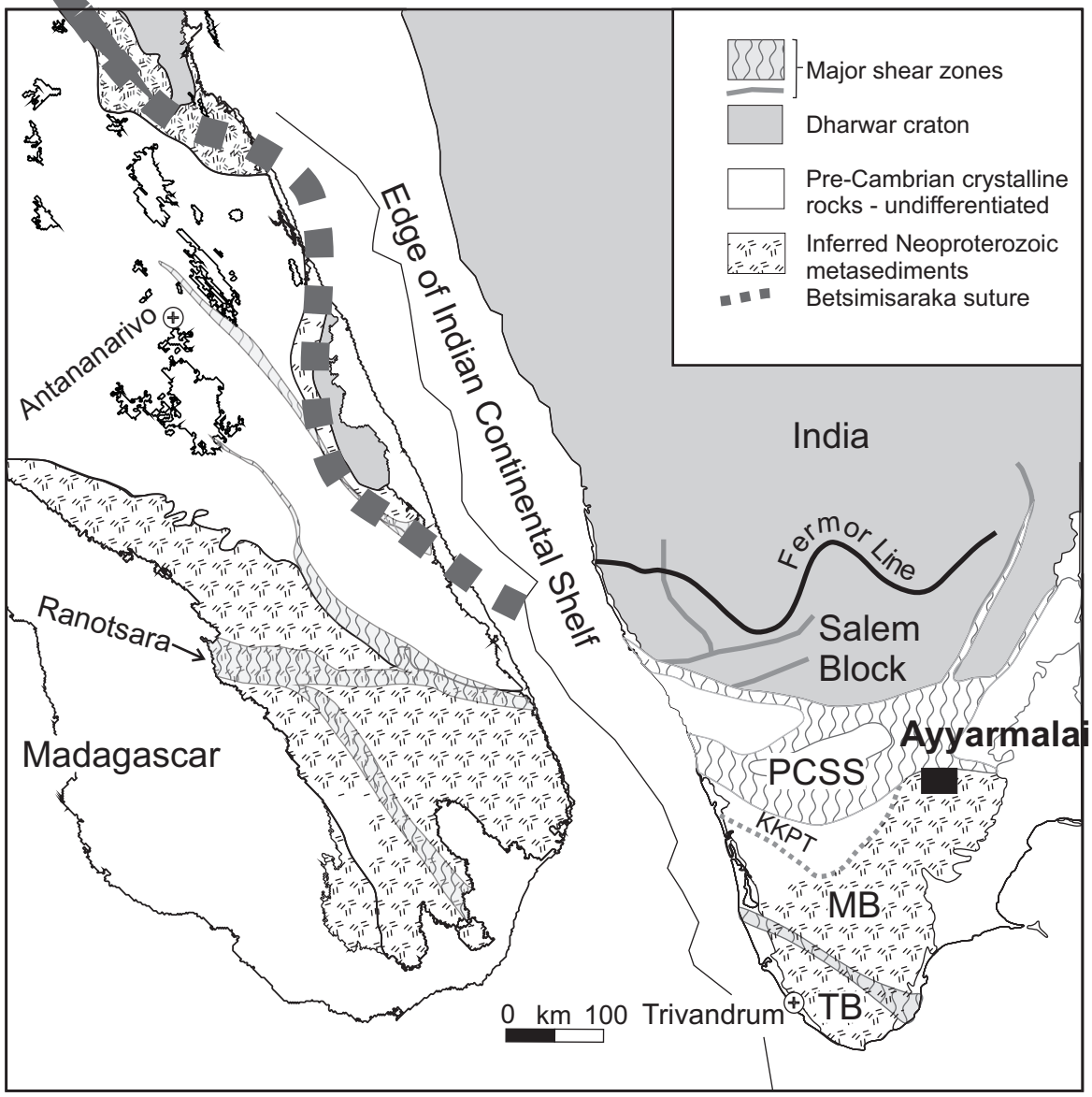
Major shear zones
Dharwar craton
Pre-Cambrian crystalline rocks - undifferentiated
Inferred Neoproterozoic metasediments
Betsimisaraka suture
Edge of Indian Continental Shelf
India
Fermor Line
Salem Block
Ayyarmalai
PCSS
KKPT
MB
TB
Trivandrum
Antananarivo
Ranotsara
Madagascar
0 km 100